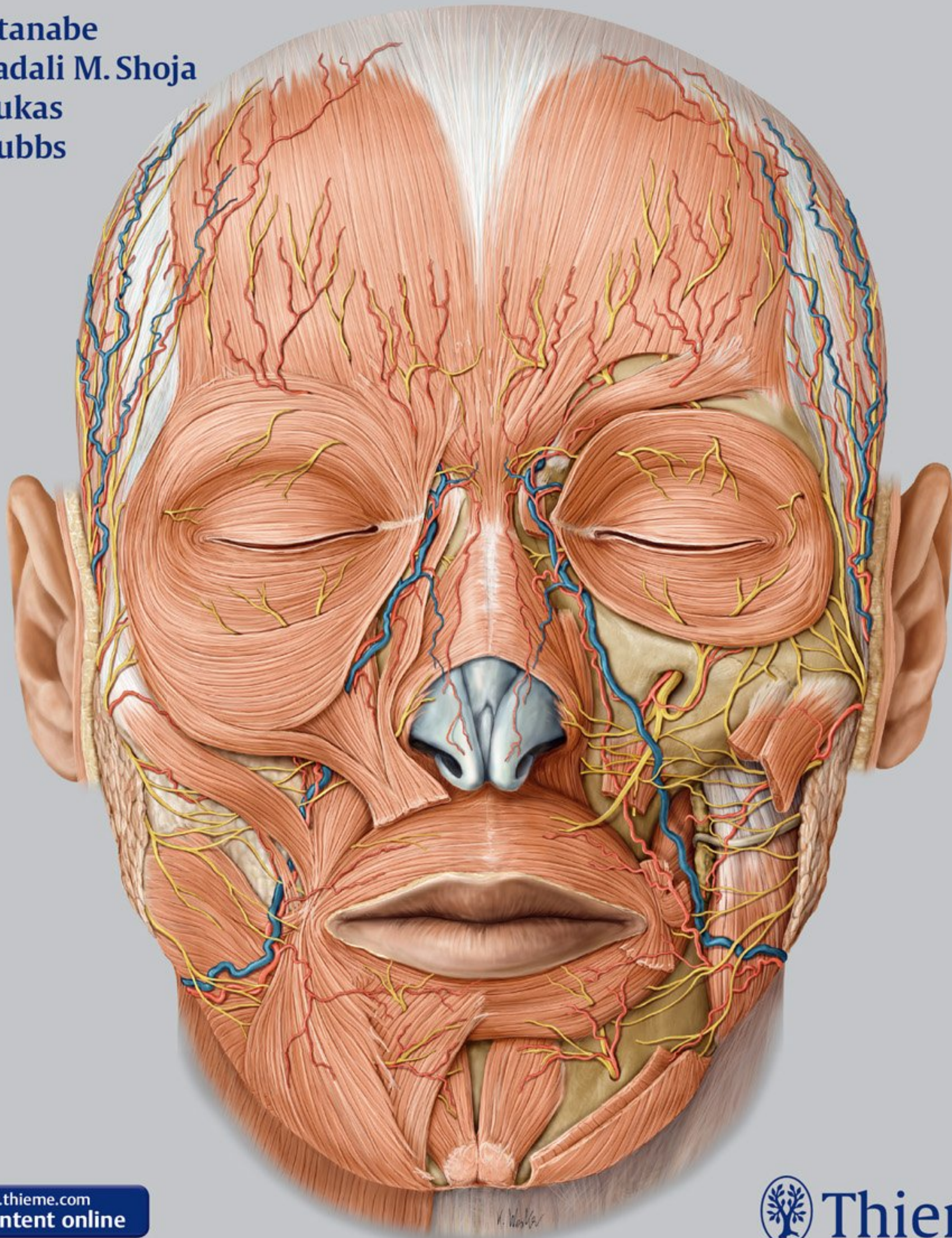


Anatomy for Plastic Surgery of the Face, Head, and Neck

Koichi Watanabe
Mohammadali M. Shoja
Marios Loukas
R. Shane Tubbs



Anatomy for Plastic Surgery of the Face, Head, and Neck

Koichi Watanabe, MD, PhD
Assistant Professor
Department of Anatomy
Kurume University School of Medicine
Fukuoka-Prefecture, Japan

Mohammadali M. Shoja, MD
Research Scientist
Section of Pediatric Neurosurgery
Children's Hospital
Birmingham, Alabama, USA

Marios Loukas, MD, PhD
Dean of Basic Sciences
Professor and Chair
Department of Anatomical Sciences
St. George's University
Grenada, West Indies

R. Shane Tubbs, MS, PA-C, PhD
Professor and Chief Scientific Officer
Seattle Science Foundation
Seattle, Washington, USA

269 illustrations

Thieme
New York • Stuttgart • Delhi • Rio de Janeiro

Executive Editor: Timothy Hiscock
Managing Editor: Elizabeth Palumbo
Director, Editorial Services: Mary Jo Casey
Editorial Assistant: Haley Paskalides
Production Editor: Barbara A. Chernow
International Production Director: Andreas Schabert
Vice President, Editorial and E-Product Development:
Vera Spillner
International Marketing Director: Fiona Henderson
International Sales Director: Louisa Turrell
Director of Sales, North America: Mike Roseman
Senior Vice President and Chief Operating Officer:
Sarah Vanderbilt
President: Brian D. Scanlan
Typesetting by Carol Pierson, Chernow Editorial Services, Inc.

Library of Congress Cataloging-in-Publication Data

Names: Watanabe, K  oichi, 1968– author. | Shoja, Mohammadali M., author. | Loukas, Marios, author. | Tubbs, R. Shane, author.
Title: Anatomy for plastic surgery of the face, head, and neck / K  oichi Watanabe, Mohammadali M. Shoja, Marios Loukas, R. Shane Tubbs.
Description: New York : Thieme, [2016] | Includes bibliographical references and index.
Identifiers: LCCN 2015031107 | ISBN 9781626230910 (alk. paper) | ISBN 9781626230927 (eISBN)
Subjects: | MESH: Head—anatomy & histology—Atlases. | Neck—anatomy & histology—Atlases. | Reconstructive Surgical Procedures—Atlases.
Classification: LCC RD1 19 | NLM WE 17 | DDC 617.9/52—dc23
LC record available at <http://lcn.loc.gov/2015031107>

  2016 Thieme Medical Publishers, Inc.
Thieme Publishers New York
333 Seventh Avenue, New York, NY 10001
USA +1 800 782 3488, customerservice@thieme.com

Thieme Publishers Stuttgart
R  digerstrasse 14, 70469 Stuttgart, Germany
+49 [0]711 8931 421, customerservice@thieme.de

Thieme Publishers Delhi
A-12, Second Floor, Sector-2, Noida-201301
Uttar Pradesh, India
+91 120 45 566 00, customerservice@thieme.in

Thieme Publishers Rio de Janeiro, Thieme Publica   es Ltda.
Edif  cio Rodolpho de Paoli, 25   andar
Av. Nilo Pe  anha, 50 – Sala 2508
Rio de Janeiro 20020-906, Brasil
+55 21 3172 2297

Printed in India by Manipal Technologies Ltd., Manipal

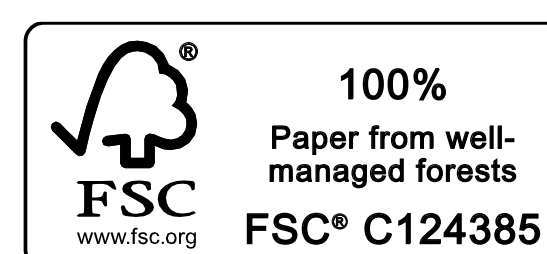
ISBN 978-1-62623-091-0

Also available as an e-book:
eISBN 978-1-62623-092-7

Important note: Medicine is an ever-changing science undergoing continual development. Research and clinical experience are continually expanding our knowledge, in particular our knowledge of proper treatment and drug therapy. Insofar as this book mentions any dosage or application, readers may rest assured that the authors, editors, and publishers have made every effort to ensure that such references are in accordance with **the state of knowledge at the time of production of the book.**

Nevertheless, this does not involve, imply, or express any guarantee or responsibility on the part of the publishers in respect to any dosage instructions and forms of applications stated in the book. **Every user is requested to examine carefully** the manufacturers' leaflets accompanying each drug and to check, if necessary in consultation with a physician or specialist, whether the dosage schedules mentioned therein or the contraindications stated by the manufacturers differ from the statements made in the present book. Such examination is particularly important with drugs that are either rarely used or have been newly released on the market. Every dosage schedule or every form of application used is entirely at the user's own risk and responsibility. The authors and publishers request every user to report to the publishers any discrepancies or inaccuracies noticed. If errors in this work are found after publication, errata will be posted at www.thieme.com on the product description page.

Some of the product names, patents, and registered designs referred to in this book are in fact registered trademarks or proprietary names even though specific reference to this fact is not always made in the text. Therefore, the appearance of a name without designation as proprietary is not to be construed as a representation by the publisher that it is in the public domain.



This book, including all parts thereof, is legally protected by copyright. Any use, exploitation, or commercialization outside the narrow limits set by copyright legislation without the publisher's consent is illegal and liable to prosecution. This applies in particular to photostat reproduction, copying, mimeographing or duplication of any kind, translating, preparation of microfilms, and electronic data processing and storage.

Contents

List of Videos	vii
Preface	ix
Contributors	xi
1 Neurocranium and Facial Skeleton	1
<i>David Kahn, Toomas Arusoo, and Eric J Wright</i>	
2 Anterior Skull Base	13
<i>Surjith Vattoth and Philip R. Chapman</i>	
3 Middle Skull Base	20
<i>Philip R. Chapman and Surjith Vattoth</i>	
4 Soft Tissue of the Scalp and Temporal Regions	33
<i>Noriyuki Koga</i>	
5 Arterial Supply of the Facial Skin	40
<i>Nobuaki Imanishi</i>	
6 Arteries of the Face and Neck	47
<i>Yelda Atamaz Pinar, Figen Govsa, and Servet Celik</i>	
7 Veins of the Face and Neck	63
<i>Yusuke Shimizu</i>	
8 Facial Nerve and Temporal Bone	72
<i>Orlando Guntinas-Lichius</i>	
9 Peripheral Branches of the Facial Nerve	79
<i>Andrew P. Trussler</i>	
10 Sensory Nerves of the Head and Neck	86
<i>Ibrahim Khansa, Jenny C. Barker, and Jeffrey E. Janis</i>	
11 Superficial Musculoaponeurotic System and the Facial Soft Tissues	101
<i>Yoko Tabira, Joe Iwanaga, Tsuyoshi Saga, and Koichi Watanabe</i>	
12 Mimetic Muscles	111
<i>Hee-Jin Kim</i>	
13 Orbital Anatomy	120
<i>Swapna Vemuri and Jeremiah P. Tao</i>	
14 Orbital Soft Tissues	126
<i>Swapna Vemuri and Jeremiah P. Tao</i>	
15 Eyelid Anatomy	134
<i>Catherine Y. Liu, Swapna Vemuri, and Jeremiah P. Tao</i>	
16 Nasal Cavity and Paranasal Sinuses	142
<i>Joe Iwanaga, Tsuyoshi Saga, and Koichi Watanabe</i>	
17 External Nose	155
<i>Hideaki Rikimaru</i>	
18 Auricle and External Acoustic Meatus	161
<i>Noritaka Komune, Junichi Fukushima, and Albert L. Rhoton, Jr.</i>	
19 Mandible and Masticatory Muscles	172
<i>Kyung-Seok Hu and Yang Hun Mu</i>	

Contents

20 Oral Cavity and Pharynx 183
Joe Iwanaga, Shinya Mikushi, and Haruka Tohara

21 Neck 200
Sherine S. Raveendran and Lucian Ion

Index 221

List of Videos

Video 1. Facial muscles and facial nerve on the anterior face

Lower face
Middle face

Video 2. Dissection of the external nose

Muscles on the external nose
Bony and cartilaginous structure

Video 3. Main trunk of the facial nerve and its branches

Landmarks of the facial nerve trunk
Temporal branch
Zygomatic branch
Buccal branch
Marginal mandibular branch
Cervical branch

Video 4. Sensory nerves of the face

Supraorbital nerve
Infraorbital nerve
Zygomaticofacial nerve
Mental nerve

Video 5. Layers of the temporal region

Superficial temporal fascia
Deep temporal fascia
Temporalis muscle

Preface

This book was planned as a head and neck surgical anatomy book for plastic surgeons, head and neck surgeons, and surgeons who practice in related fields. Unfortunately, few surgical textbooks emphasize anatomy, especially textbooks in the field of plastic surgery. In most surgical textbooks, the procedures are described only in minute detail. Conversely, traditional anatomical textbooks do not provide adequate information on the regional anatomy, preventing surgeons from obtaining the knowledge necessary to expertly perform various surgical procedures. One reason for this is that although the basic anatomy of the human body was almost completely described more than 100 years ago, the anatomy in the head and neck region, especially that applicable to plastic surgery, is still developing. Additionally, anatomical textbooks often do not provide the most up-to-date information. Therefore, we have attempted to include the latest anatomical understanding of the head and neck anatomy from a plastic surgeon's perspective.

In writing this preface, I (KW) discussed head and neck anatomy with my mentors in two specialties: gross anatomy and plastic surgery. This allowed me to consider anatomy from two different viewpoints.

First, my mentor in gross anatomy made the following observations: The anatomy of the head and neck is extremely complicated and the details differ among individuals and during different stages of life. These differences include the thickness of the tissues, their changes in response to aging, and even anatomical variations in vessels, nerves, and muscles. Each organ in the head and neck region has a very distinct function. Consequently, pathologies involving the head that require surgery will be operated on by surgeons specializing in neurosurgery, otorhinolaryngology, ophthalmology, dental medicine, and plastic surgery. While in-depth knowledge in the anatomical area of specialization is extremely important in treating patients, the surgeon as well as the medical staff must also be highly familiar with not just related regions of the body but also with unrelated regions. In medical education, unfortunately, the importance of anatomical education has been downplayed globally in recent years. This may be because nowadays medical stu-

dents have less time to study anatomy, given the many new fields of medicine that they are expected to be familiar with. Apparently, some medical schools no longer offer anatomical dissection. Thus, not surprisingly, the number of anatomists, especially gross anatomists, is decreasing. This tendency has critical, negative implications for surgery. Gross anatomy is the basis of knowledge for every surgeon. Surgeons must be experts in gross anatomy if they hope to acquire the surgical skills to become experts in surgery.

My second mentor, a specialist in plastic surgery, offered the following: The most important aspect of performing plastic surgery is knowledge of three-dimensional regional anatomy. For example, each nerve and blood vessel takes up space three dimensionally. It is important to recognize how these structures travel on the surface plane, but it is more important for the success of the actual surgery to know which tissue layers these structures run through. Anatomical atlases and textbooks provide detailed images of these structures, but the knowledge gained from them is two-dimensional. Novice surgeons typically memorize the two-dimensional image of their surgical field. Because of this, surgical results are sometimes unsatisfactory, or unexpected surgical complications may occur. To perform surgeries with a high degree of difficulty, a surgeon has to be able to vividly visualize the three-dimensional regional anatomy of the surgical field. Plastic surgery residents have to study the regional anatomy in anatomical atlases and textbooks, and confirm their anatomical knowledge in practical operations. By repeating this pattern many times, a resident is able to establish and practice three-dimensional anatomical knowledge. By having surgical training based on accurate anatomical knowledge, a surgeon will be better equipped to perform high-degree operations.

We hope that our textbook will not only help to improve the surgical skill of individual surgeons, but will also promote the development of head and neck surgery. I would like to thank Dr. Koh-ichi Yamaki, Professor of Anatomy, and Dr. Kensuke Kiyokawa, Professor of Plastic Surgery, for kindly contributing the above comments to the preface.

Contributors

Toomas Arusoo, MS

Medical Student, Year 2
Michigan State University College of Human
Medicine
Grand Rapids, Michigan, USA

Jenny C. Barker, MD, PhD

Resident
Department of Plastic Surgery
Ohio State University Wexner Medical Center
Columbus, Ohio, USA

Servet Celik, MD

Assistant Professor
Department of Anatomy
Faculty of Medicine
Ege University
Izmir, Turkey

Philip R. Chapman, MD

Chief, Neuroradiology
Associate Professor, Neuroradiology Section
University of Alabama at Birmingham School of
Medicine
Birmingham, Alabama, USA

Junichi Fukushima, MD, PhD

Department of Otorhinolaryngology
Graduate School of Medical Science
Kyushu University
Fukuoka, Japan

Figen Govsa, MD

Professor
Department of Anatomy
Ege University, Faculty of Medicine
Izmir, Turkey

Orlando Guntinas-Lichius, MD

Professor and Chairman
ENT Department
Jena University Hospital
Dean of Students
Medical Faculty
Friedrich-Schiller University
Jena, Germany

Kyung-Seok Hu, DDS, PhD

Associate Professor
Department of Oral Biology
Division in Anatomy & Developmental Biology
Yonsei University College of Dentistry
Seoul, Republic of Korea

Nobuaki Imanishi, MD

Associate Professor
Department of Anatomy
School of Medicine, Keio University
Tokyo, Japan

Lucian Ion, FRCS(Plast)

Consultant Plastic Surgeon
Director, Aesthetic Plastic Surgery Ltd
London, UK
Honorary Consultant
Chelsea and Westminster Hospital
London, UK

Joe Iwanaga, DDS

Assistant Professor
Department of Anatomy
Kurume University School of Medicine
Fukuoka, Japan

Jeffrey E. Janis, MD, FACS

Professor and Executive Vice Chairman
Chief of Plastic Surgery
University Hospitals
Department of Plastic Surgery
Ohio State University Wexner Medical Center
Columbus, Ohio, USA

David Kahn, MD

Clinical Associate Professor Plastic Surgery
Section Chief, Cosmetic Surgery
Division of Plastic Surgery
Stanford University
Palo Alto, California, USA

Ibrahim Khansa, MD

Resident
Department of Plastic Surgery
Ohio State University Wexner Medical Center
Columbus, Ohio, USA

Hee-Jin Kim, DDS, PhD

Professor
Division in Anatomy & Developmental Biology
Department of Oral Biology
Yonsei University College of Dentistry
Seoul, Korea

Kensuke Kiyokawa, MD, PhD

Professor and Chairman
Department of Plastic & Reconstructive Surgery &
Maxillofacial Surgery
Kurume University School of Medicine
Fukuoka, Japan

Contributors

Noriyuki Koga, MD, PhD
Assistant Professor
Department of Plastic Surgery, Reconstructive and
Maxillofacial Surgery
Kurume University School of Medicine
Kurume, Japan

Noritaka Komune, MD, PhD
Fellow
Department of Otorhinolaryngology and Head and Neck
Surgery
Kyushu University Hospital
Fukuoka-ken, Japan

Catherine Y. Liu, MD, PhD
Resident, Ophthalmology
Gavin Herbert Eye Institute
University of California, Irvine
Irvine, California, USA

Marios Loukas, MD, PhD
Dean of Basic Sciences
Professor and Chair
Department of Anatomical Sciences
St. George’s University
Grenada, West Indies

Shinya Mikushi, DDS, PhD
Nagasaki University Hospital
Department of Special Care Dentistry
Clinic for Oral Care and Dysphagia Rehabilitation
Nagasaki, Japan

Yang Hun Mu, DDS, PhD
Assistant Professor
Department of Anatomy College of Medicine
Dankook University
Chungnam, Korea

Yelda Atamaz Pinar, MD
Professor
Department of Anatomy
Faculty of Medicine
EGE University, Faculty of Medicine
Izmir, Turkey

Sherine S. Raveendran, FRCSEd, EBOPRAS, MSc, MS, MBBS
Director
Toronto Medical Aesthetics
Markham, Ontario, Canada

Albert L. Rhoton, Jr., MD
R. D. Keene Family Professor and Chairman Emeritus
Department of Neurological Surgery
University of Florida
Gainesville, Florida, USA

Hideaki Rikimaru, MD, PhD
Department of Plastic Reconstructive Surgery and
Maxillofacial Surgery
Kurume University School of Medicine
Fukuoka, Japan

Tsuyoshi Saga, PhD
Associate Professor
Department of Anatomy
Kurume University School of Medicine
Fukuoka, Japan

Yusuke Shimizu, MD, PhD
Associate Professor
Department of Plastic and Reconstructive Surgery
Keio University, School of Medicine
Tokyo, Japan

Mohammadali M. Shoja, MD
Research Scientist
Section of Pediatric Neurosurgery
Children’s Hospital
Birmingham, Alabama, USA

Yoko Tabira, PhD
Research Associate
Department of Anatomy
Kurume University School of Medicine
Kurume, Japan

Jeremiah P. Tao, MD, FACS
Chief, Oculoplastic & Orbital Surgery
American Society of Ophthalmic Plastic and Reconstructive
Surgery Fellowship Director
Ophthalmology Residency Director
Associate Professor
Gavin Herbert Eye Institute
University of California, Irvine
Irvine, California, USA

Haruka Tohara, DDS, PhD
Gerodontology and Oral Rehabilitation,
Department of Gerontology and Gerodontology
Graduate School of Medical and Dental Sciences
Tokyo Medical and Dental University
Yushima, Bunkyo
Tokyo, Japan

Andrew P. Trussler, MD, FACS
Plastic Surgeon, Private Practice
Austin, Texas, USA

R. Shane Tubbs, MS, PA-C, PhD
Professor and Chief Scientific Officer
Seattle Science Foundation
Seattle, Washington, USA

Surjith Vattoth, MD, FRCR
Senior Consutant, Neuroradiologist
Hamad Medical Corporation
Doha, Qatar

Swapna Vemuri, MD
Fellow, Oculoplastic and Orbital Surgery
Gavin Herbert Eye Institute
University of California, Irvine
Irvine, California, USA

Koichi Watanabe, MD, PhD

Assistant Professor
Department of Anatomy
Kurume University School of Medicine
Fukuoka-Prefecture, Japan

Koh-ichi Yamaki, MD, PhD

Professor and Chair
Department of Anatomy
Kurume University School of Medicine
Kurume, Japan

Eric J. Wright, MD

Chief Resident
Division of Plastic & Reconstructive Surgery
Stanford University Medical Center
Palo Alto, California, USA

1 Neurocranium and Facial Skeleton

David Kahn, Toomas Arusoo, and Eric J Wright

Introduction

The skull can be divided into two parts: the *neurocranium*, which forms a protective case around the brain, and the *viscerocranium*, which forms the skeleton of the face. This chapter details the viscerocranium and bones of the neurocranium that pertain to the viscerocranium.

Neurocranium

The neurocranium in adults is formed by a series of eight bones: the singular frontal, ethmoid, sphenoid, occipital bones centered on the midline, and the temporal and parietal bones occurring as bilateral pairs.¹ The primarily flat frontal, parietal, and occipital bones form the calvaria (skullcap) by intramembranous ossification of head mesenchyme derived from the neural crest. The primarily irregular, yet considerably flat, sphenoid and temporal bones contribute to the cranial base via endochondral ossification of cartilage or from more than one type of ossification. The irregular ethmoid bone slightly contributes to the neurocranium but is primarily part of the viscerocranium. In reality, the flat bones and flat portions of the bones forming the neurocranium consist of convex external and concave internal curved surfaces.¹

Fibrous interlocking sutures unite most calvarial bones in adulthood, although during childhood, the sphenoid and occipital bones are unified by synchondroses.² Some sutures, comprising narrow closures of connective tissue at birth, remain open until adulthood. The sagittal suture is derived from neural crest cells and the coronal suture from paraxial mesoderm.² The newborn skull contains *fontanelles*, the most prominent being the anterior fontanel, which are widened sutures at points where more than two bones meet. The anterior fontanel, found where the two parietal and frontal bones meet, closes in most cases by 18 months of age, and the posterior fontanel closes by 1 to 2 months of age.²

Two primary centers of ossification traverse the frontal (metopic) suture in the second year, dividing the frontal bone into halves. Usually, the frontal suture disappears by age 6 years, when the halves fuse, but it can persist into adulthood as a metopic suture either totally, running from the midline of the glabella to the bregma, or partially.² The *glabella* is a smooth anterior projecting prominence on the frontal bone superior to the root of the nose, and the *bregma* is the junction of the coronal and sagittal sutures.

The maxillae and mandible provide the sockets and supporting bone for the maxillary and mandibular teeth. The maxillae contribute the greatest part of the upper facial skeleton,

forming the skeleton of the upper jaw, which is fixed to the cranial base. (The mandible is detailed in Chapter 19.)

On the lateral aspect of the skull is the thin pterion. The pterion, located two finger breadths superior to the zygomatic arch and a thumb's breadth posterior to the frontal process of the zygomatic bone, is formed by the articulations of the frontal, parietal, sphenoid, and temporal bones.¹ The pterion overlies the anterior branch of the middle meningeal artery. Therefore, an injury to this region can damage the vessel, producing an epidural hematoma.¹

The air-filled paranasal sinuses, including the maxillary, frontal, and ethmoidal sinuses, are discussed. The sphenoidal sinuses are discussed in Chapters 2 and 16. The bony articulations of the neurocranium and viscerocranium are described in **Table 1.1**, and the general processes of ossification are displayed in **Table 1.2**.

Frontal Bone

The frontal bone forms the forehead via its squamous, orbital, and nasal parts and two cavities, the frontal sinuses.

Squamous Part

The flat squamous part is the largest part of the frontal bone forming most of the forehead.³ The supraorbital margin of the frontal bone is the angular boundary between the squamous and the orbital parts (**Fig. 1.1**).⁴

On the external surface of the squamous part, about 3 cm above the midpoint of this margin, are the frontal tuberosities.⁴ These tubercles are more prominent in children and adult women. Ventrally, a shallow groove separates the frontal tuberosities from the paired and curved superciliary arches.⁴ These arches extend laterally from the medially located, smooth, and elevated glabella and are more prominent in males. Partly dependent on frontal sinus size, superciliary arch prominence is occasionally associated with small sinuses.⁴

The supraorbital notch (or foramen), which transmits the supraorbital vessels and nerve, lies at the junction between the sharp, lateral two-thirds and the rounded medial third of the supraorbital margin.⁴ The variably occurring frontal notch (or foramen) occurs medial to the supraorbital notch in 50% of skulls.⁴

Surgical Annotation

Recent interest in the surgical treatment of migraines has led to numerous anatomical studies identifying areas of nerve compression. The supraorbital nerve, as it emerges from the

Table 1.1 Neurocranium and viscerocranium articulations

Bone	Single	Paired	Articulates with
Frontal	X		Parietal, sphenoid, zygomatic, maxilla, ethmoid, nasal, lacrimal
Ethmoid	X		Frontal, sphenoid, maxilla, palatine, vomer, nasal, lacrimal, inferior nasal concha
Temporal		X	Parietal, occipital, sphenoid, zygomatic, mandible
Nasal		X	Frontal, maxilla, nasal
Vomer	X		Sphenoid, maxilla, ethmoid, palatine
Inferior nasal concha		X	Maxilla, ethmoid, palatine, lacrimal
Maxilla		X	Frontal, sphenoid, zygomatic, maxilla, ethmoid, palatine, vomer, nasal, lacrimal, inferior nasal concha
Palatine		X	Sphenoid, maxilla, ethmoid, palatine, vomer, inferior nasal concha
Zygomatic		X	Frontal, temporal, maxilla, sphenoid
Lacrimal		X	Frontal, maxilla, ethmoid, inferior nasal concha

Source: Data from Norton NS. Netter’s Head and Neck Anatomy for Dentistry. 1st ed. Philadelphia, PA: Elsevier Saunders; 2006.

supraorbital foramen or notch, has been identified as a migraine trigger area.⁵ The supraorbital nerve can have compression from both a foramen as well as a notch as a result of the associated fascial bands. In addition to the soft tissue procedure, a supraorbital foraminotomy or fascial band release has been shown to improve postoperative outcomes.⁶ A transpalpebral incision can be used to access the supraorbital nerves to perform the decompression. An incision is made in the upper tarsal crease, with subsequent dissection identifying the supraorbital nerve. Muscles such as the corrugator supercilii are resected, and the foraminotomy is performed. Endoscopic techniques have also been described.⁷ With the use of the endoscopic technique, release of the zygomaticotemporal branch can also be performed.

The supraorbital margin extends laterally, forming the prominent zygomatic process, which articulates with the zygomatic bone. A posterosuperiorly curving line, which continues onto the squamous part of the temporal bone, divides into superior and inferior temporal lines.⁴ The temporal surface of the frontal bone is inferior and posterior relative to these temporal lines. The anterior surface of the temporal surface forms the anterior part of the temporal fossa. The rough inferior surface of the posterior margin of the squamous part articulates with the greater wing of the sphenoid.⁴

The nasal part of the frontal bone is discussed in the *Nasal Bone: Nasal Bridge and Bony Septum* section of this chapter. The interior surface of the frontal bone is detailed in Chapter 2.

Orbital Parts of the Frontal Bone

The two orbital parts of the frontal bone are thin, curved, and triangular laminae, consisting entirely of compact bone (**Fig. 1.2**).⁴ Forming the largest part of the orbital roofs, the orbital parts are separated by a wide, quadrilateral ethmoidal notch that is occupied by the cribriform plate of the ethmoid bone.⁴ The labyrinths of the ethmoid bone, which contain the ethmoidal air cells, articulate with the inferior surface of the lateral margins of the ethmoidal notch. This articulation converts two transverse grooves across each margin into anterior and posterior ethmoidal canals. These canals transmit the anterior and posterior ethmoidal nerves and vessels into the medial orbit.⁴

The posterolaterally ascending frontal sinuses open anterior to the ethmoidal notch and lateral to the nasal spine (**Fig. 1.3**). Deflecting from the median plane, these rarely symmetrical sinuses ascend between the frontal laminae and are separated by a thin septum.⁴ Each sinus communicates with the ipsilateral nasal cavity’s middle meatus via the frontonasal canal.⁴

Table 1.2 Neurocranium and viscerocranium ossification patterns

Bone	Parts	Ossification
Frontal	Squamous, orbital, nasal portions	Intramembranous
Ethmoid	Perpendicular plate, cribriform plate, ethmoid labyrinth	Endochondral
Temporal	Squamous part, tympanic part	Intramembranous
	petromastoid part, styloid process	Endochondral
Nasal		Intramembranous
Vomer		Intramembranous
Inferior Nasal Concha		Endochondral
Maxilla	Body; frontal, zygomatic, palatine, alveolar processes	Intramembranous
Palatine	Perpendicular plate, horizontal plate, pyramidal process	Intramembranous
Zygomatic	Frontal, temporal, maxillary processes	Intramembranous
Lacrimal		Intramembranous

Source: Data from Norton NS. Netter’s Head and Neck Anatomy for Dentistry. 1st ed. Philadelphia, PA: Elsevier Saunders; 2006.

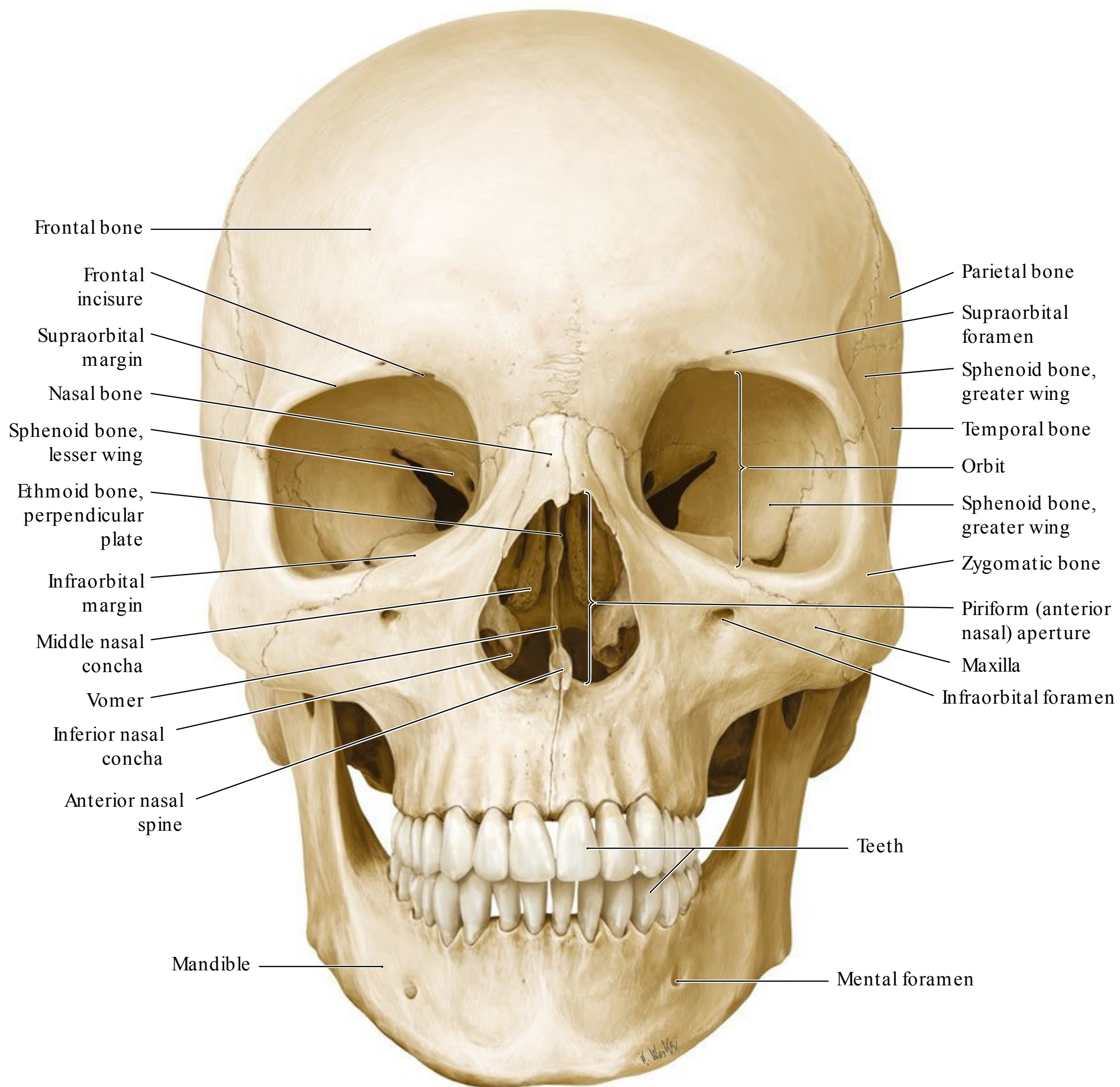


Fig. 1.1 Anterior view of the skull. The boundaries of the viscerocranium in relation to the neurocranium can be appreciated in this view. Visible features include the anterior nasal aperture, marking the start of the bony respiratory tract; a metopic suture projects superiorly from

the nasion; and the supraorbital foramen, infraorbital foramen, and mental foramen through which cutaneous nerves pass, are visible. (Reproduced from THIEME Atlas of Anatomy, General Anatomy and Musculoskeletal System, © Thieme 2005, Illustration by Karl Wesker.)

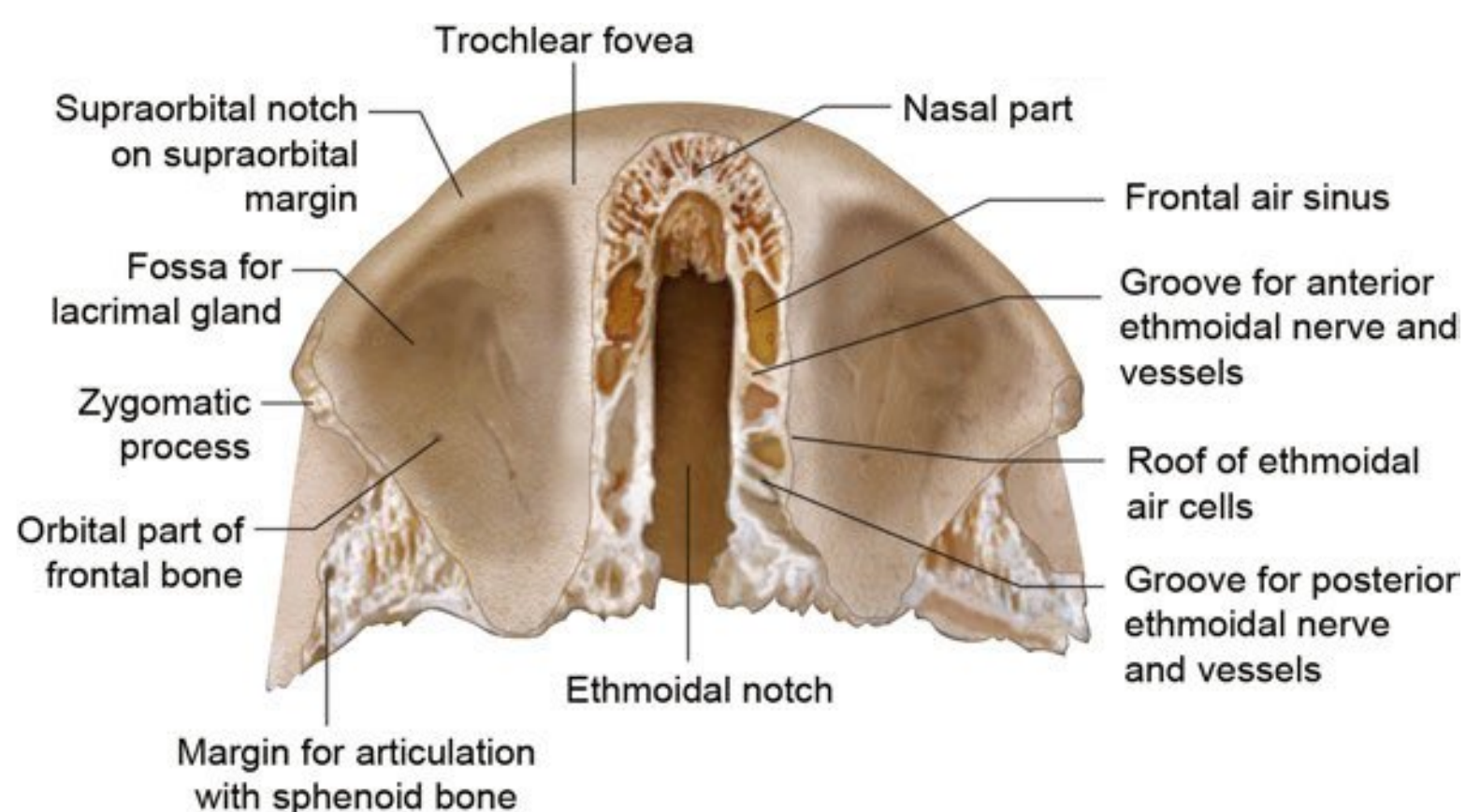


Fig. 1.2 Inferior view of the frontal bone. From this view, the ethmoidal notch and ethmoidal air sinuses can clearly be appreciated. Additional visibility of the orbital part surface features, including the fossa for the lacrimal gland, the sphenoidal articulating surface, and the zygomatic process, is obtained from this view.

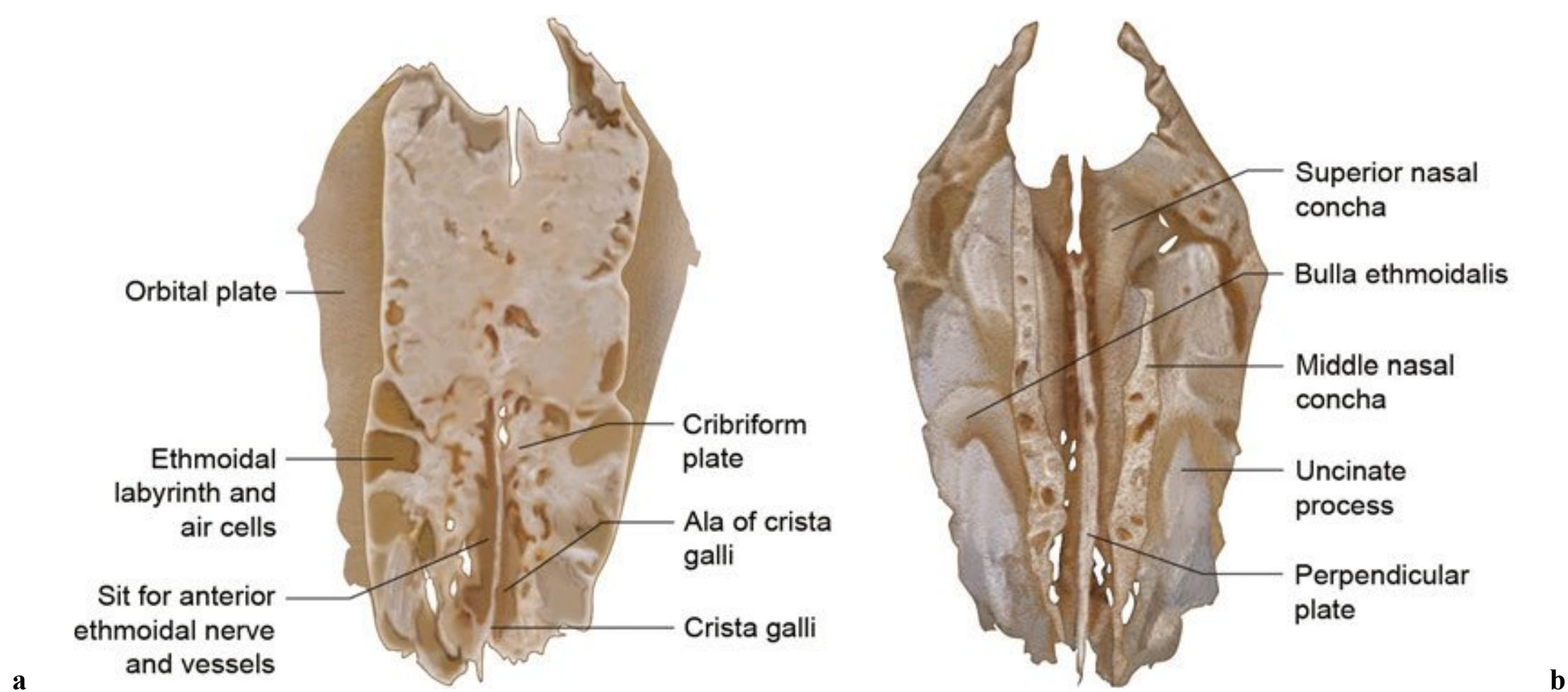


Fig. 1.3 (a) Superior view of the ethmoid bone. This view of the ethmoid bone provides a better appreciation for the ethmoidal labyrinth and air cells, the cribriform plate, and the crista galli and its

associated alae. **(b)** Inferior view of the ethmoidal bone. Viewing the ethmoid bone from below allows better appreciation of the nasal conchae, uncinate process, and the perpendicular plate.

Frontal Sinus Fractures

Surgical Annotation

Frontal sinus fractures can serve as a source of infection and cosmetic deformity. Approximately 10% of facial fractures involve the frontal sinuses.⁸ When outflow of the sinus is blocked as a result of injury to the nasofrontal duct, frontal sinus mucocoeles can develop. In accessing the injury, management depends on which wall of the sinus is fractured, the extent of fracture displacement, and the involvement of the nasofrontal duct. Correction of the anterior table of the sinus, which is done mainly to correct the cosmetic deformity, can be performed through an existing laceration or coronal incision. When the posterior table is displaced, the coronal incision allows access to perform a cranialization, which involves removing the posterior wall and allowing for the sinus to be part of the intracranial cavity. The sinus mucosal surface must be removed and the outflow tract and dead space obliterated to prevent postinjury infection.

Different techniques for performing the obliteration have been described.⁸ Management of sinus preservation can also be performed with few complications depending on the fracture pattern.⁹

Each smooth and concave orbital surface contains a shallow anterolateral fossa for the lacrimal gland. The posterior border of the orbital plate articulates with the lesser wings of the sphenoid.⁴

Ethmoid Bone

The fragile cuboidal ethmoid bone lies anteriorly in the cranial base, contributing to the medial orbital walls, nasal septum, roof, and lateral walls of the nasal cavity. The ethmoid is composed of a horizontal, perforated cribriform plate, a median perpendicular plate, and the two lateral labyrinths.³

Cribriform Plate

As mentioned, the horizontal cribriform plate fills the ethmoidal notch of the frontal bone (**Fig. 1.3a**). Penetrated by numerous foramina that contain olfactory nerve branches, the plate forms a large part of the nasal roof.³ The triangular and median crista galli projects superiorly from the plate and joins the frontal bone anteriorly via its two alae.³ Depressions in the cribriform plate on either side of the crista galli exist for the overlying olfactory bulb and gyrus rectus. Antero and lateral to the crista, foramina exist to transmit the anterior ethmoidal nerve and vessels from the nasal cavity to the foramen cecum.⁴

Perpendicular Plate

The perpendicular plate is discussed in the Nasal Bone: Nasal Bridge and Bony Septum section of this chapter.

Ethmoidal Labyrinths

On average, the ethmoidal labyrinths consist of 20 thin-walled air cells arranged as anterior, middle, and posterior groups containing 11, 3, and 6 air cells, respectively.⁴ The lateral orbital plate forms part of the medial orbital wall (**Fig. 1.4**). Adjoining articulations, save those that open into the nasal cavity, close all air cells. The air cells of the superior and posterior surfaces are closed by the ethmoidal notch of the frontal bone and both the sphenoidal conchae and orbital process of the palatine bone, respectively.⁴

The orbital plate covers the middle and posterior ethmoidal air cells articulating superiorly with the orbital plate of the frontal bone, anteriorly with the lacrimal bone, inferiorly with the maxilla and orbital process of the palatine bone, and posteriorly with the sphenoid bone.⁴ Anterior to the orbital plate, the lacrimal bone and frontal process of the maxilla complete the walls.

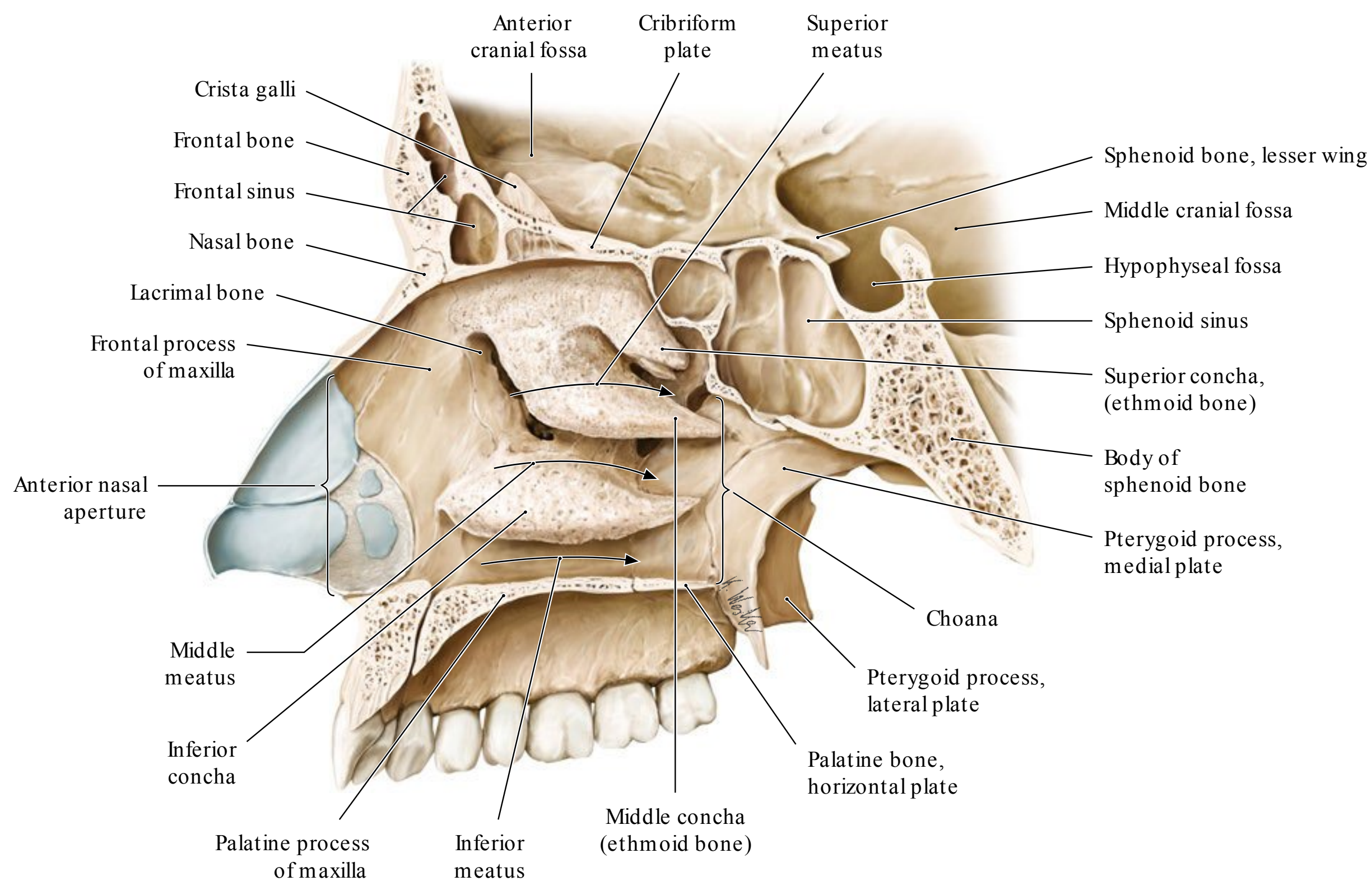


Fig. 1.4 Medial view of the right nasal cavity. This view of the nasal cavity allows better appreciation of the conchae, meatuses, portions of the hard palate, the frontal sinus, ethmoidal contributions to the nasal

cavity, and the anterior nasal aperture. (Reproduced from THIEME Atlas of Anatomy, Head and Neuroanatomy, © Thieme 2010, Illustration by Karl Wesker.)

Projecting posteroinferiorly from the labyrinth, the thin uncinate process crosses the ostium of the maxillary sinus to join the ethmoidal process of the inferior nasal concha.⁴

Descending from the inferior surface of the cribriform plate, the medial surface of the labyrinth forms part of the lateral nasal wall as the thin, lamellated, and convoluted middle nasal concha (**Fig. 1.3b**). Its anteroninferior lateral surface forms part of the middle meatus (**Fig. 1.4**).⁴ On the lateral wall of the middle meatus, middle ethmoidal air cells produce the ethmoidal bulla and open either on the bulla or above it. Posterior ethmoidal air cells open into the superior meatus, which is bounded by the superior nasal concha of the ethmoid.⁴ A curved infundibulum extends anteriorly and superiorly from the middle meatus, communicating with the anterior ethmoidal sinuses and in half of skulls continues superiorly as the frontonasal duct, which drains the frontal sinus.⁴

Temporal Bone

The paired temporal bones help form the base and lateral walls of the skull and are discussed in further detail in subsequent chapters (**Fig. 1.1**). The temporal bone houses the auditory and vestibular apparatuses and contains mastoid air cells.³ Each bone has eight centers of ossification that give rise to the three major centers observed before birth.² The temporal bone comprises the squamous, petromastoid, and tympanic parts, as well

as the styloid process.³ The temporal bone also has two associated canals. On its lateral surface, the external acoustic meatus conveys sound waves to the tympanic membrane. On its medial surface, the internal acoustic meatus conveys the facial and vestibulocochlear nerves.⁴

Squamous Part

The largest, squamous part lies anterosuperiorly and contains the thin and largest temporal portion, a zygomatic process and a mandibular fossa (**Fig. 1.5**).³ Its external temporal surface forms part of the temporal fossa. The concave, internal cerebral surface of the squamous part is grooved by the middle meningeal vessels.³ The lower border, fused to the anterior petrous part often contains traces of a petrosquamosal suture. Posteriorly, the squamous part fuses with the mastoid part. The anteroinferior border articulates with the greater wing of the sphenoid, and the superior border articulates with the inferior parietal bone at the squamosal suture.⁴

The zygomatic process extends anterolaterally from the squamous portion. It forms the zygomatic arch via an articulation between its obliquely posteroinferiorly sloping, deeply serrated anterior end, and the temporal process of the zygomatic bone.³ Its inferior surface forms a short articular tubercle, which contacts the articular disc of the temporomandibular joint and forms the anterior limit of the mandibular fossa.⁴

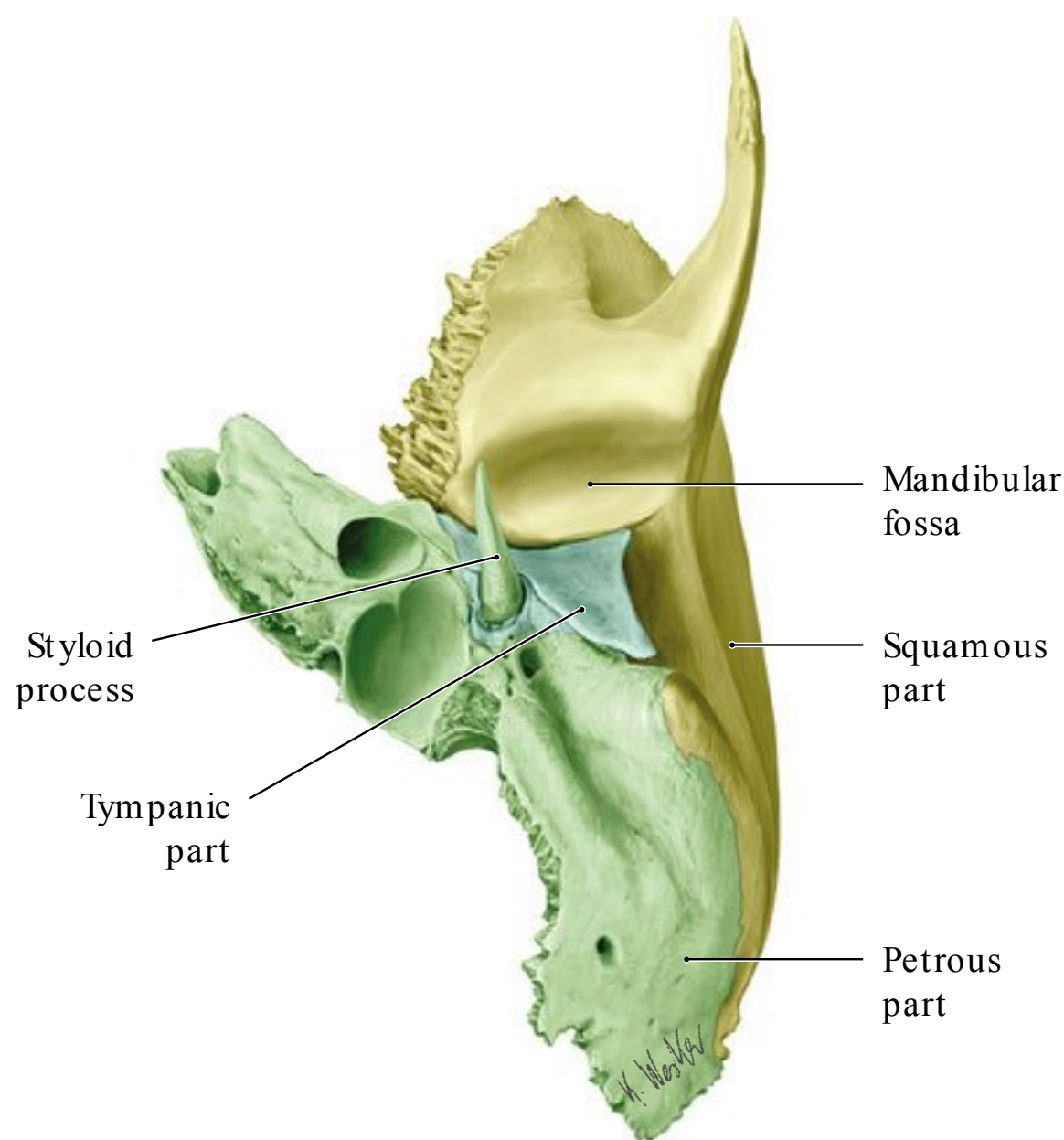


Fig. 1.5 Left temporal bone: inferior view. The squamous part, which bears the mandibular fossa; the petromastoid part, which contains the auditory and vestibular apparatus; and the tympanic part, which forms much of the external auditory canal, are best appreciated from this inferior view. (Reproduced from THIEME Atlas of Anatomy, Head and Neuroanatomy. © Thieme 2010, Illustration by Karl Wesker.)

The mandibular fossa presents an anterior articular area and a posterior nonarticular area, formed by the tympanic element. This smooth, concave articular surface, formed by the squamous part, contacts the mandibular condyle's temporomandibular joint articular disc. The squamotympanic fissure separates the posterior mandibular fossa from the tympanic part.⁴

Petromastoid Part

The petromastoid part is relatively large and better described as two parts. The trabecular mastoid part, which internally contains the mastoid air cells and mastoid antrum, constitutes the posterior region of the temporal bone. The posteriorly projecting mastoid process, which is larger in adult men, attaches the sternocleidomastoid, splenius capitis, and longissimus capitis to its lateral surface and the posterior belly of the digastric on its medial surface.⁴

The petrous part formed of compact bone inclines superiorly and anteromedially from the cranial base.⁴ It houses the auditory and vestibular apparatuses and separates the temporal and occipital lobes of the brain.³ The mass of the petrous part is wedged between the sphenoid and occipital bones.⁴ The petrous part's base, apex, three surfaces, and three borders are described in subsequent chapters.

The petrous portion extends anteriorly and medially, forming the foramen lacerum via sphenoid articulation. On the medial side lies the internal acoustic meatus and superior and inferior petrosal sinus grooves.³

The tympanic part is located below the squamous part and anterior to the mastoid process. Internally fused with the

petrous part and posteriorly fused with the squamous part and mastoid process, the tympanic part forms a thin, incomplete ring.⁴ The posterior surface forms the anterior wall, floor, and posterior wall of the external acoustic meatus. The anterior surface forms the posterior wall of the mandibular fossa.³ The pointed, slender styloid process projects anteroinferiorly from the inferior surface of the temporal bone. Further explanation of temporal bone relationships is covered in subsequent chapters.

Viscerocranium

The viscerocranium consists of 15 irregular bones. These are the singular midline-centered mandible, ethmoid, and vomer, and the six bilateral pairs of bones, including the maxillae, inferior nasal conchae, and the zygomatic, palatine, nasal, and lacrimal bones.

Nasal Bone: Nasal Bridge and Bony Septum

The nasal bones, placed side by side between the frontal processes of the maxillae, jointly form the nasal bridge and internasal suture. Each small, oblong, and variable bone has external and internal surfaces and superior, inferior, lateral, and medial borders.⁴ The transversely convex external surface is centrally perforated by a vein-traversing foramen. A longitudinal groove for the anterior ethmoidal nerve traverses the transversely concave internal surface (**Fig. 1.6**).⁴

The thick, serrated superior border articulates with the nasal part of the frontal bone, forming the frontonasal suture (**Fig. 1.7**).⁴ The nasion is a craniometric point on the cranium where the frontonasal and internasal sutures meet. The medial border articulates with the contralateral nasal bone and pro-

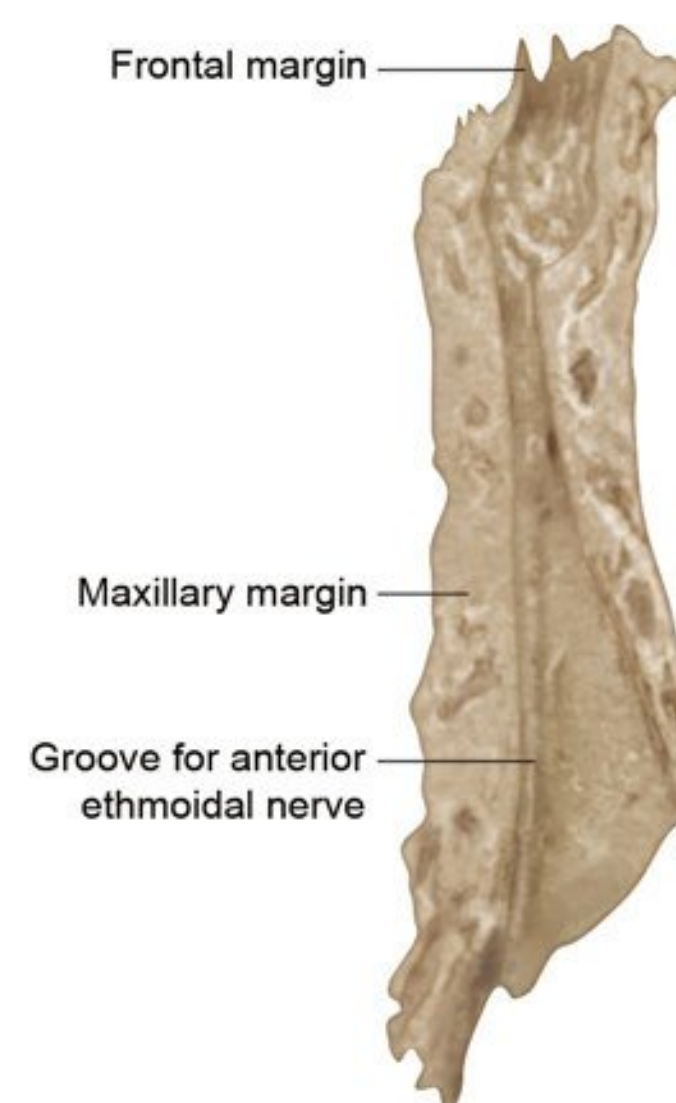


Fig. 1.6 Left nasal bone: internal view. The four articulating borders and the groove for the anterior ethmoidal nerve are appreciated from this view.

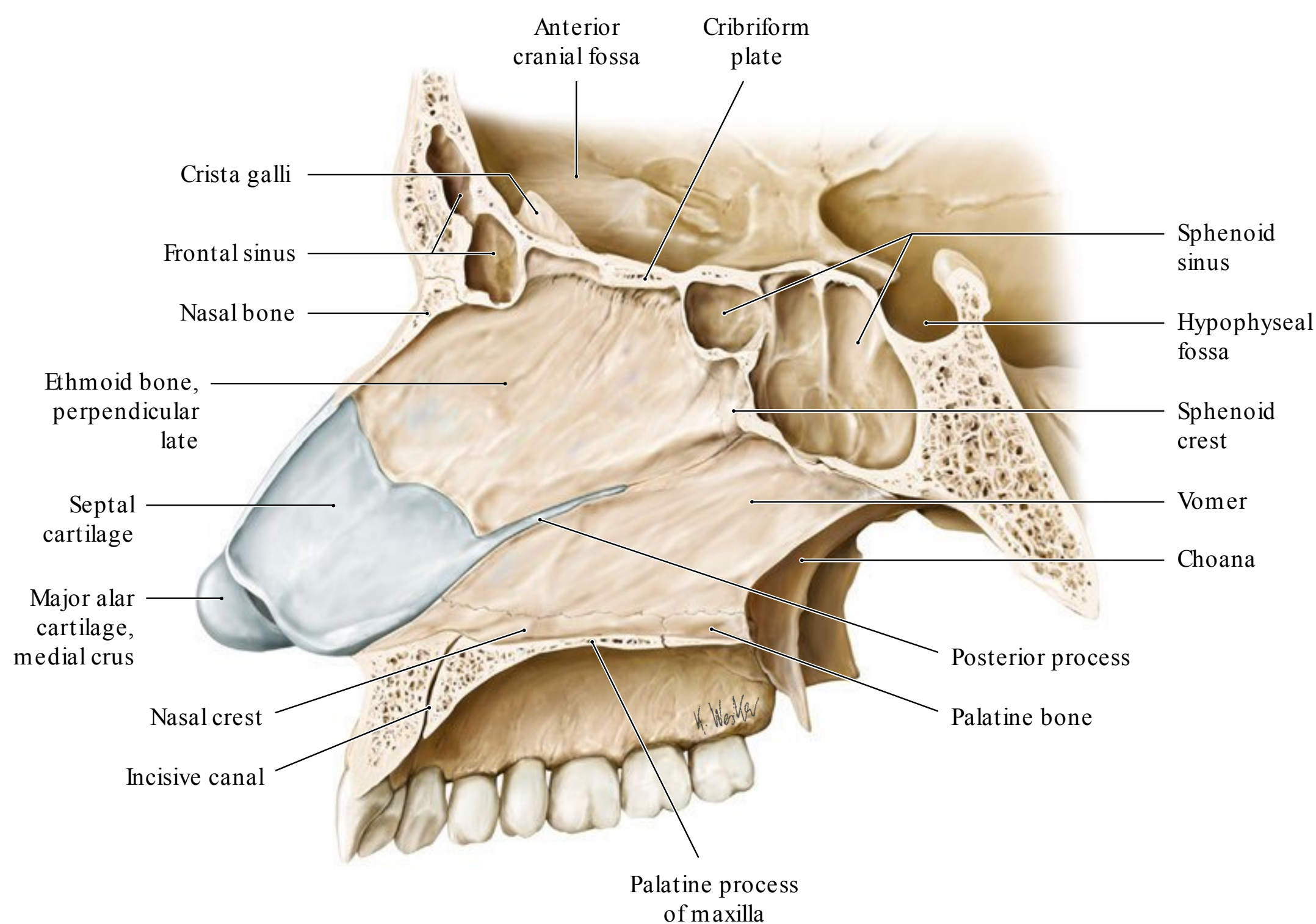


Fig. 1.7 Nasal septum. Parasagittal section viewed from the left side. The lateral wall of the left nasal cavity, including adjacent bones, has been removed. The contributions of the frontal, nasal, vomer, and

ethmoid bones to the bony nasal septum can be appreciated from this view. (Reproduced from THIEME Atlas of Anatomy, Head and Neuroanatomy. © Thieme 2010, Illustration by Karl Wesker).

jects caudally as a vertical crest. This crest forms part of the bony nasal septum and further articulates with the nasal spine of the frontal bone dorsally, the perpendicular plate of the ethmoid bone, and the nasal septal cartilage.⁴

Surgical Annotation

Nasoethmoidal orbital fractures involve injury to numerous osseous structures in the upper midface. The frontal process of the maxilla is isolated from the abutting osseous structures. This fracture pattern allows for displacement of the medial canthal tendon, leading to traumatic telecanthus. This type of injury is commonly seen after direct impact to the upper nasal area. The fracture can present a surgical challenge to obtain adequate exposure of the numerous anatomical structures within this area. An existing laceration can be used to obtain access; however, a coronal incision, lower eyelid incision, and gingival buccal incision are needed to allow for access.¹⁰ Re-establishment of the medial canthal tendon position is essential during this procedure and can be accomplished by direct plating or transnasal wiring, depending on the extent of comminution of the area.¹¹ Use of bone grafting is dependent on the need to re-establish the nasal height. Lacrimal system injury can occur given its close proximity and will require repair.

The notched inferior border is continuous with the upper lateral nasal cartilage at its cephalic margin. The lateral border articulates with the frontal process of the maxilla, forming the nasomaxillary suture lines.

The nasal part of the frontal bone lies between the supraorbital margins. A nasal notch inferiorly articulates with the nasal bones and laterally articulates with the frontal processes of the maxilla and the lacrimal bones.⁴ This notch supports the nasal bridge via an anteroinferior projection from its posterior surface. This projection runs behind the nasal bones and the frontal processes of the maxillae, ending in a sharp nasal spine.⁴ The nasal spine laterally forms part of the nasal cavity and makes a small contribution to the nasal septum via anterior articulations with the crest of the nasal bone and posterior articulations with the perpendicular plate of the ethmoid.⁴

The flat, median, and quadrilateral perpendicular plate of the ethmoid bone descends from the cribriform plate. This plate usually deviates slightly to form the upper part of the nasal septum. It articulates via its anterior border with the nasal spine of the frontal bone and the crests of the nasal bones.⁴ Posteriorly, the plate articulates with the crest of the sphenoid body superiorly and the vomer inferiorly. The broad inferior border attaches to the nasal septal cartilage. The superior surface contains grooves and canals for medial cribriform plate foramina; all other surfaces are smooth.⁴

Vomer

The thin, medially situated vomer bone forms the posterior, inferior part of the nasal septum. Both surfaces of the vomer contain a prominent groove for the nasopalatine nerve and vessels that runs obliquely anteriorly and inferiorly (**Fig. 1.8**).⁴

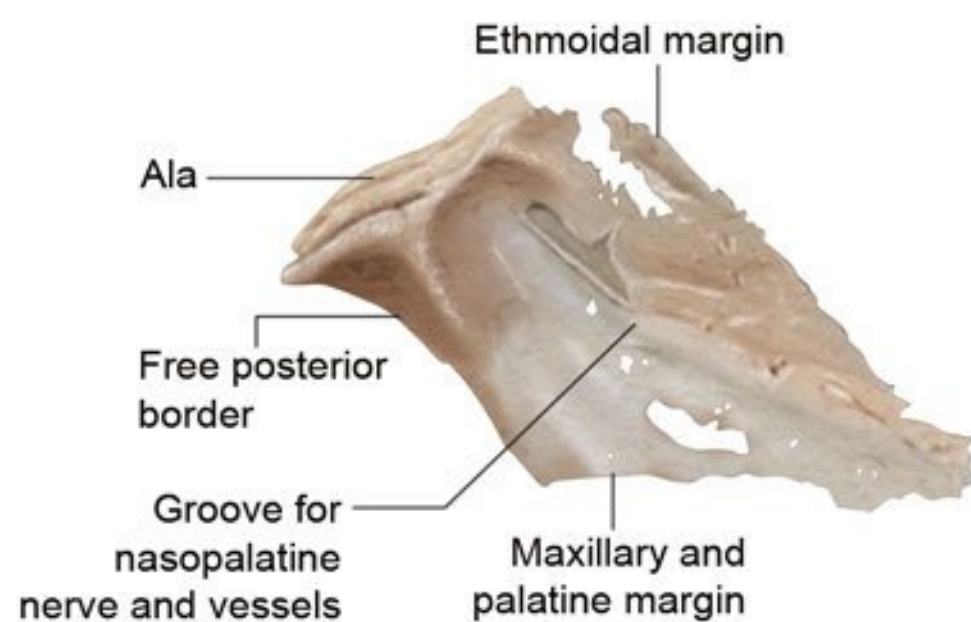


Fig. 1.8 Vomer: lateral border. The four articulating borders and the groove for the nasopalatine nerve and vessels are realized from this view.

The superior border is the thickest of the vomer's four borders. Presenting as a deep furrow, articulating with the rostrum of the body of the sphenoid, it is bound on either side by horizontally projecting alae.⁴ The alae articulate with the sphenoidal conchae and with both the sphenoidal processes of the palatine bones and the vaginal processes of the medial pterygoid plates of the sphenoid rostrally and caudally, respectively.⁴

The rostral and inferiorly sloping anterior border fuses with the perpendicular plate of the ethmoid in its upper half. The lower half is grooved to articulate with the inferior margin of the nasal septal cartilage. The anterior extremity descends between the incisive canals, articulating with the posterior margin of the maxillary incisor crest.⁴ Median nasal crests of the palatine and maxillae bones articulate with the inferior vomer border. The dorsally bifid, concave posterior border separates the nasal apertures and does not articulate with any other bones.³

Inferior Nasal Concha

Consisting of a lamina of cancellous bone, the curved inferior nasal concha forms part of the lateral wall of the nasal cavity. The perforated, convex medial surface includes longitudinal grooves for traversing vessels. The concave lateral surface forms part of the inferior meatus (**Fig. 1.9**).⁴ The superior border, divided into three regions, articulates with the conchal crests of the maxilla anteriorly and the palatine posteriorly.⁴

The middle of these three regions comprises three articulating processes. As discussed herein, the rostral lacrimal process helps form the nasolacrimal canal via articulations with the lacrimal bone and maxilla. The ascending ethmoidal process joins the uncinate process of the ethmoid. Intermediately, the ventral and laterally curving maxillary process articulates with the medial maxilla at the opening of the maxillary sinus.⁴ The anterior and posterior ends of the inferior nasal concha tapering and the inferior border are free, thick, and cellular.³

Maxilla

The maxilla jointly forms most of the upper jaw and face. Each bone forms the bulk of the floor and lateral wall of the nasal

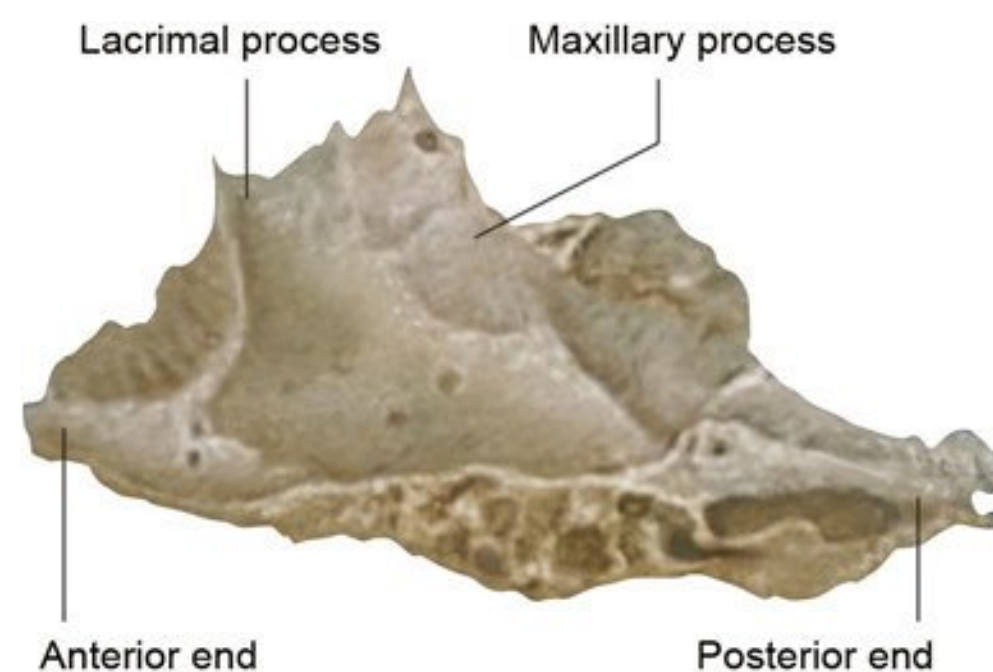


Fig. 1.9 Left inferior nasal concha: lateral view. Forming part of the inferior meatus, the superior border and its three processes and the free inferior border can be appreciated from this view.

cavity and the orbital floor. It also contributes to the infratemporal and pterygopalatine fossae. The maxilla comprises a body and frontal, zygomatic, palatine, and alveolar processes.³

Body

Anterior Surface

Enclosing the maxillary sinus, the pyramidal body of the maxilla has anterior, infratemporal (posterior), orbital, and nasal surfaces (**Fig. 1.10a**).⁴ The anterolaterally facing anterior surface contains inferior elevations and the alveolar processes dorsal to the roots of teeth. The canine eminence overlies the canine tooth socket and separates the shallow incisive fossa, posterior to the incisors, from the deeper, more lateral canine fossa. Dorsal to the canine fossa lies the infraorbital foramen, which transmits the infraorbital vessels and nerve.⁴ The anterior median intermaxillary suture is formed between the two maxillae, the inferior border of the nasal aperture, and the central incisor teeth.

Posterior Surface

The concave posterior (infratemporal) surface forms the anterior wall of the infratemporal and pterygopalatine fossae.⁴ Separating the posterior and anterior maxillary body surfaces are the ascending zygomaticoalveolar ridge (jugal crest) and the zygomatic process (**Fig. 1.10b**).⁴ Posteroinferiorly located is the maxillary tuberosity, which articulates with the pyramidal process of the palatine bone.⁴

Orbital Surface

The orbital surface forms most of the orbital floor. Along its medial border, the orbital surface articulates with the lacrimal bone, the orbital plate of the ethmoid, and the orbital processes of the palatine bone. It also forms the infraorbital groove, part of the infraorbital canal, and the anterior edge of the inferior orbital fissure.⁴

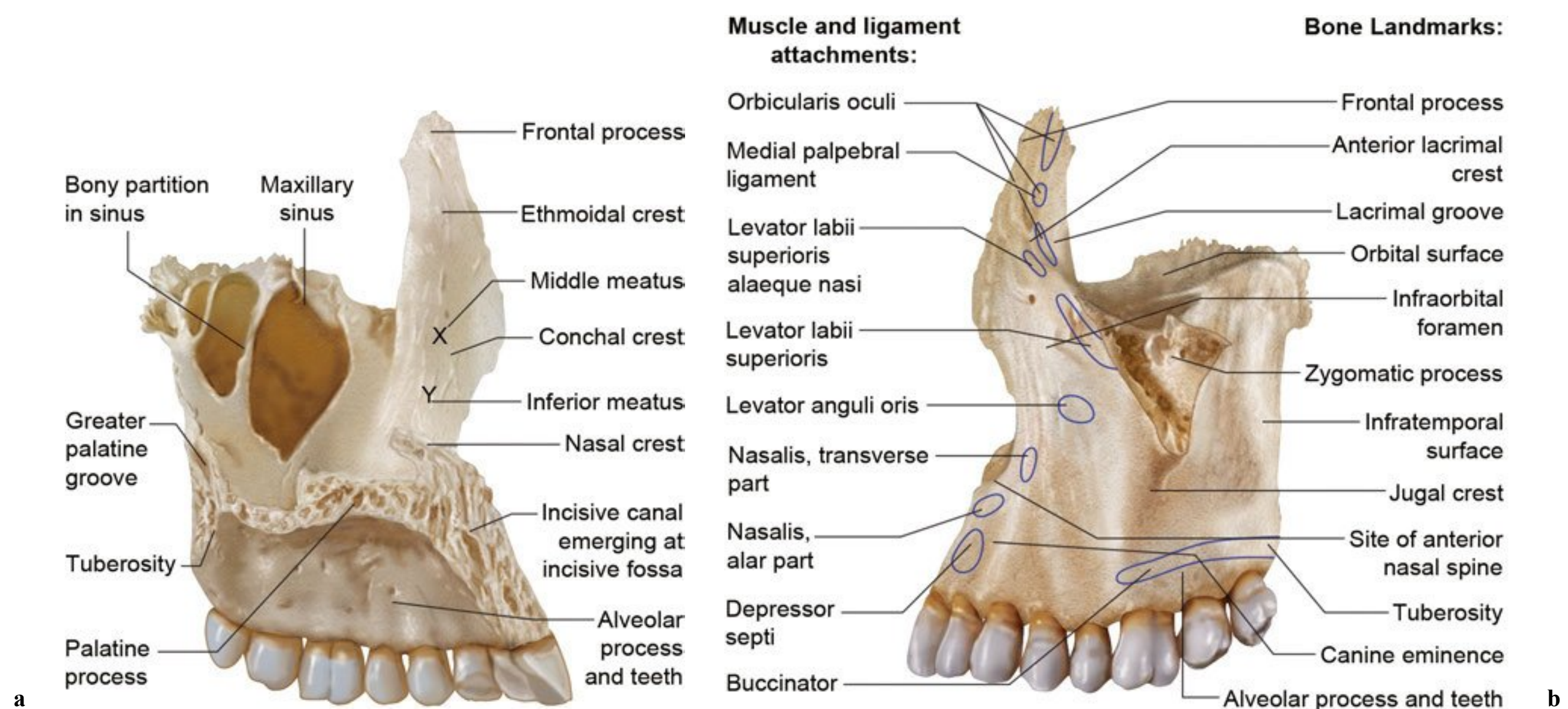


Fig. 1.10 (a) Medial view of the left maxilla. Much of the body; the palatine, frontal, and alveolar process; and the maxillary sinus can be realized from this view. Additionally, the emerging incisive canal, greater palatine groove, and the conchal and nasal crests can be

appreciated via this medial view. **(b)** Lateral view of the left maxilla. The remainder of the body and its associated jugal crest and orbital and infratemporal surfaces are viewed best laterally. Additionally, the lateral frontal zygomatic process can be appreciated via this lateral view.

Nasal Surface

The large maxillary hiatus, which leads to the maxillary sinus, defines the posterosuperior nasal surface. The aerated sinus is partially closed by ethmoid and lacrimal bone articulations. Inferior to the sinus is part of the inferior meatus and posteriorly a roughened surface for articulation with the perpendicular plate of the palatine bone.⁴ Anterior to the hiatus is the nasolacrimal groove, comprising about two-thirds of the circumference of the nasolacrimal canal; the remainder is contributed by the descending part of the lacrimal bone and the lacrimal process of the inferior nasal concha.⁴ This canal leads the nasolacrimal duct to the inferior meatus. Anteriorly, the oblique conchal crest articulates with the inferior nasal concha, separating the inferior meatus from the more superior atrium of the middle meatus.⁴

Zygomatic Process

The anterior, infratemporal and orbital surfaces converge at the laterally projecting zygomatic process. This serrated process articulates with the maxillary process of the zygomatic bone. The thick, arched, and inferiorly projecting alveolar process supports the maxillary teeth. These socketed processes vary in depth, width, and septation according to the tooth type.⁴

Frontal Process

The posterosuperiorly projecting frontal process articulates superiorly with the nasal part of the frontal bone, anteriorly with the nasal bone, and posteriorly with the lacrimal bone.⁴ The vertical lacrimal crest divides the frontal process; posterior to this crest, vertical grooves of the frontal process and the lacri-

mal bone combine to complete the lacrimal fossa.⁴ The medial surface of the frontal process forms part of the lateral nasal wall. Subapical articulations with the ethmoid close the anterior ethmoidal air cells, and an oblique ethmoidal crest, which forms the superior border of the middle meatus, posteriorly articulates with the middle nasal concha.⁴

Palatine Process

Projecting from the most inferior part of the medial maxilla is the thick, horizontal palatine process. Together, the articulated contralateral palatine processes form most of the nasal floor and three-quarters of the osseous (hard) palate.⁴ The horizontal plate of the palatine bone forms the remainder, subsequently forming the transverse palatamaxillary suture. Posterolaterally, two grooves in the palatine process transmit the greater palatine vessels and nerves. These two lateral incisive canals, each ascending into its half of the nasal cavity, open into the infundibular incisive fossa and transmit the terminations of the greater palatine artery and nasopalatine nerve.⁴

Occasionally, the median anterior and posterior incisive foramina are present.⁴ The median intermaxillary palatal suture runs posterior to the infundibular incisive fossa.

The thicker anteromedial border articulates with the contralateral palatine process, forming a raised nasal crest that creates a groove for the vomer. Anteriorly, this ridge rises as an incisor crest, which articulates contralaterally with the paired process, forming the anterior nasal spine.⁴

Maxillary Sinus

The pyramidal maxillary sinus, located in the body of the maxilla, is the largest of the paranasal sinuses (**Fig. 1.11**). The medial

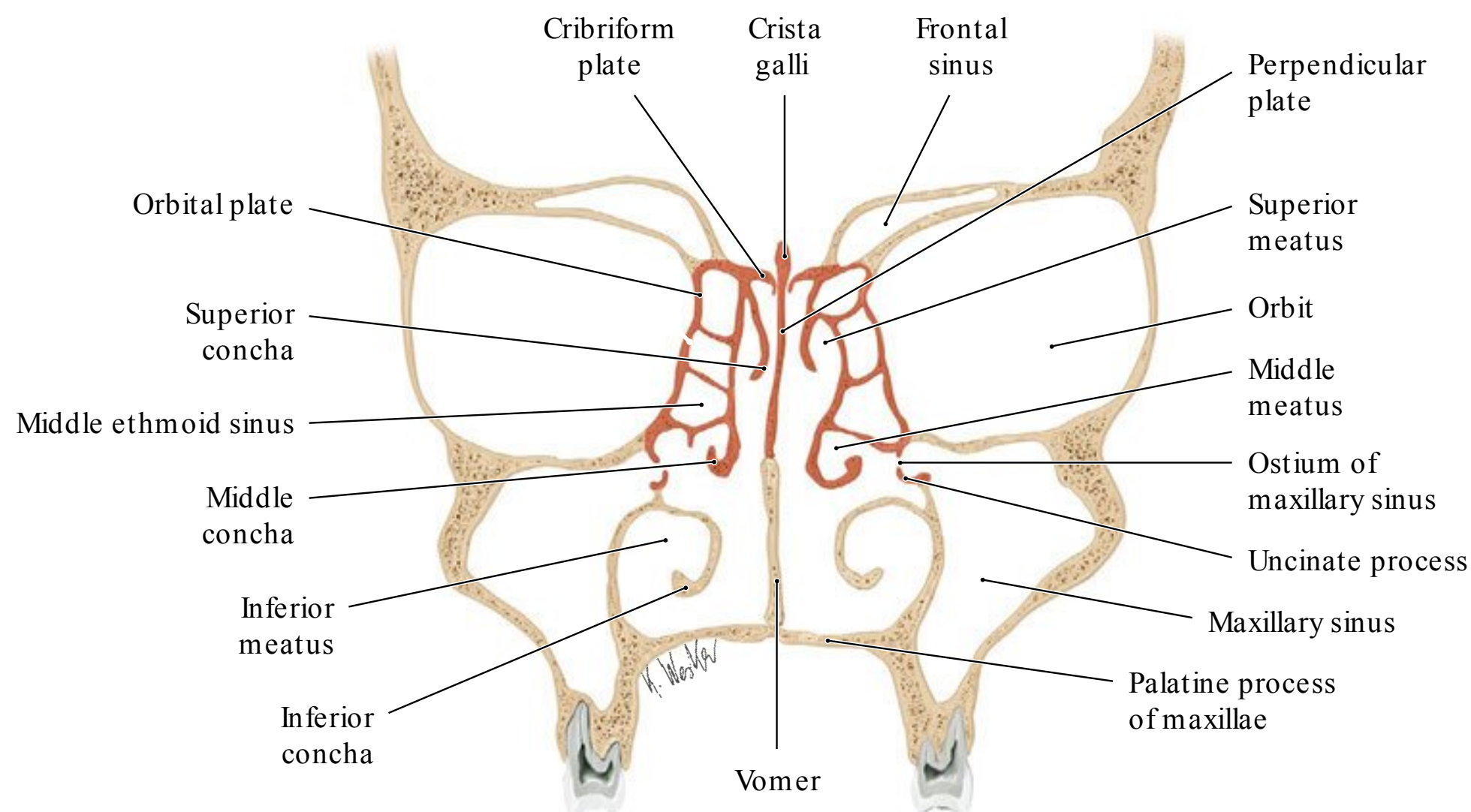


Fig. 1.11 Bony structure of the paranasal sinuses: anterior view. This coronal section elucidates the relationship of the paranasal sinuses with their associated structures to the viscerocranium. (Reproduced from

THIEME Atlas of Anatomy, Head and Neuroanatomy. © Thieme 2010, Illustration by Karl Wesker.)

wall forms part of the lateral wall of the nose, and the roof forms the largest portion of the orbital floor. The maxilla forms the floor, anterior wall, and posterior wall of the sinus via its alveolar process and part of the palatine process, the facial surface, and infratemporal surface respectively. The apex of the sinus extends into the zygomatic process of the maxilla.⁴

High on the posterior medial wall of the maxillary sinus is the ostium of the sinus. Portions of the perpendicular plate of the palatine bone, the uncinate process of the ethmoid bone, the inferior nasal concha, the lacrimal bone, and overlying nasal mucosa limit the size of the ostium.⁴ The ostium usually opens into the posterior part of the ethmoidal infundibulum, which communicates with the middle meatus, although an accessory ostium is sometimes present posterior to the major ostium.⁴

Palatine Bone

The paired palatine bones each comprise a horizontal and perpendicular plate, arranged as L-shaped pyramidal, orbital, and sphenoidal processes (Fig. 1.12).³ The palatine bones contribute to the floors of the palate, orbit, and nasal cavity; to the lateral wall of the nasal cavity; to the pterygopalatine and pterygoid fossae; and to the inferior orbital fissures. These bones are placed in the posterior nasal cavity between the maxillae and pterygoid processes of the sphenoid bone.³

Horizontal Plate

The quadrilateral horizontal plate has nasal and palatine surfaces and anterior, posterior, lateral, and medial borders. The nasal surface transversely forms the posterior nasal floor. The palatine surface forms the posterior quarter of the bony palate via midline articulations with its pair at the medial border and with the palatine process of the maxilla at its anterior border.⁴ The midline articulating horizontal plates form the posterior part of the nasal crest, which articulates with the posteroinf-

rior edge of the vomer. The posterior border projects posteriorly as the posterior nasal spine. The lateral border, continuous with the perpendicular plate of the palatine bone, contains the greater palatine foramen.³

Perpendicular Plate

The perpendicular plate has nasal and maxillary surfaces and anterior, posterior, superior, and inferior borders.⁴ The nasal surface of the perpendicular plate inferiorly contributes to the inferior meatus. Superiorly, a horizontal conchal crest articulates with the inferior concha. Moving superiorly are a depres-

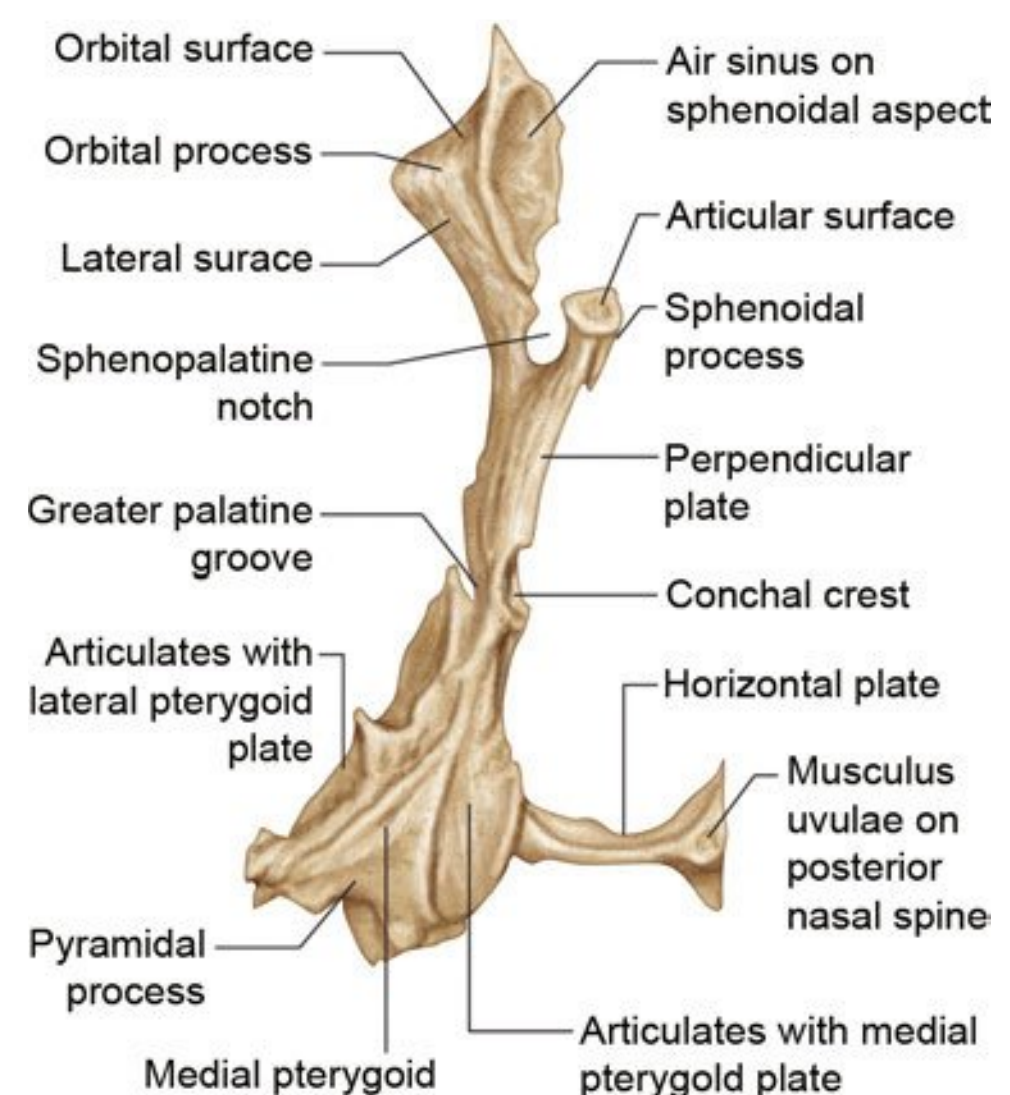


Fig. 1.12 Posterior view of the left palatine bone. The palatine bone, which comprises the horizontal and perpendicular plates, pyramidal, orbital, and sphenoidal processes and some of their articulating surfaces, can be understood from this posterior view.

sion that forms part of the middle meatus, an ethmoidal crest for the middle nasal concha, and a horizontal groove that forms part of the superior meatus.⁴

The maxillary surface articulates with the nasal surface of the maxilla. Posterosuperiorly, it forms a medial wall to the pterygopalatine fossa and anteriorly forms part of the medial wall of the maxillary sinus. The palatine groove (i.e., canal on maxillary articulation) descends posteriorly on the maxillary surface and transmits the greater palatine vessel and nerve.⁴

The anterior border articulates with the maxillary process of the inferior concha, appearing in the medial wall of the maxillary sinus. The posterior border articulates with the medial pterygoid plate. The sphenopalatine foramen is formed by the sphenopalatine notch on the superior border articulating with the body of the sphenoid. This foramen provides connections from the pterygopalatine fossa to the posterior part of the superior meatus.⁴

Pyramidal Process

The pyramidal process extends posterolaterally from the horizontal and perpendicular palatine plate junction to an angle between the pterygoid plates of the sphenoid bone.³ The posterior surface completes the lower part of the pterygoid fossa, and the anterior lateral surface articulates with the maxillary tuberosity.⁴ The inferior surface contains the lesser palatine foramina.³

Orbital Process

The orbital process, extending superolaterally from the anterior perpendicular plate, has three articulating and two non-articulating surfaces. The anterior (maxillary) surface articulates

anterolaterally with the maxilla. The posterior (sphenoidal) surface bears the opening of an air sinus that usually communicates with the sphenoid sinus, which is closed by the sphenoidal concha.⁴ The medial (ethmoidal) surface articulates with the labyrinth of the ethmoid bone, on which the sinus of the orbital process can form, thus communicating with the posterior ethmoidal air cells. Rarely, the sinus of the orbital process can open on both the ethmoidal and sphenoidal surfaces. Separating the nonarticulating superior (orbital) and lateral surfaces is a rounded border that forms a medial part of the lower margin of the inferior orbital fissure.⁴

Sphenoidal Process

The superior surface of the superomedially projecting sphenoidal process articulates with the sphenoidal concha and contributes to the palatovaginal canal formation. The superior and lateral surfaces and the posterior border of the sphenoidal process articulate with the root of, the medial surface of, and the vaginal process of the medial pterygoid plate, respectively.⁴ The medial border of the sphenoidal process articulates with the ala of the vomer, and the inferomedial surface forms part of the roof and lateral wall of the nose.⁴

Zygomatic Bone

The quadrangular zygomatic (zygoma) bones form the prominences of the cheeks and rests on the maxillae. The zygoma forms the anterolateral rims, walls, floor, much of the infraorbital margins of the orbits, and the walls of the temporal and infratemporal fossae.³ It includes lateral, temporal, and orbital surfaces; two processes, the frontal and temporal; three foramina; and five borders (**Fig. 1.13**).⁴

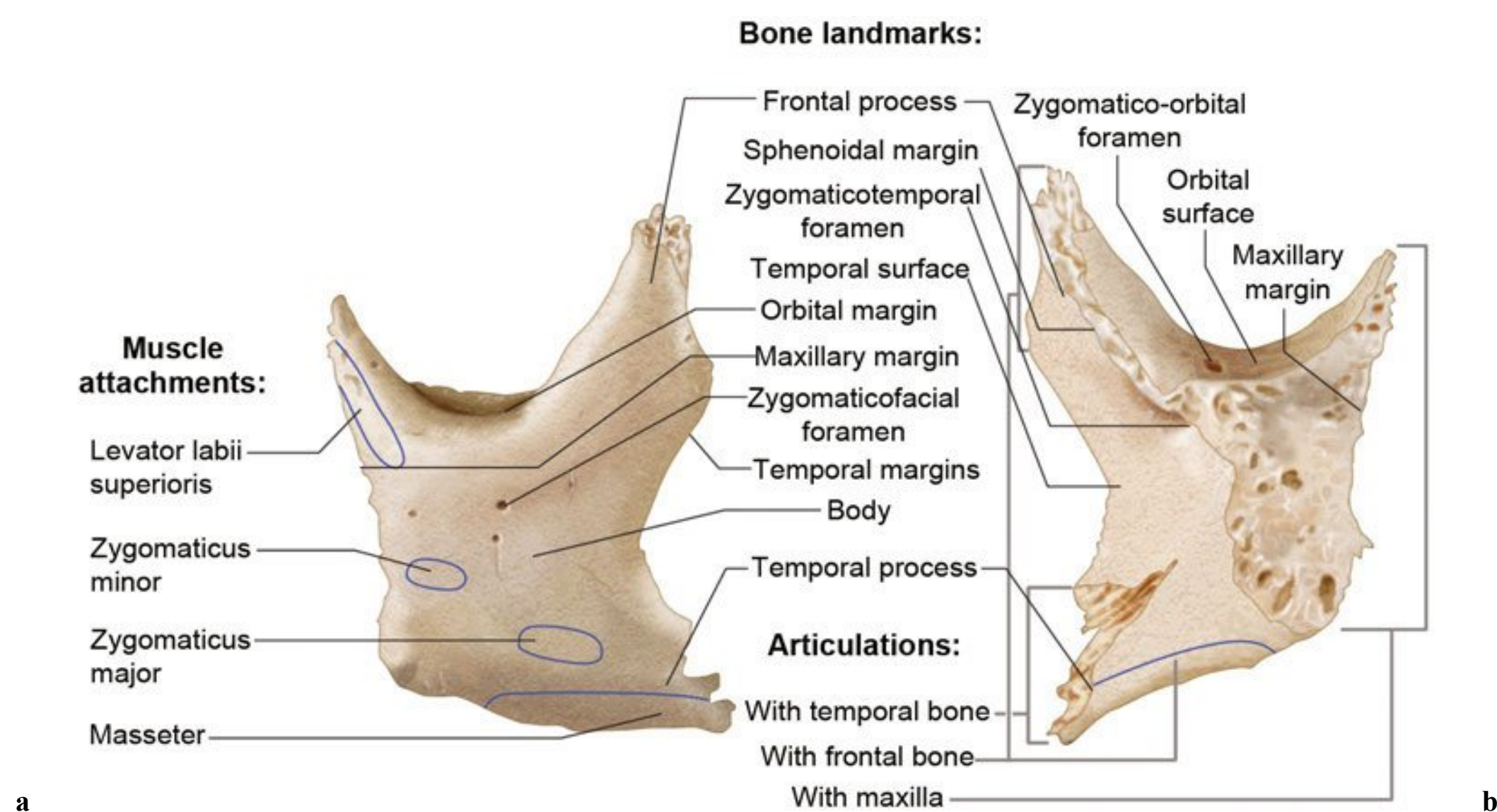


Fig. 1.13 (a) External view of the left zygomatic bone. The facial surface of the zygomatic body displays the zygomaticofacial foramen near the orbital surface. The frontal and temporal processes, as well as the orbital, temporal, and maxillary margins, are visible from this anterior view. (b) Internal view of left zygomatic bone. The internal

view provides a better appreciation for the serrated maxillary and sphenoidal margins and those surfaces that articulate with the frontal bone, temporal bone, and maxilla. The zygomatico-orbital foramen on the orbital surface is also viewed from this angle.

Surfaces

The convex lateral (facial) surface contains the centrally located zygomaticofacial foramen, allowing passage of the zygomaticofacial nerve and vessels. This foramen is often double and occasionally absent. The zygomaticus minor and major originate inferior to the foramen anteriorly and posteriorly, respectively.⁴

The posteromedial (temporal) surface articulates medially with the zygomatic process of the maxilla. This smooth, concave surface transmits the zygomaticotemporal nerve via the zygomaticotemporal foramen near the base of the frontal process.⁴

The orbital surface extends up on the medial aspect of the frontal process and forms the anterolateral part of the orbital floor and adjoining lateral wall. This smooth, concave surface usually contains the zygomatico-orbital foramina representing canal openings leading to the zygomaticofacial and zygomaticotemporal foramina.⁴

Borders

The anteroinferior (maxillary) border articulates with the maxilla. Its medial end tapers to a point that provides partial attachment for the levator labii superioris muscle. The sinuous posterosuperior (temporal) border is continuous with the posterior border of the frontal process and, thus, the upper border of the zygomatic arch.⁴ The temporal fascia attaches to this border. The serrated posteromedial border articulates superiorly with the greater wing of the sphenoid and inferiorly with the orbital surface of the maxilla. This surface usually forms the lateral edge of the inferior orbital fissure by the presence of a non-articulating concave indent.⁴ A posteroinferior border, roughened for masseter attachment and the anterosuperior (orbital) border, forms the inferolateral circumference of the orbital opening.⁴

Processes

The thick, serrated frontal process articulates with the zygomatic process of the frontal bone superiorly and with the greater wing of the sphenoid bone posteriorly.⁴ Varying in size and form, Whitnall's tubercle is usually present on the orbital aspect, 1 cm below the frontozygomatic suture.⁴ The zygomatic arch is formed by articulations between the long, narrow, and

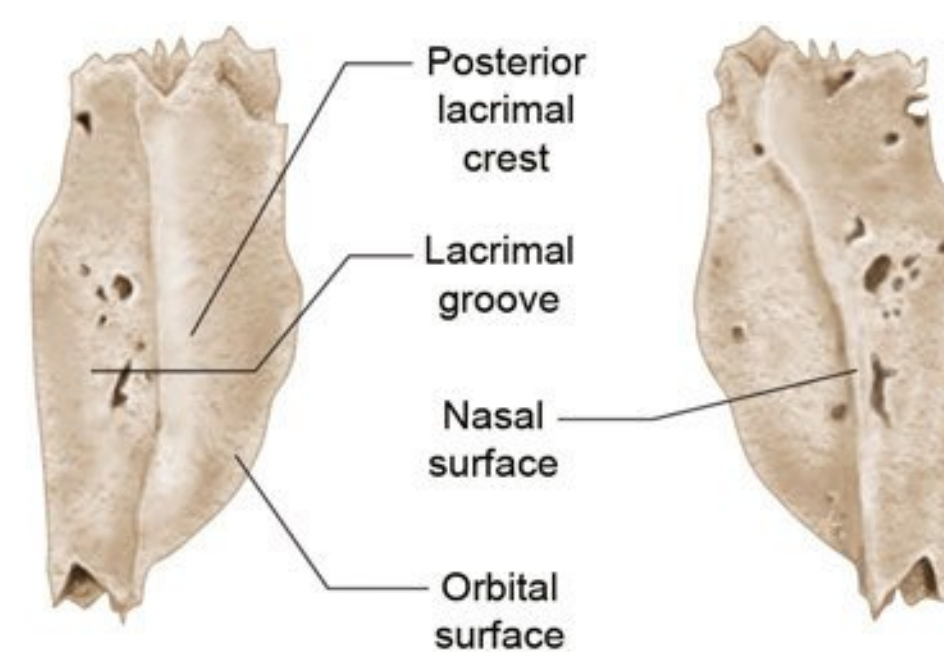


Fig. 1.14 External view of the right lacrimal bone. This view elucidates the orbital surface of the lacrimal bone with its associated lacrimal groove, which lies anterior to the posterior lacrimal crest.

serrated temporal process of the zygoma and the zygomatic process of the temporal bone.³

Lacrimal Bone

The paired small, thin, fragile lacrimal bones contribute to the anterior medial wall of the orbit.³ A vertical posterior lacrimal crest divides the lateral (orbital) surface of the lacrimal bone (**Fig. 1.14**). Rostral to this crest, the rostral edge of a vertical groove meets the posterior border of the frontal process of the maxilla, completing the fossa for the lacrimal sac. The medial wall of this groove joins the nasolacrimal groove of the nasal maxilla and the lacrimal process of the inferior nasal concha, contributing to the formation of the nasolacrimal canal. The upper opening of the nasolacrimal canal is completed by the maxilla and the lacrimal hamulus, caudal and ventral to the posterior lacrimal crest.⁴

The medial (nasal) surface forms part of the middle meatus via its anteroinferior region. The posterosuperior part of the medial surface meets the ethmoid, completing some anterior ethmoidal air cells. The lacrimal bones contain anterior, posterior, superior, and inferior borders. They articulate with the frontal process of the maxilla, the orbital plate of the ethmoid, the frontal bone, and the orbital surface of the maxilla, respectively.⁴

References

1. Moore KL, Dalley AF, Agur AMR. Clinically Oriented Anatomy. 6th ed. Baltimore, MD, and Philadelphia, PA: Lippincott Williams & Wilkins; 2010
2. Sadler TW. Langman's Medical Embryology. 12th ed. New York, NY: Lippincott Williams & Wilkins; 2012
3. Norton NS. Netter's Head and Neck Anatomy for Dentistry. 1st ed. Philadelphia, PA: Elsevier Saunders; 2006
4. Standring S, Gray HFRS. Gray's Anatomy: The Anatomical Basis of Clinical Practice. 39th ed. Philadelphia, PA: Elsevier Churchill Livingstone; 2005
5. Fallucco M, Janis JE, Hagan RR. The anatomical morphology of the supraorbital notch: clinical relevance to the surgical treatment of migraine headaches. *Plast Reconstr Surg* 2012;130(6):1227–1233 [PubMed](#)
6. Chepla KJ, Oh E, Guyuron B. Clinical outcomes following supra-orbital foraminotomy for treatment of frontal migraine headache. *Plast Reconstr Surg* 2012;129(4):656e–662e [PubMed](#)
7. Kung TA, Guyuron B, Cederna PS. Migraine surgery: a plastic surgery solution for refractory migraine headache. *Plast Reconstr Surg* 2011;127(1):181–189 [PubMed](#)
8. Tiwari P, Higuera S, Thornton J, Hollier LH. The management of frontal sinus fractures. *J Oral Maxillofac Surg* 2005;63(9):1354–1360 [PubMed](#)
9. Bell RB, Dierks EJ, Brar P, Potter JK, Potter BE. A protocol for the management of frontal sinus fractures emphasizing sinus preservation. *J Oral Maxillofac Surg* 2007;65(5):825–839 [PubMed](#)
10. Pawar SS, Rhee JS. Frontal sinus and naso-orbital-ethmoid fractures. *JAMA Facial Plast Surg* 2014;16(4):284–289 [PubMed](#)
11. Kochhar A, Byrne PJ. Surgical management of complex midfacial fractures. *Otolaryngol Clin North Am* 2013;46(5):759–778 [PubMed](#)

Introduction

The skull base is traditionally divided into anterior, central, and posterior zones based principally on the appearance of the skull base as viewed from above (**Fig. 2.1**). This approach supports the general delineation of the intracranial compartment into the anterior, middle, and posterior fossae. The anterior skull base forms the broad floor of the anterior cranial fossa, which is filled predominantly with the frontal lobes of the brain. The anterior skull base is traditionally defined as the region of the skull base lying anterior to the lesser wing of sphenoid and planum sphenoidale (**Fig. 2.2**). The lesser wing of the sphenoid spans anterolaterally from the anterior clinoid process. The posterior and superior margins of the lesser wing form a curvilinear ridge that takes on the shape of a wing—hence its name. The lesser wing of the sphenoid bone fuses anteriorly with the posterior margin of the orbital plate of the frontal bone. The planum sphenoidale is the superomedial plate of sphenoid bone seen posterior to the cribriform plate of ethmoid and anterior to the anterior wall of sella turcica (tuberculum sellae). Medially, the anterior skull base forms the roof of the nasal cavity and ethmoid sinus, including the cribriform plate of the ethmoid. Laterally, the orbital plates of the frontal bones form the orbital roof portion of the anterior skull base on either side. Posteriorly, the midline or parasagittal anterior skull base is constituted by the planum sphenoidale and laterally by the lesser wing of the sphenoid bone.¹ The middle or central skull base is separated from the anterior skull base by a horizontal line along the anterior sellar margin extending laterally along the posterior margin of lesser wing of the sphenoid bone bilaterally, which includes the medial anterior clinoid processes.²

Midline or Parasagittal Anterior Skull Base Forming the Roof of the Nasal Cavity and Ethmoid Sinuses

The anterior skull base, especially in the region of the nasal vault and ethmoid roof, is only minimally ossified at birth and ossifies gradually from cartilage. The roof of the nasal cavity begins to ossify by around the age of 3 months and is predominantly ossified at 6 months. The crista galli, a midline triangle-shaped, superiorly projecting bony process of the ethmoid bone, begins to ossify from the tip at 3 months and is usually ossified by the first year. The name is derived from the Latin and means crest of the cock (rooster's comb). The crista galli provides attachment to the anteroinferior part of the falx cerebri

and should not be confused with the frontal crest, a more anterior midline bony ridge-like portion of the frontal bones, which also provides attachment to the falx cerebri (**Fig. 2.3**). The crista galli is pneumatized in 10 to 15% of patients as identified on computed tomography (CT) scans. Although the crista galli is technically part of the ethmoid bone, pneumatization generally occurs as an extension of the left or right frontal sinus.³ The perpendicular plate of the ethmoid, which forms the superior portion of the bony nasal septum and is seen directly below the crista galli, begins to ossify at 6 months and fuses with the vomer, which forms the inferior portion of the bony nasal septum by around 2 years of age.¹

The cribriform plate (lamina cribrosa) of the ethmoid in the adult is a horizontal perforated bony plate at the medial aspect of ethmoid bone, with deep grooves lying on either side of the midline crista galli. It forms part of the roof of the nasal cavity and constitutes the floor of the olfactory fossa lodging the olfactory bulbs (**Fig. 2.4**). The olfactory fossa is the lowest point in the anterior skull base. The perforations and foramina in the middle of the grooves are small and transmit the afferent olfactory nerve fibers from the nasal vault mucosa to the olfactory bulbs intracranially. The larger foramina at the medial aspect of the grooves transmit nerves to the superior nasal septum and those at the lateral aspect to the superior turbinate region. More than two-thirds of the population will have ossified posterior cribriform plates by 1 year of age, and most of the anterior skull base, including the cribriform plates, are ossified after 2 years; however, small gaps can be seen in the nasal roof until early in year 3 of life.

The ethmoid roof is formed by the vertically oriented lateral lamella of the cribriform plate of the ethmoid bone medially and the more horizontal fovea ethmoidalis of the orbital plate of frontal bone superolaterally. The vertical lateral lamella lies just lateral to the horizontal cribriform plate proper. The lateral lamella is 10 times thinner than the fovea ethmoidalis.⁴ The skull-base attachment of the middle turbinate of the nasal cavity to the anterior cribriform plate is quite delicate, and its detachment at surgery can damage the dura mater with resultant cerebrospinal fluid leak.

Ethmoid air cells lie inferior to the plane of cribriform plate until 3 months of age. By 6 months, they extend above the horizontal cribriform plate plane, and the more superolateral fovea ethmoidalis portion of ethmoid sinus roof begins to develop from the orbital plate of the frontal bone by 18 months and matures by 2 years of age. Knowledge of this lateral-to-medial slope of the anterior skull base is extremely important during transethmoidal surgical approaches to anterior skull-base lesions. Using the same axial plane of surgical dissection, which is safe along the more lateral ethmoid roof, could injure the brain and dura mater if extended medially to the region of cribriform plate.⁵

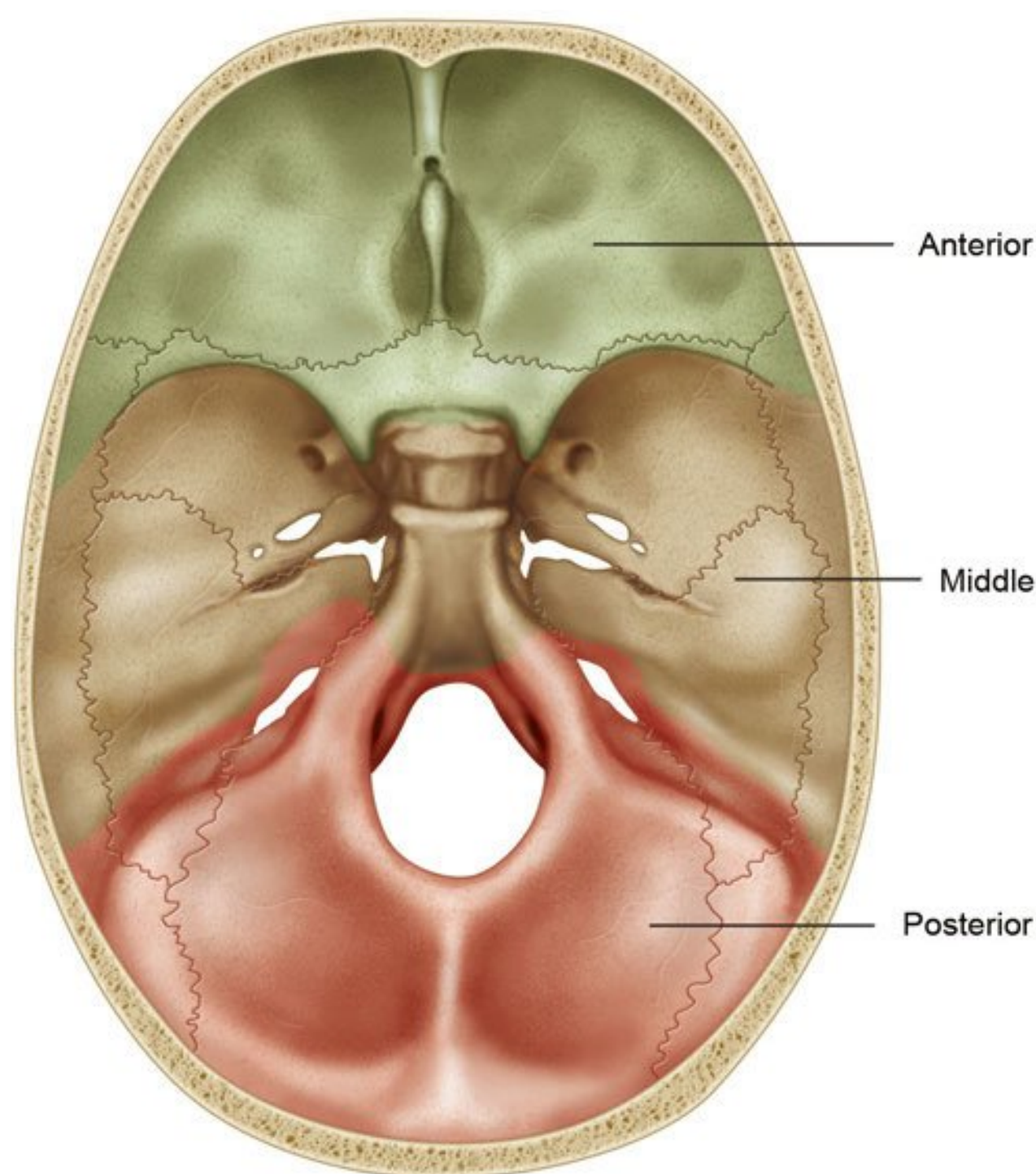


Fig. 2.1 View of the skull base from above. Traditionally, the skull base is divided into anterior, middle, and posterior components.

A horizontal line drawn along the roof of the ethmoid sinus passes through the orbit superior to the orbital vertical midpoint in most cases (88%), with 10% crossing at the midpoint and only 2% below that plane.⁶ Preoperative imaging should be critically reviewed to assess for a low-lying skull base. The safest anatomy is when the horizontal line drawn from the roof of the ethmoid crosses the upper third of the orbit; precautions to avoid injury to the skull base should be taken when the horizontal plane of the ethmoid roof crosses below the vertical midpoint of the orbit.¹

The skull base also slopes downward in an anterior to posterior direction in the sagittal plane from the frontal recess to the planum sphenoidale along the ethmoid roof. The degree of slope is highly variable and should be assessed by preoperative imaging. During endoscopic sinus surgery, the skull base could be injured while using a front-to-back technique. Skull-base injury can be avoided by early identification using the back-to-front technique of endoscopic surgery whereby the skull base is easily located at the roof of sphenoid sinus after identifying the superior meatus and sphenoid ostium.^{7–11}

The Keros classification of the ethmoid roof and olfactory fossa into three types takes into account the vertical height of the lateral lamella of the ethmoid and the resultant depth of the olfactory fossa (**Fig. 2.5**). An olfactory fossa that is only 1 to 3 mm deep because of a nearly nonexistent lateral lamella constitutes a Keros type 1 (12%). The olfactory fossa is 4 to 7 mm deep in Keros type 2 (70%) and 8 to 16 mm deep in type 3 (18%) with progressively increasing vertical height of the lateral lamella.¹² Asymmetry of more than 2 mm is seen in 8% of cases.¹³ During endoscopic surgery, Keros type 3 has the largest risk for iatro-

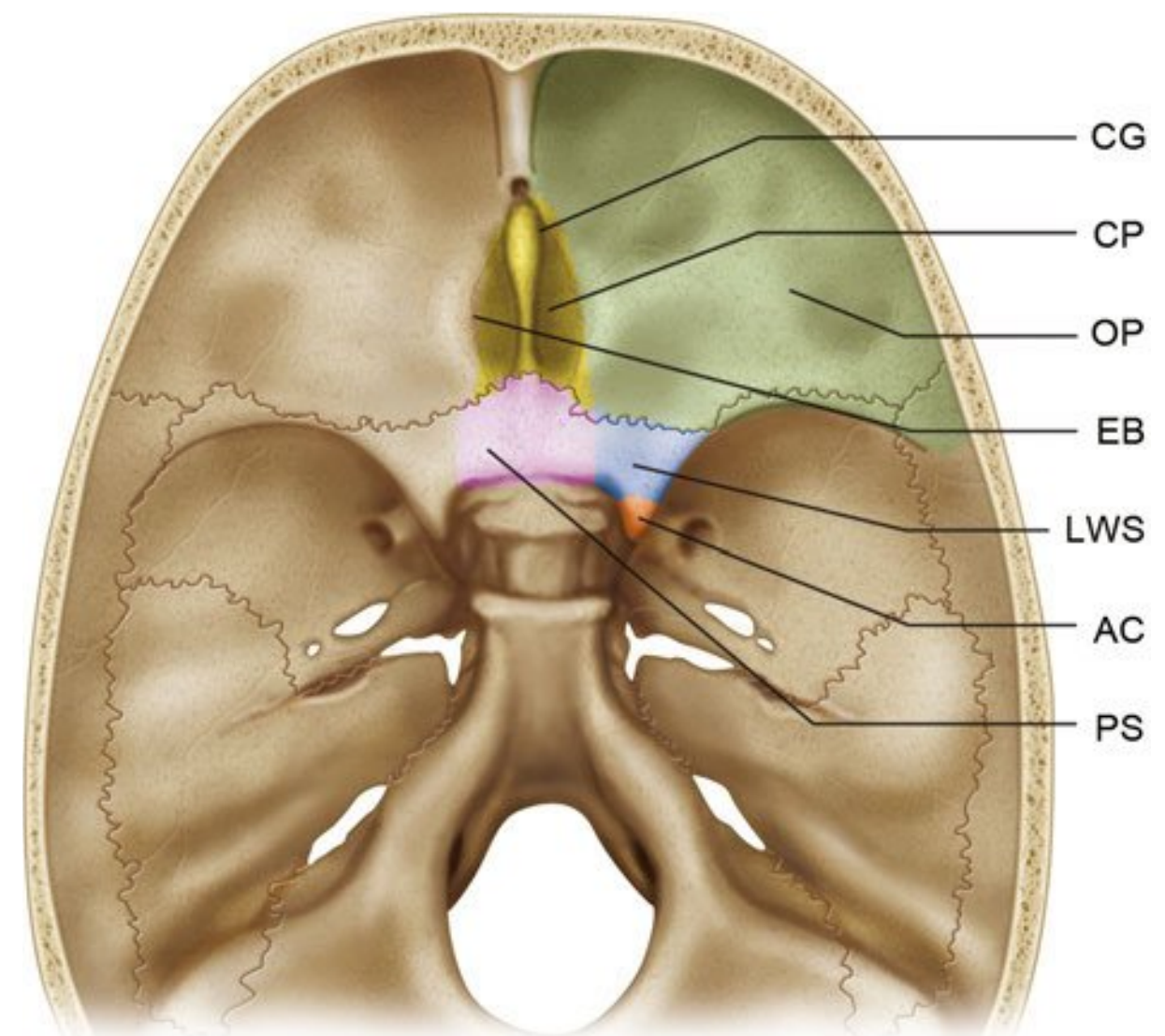


Fig. 2.2 Magnified view of the anterior skull base. The anterior clinoid process (AC) merges anteriorly with the lesser wing of the sphenoid bone (LWS). Medially, the lesser wing of the sphenoid merges with a flat portion of the sphenoid bone that serves as the ventral roof to the sphenoid sinus, the planum sphenoidale (PS). The lesser wing of the sphenoid is joined anteriorly with the orbital plate (OP) of the frontal bone. The orbital plate of the sphenoid bone serves as the roof of the orbit. The ethmoid bone (EB) is in the center of the anterior skull base and contains the cribriform plate (CP) and the crista galli (CG).

genic injury to the lateral lamella. Also, the anterior ethmoidal artery could be iatrogenically injured in the anterior ethmoidal foramen (along with the anterior ethmoidal vein and nerve) (**Fig. 2.6**) lying between the ethmoid and frontal bones just anterolateral to the cribriform plate and cause catastrophic bleeding into the orbit. The posterior ethmoidal foramen containing the posterior ethmoidal artery, vein, and nerve lies between the ethmoid and sphenoid bones, just posterolateral to the cribriform plate of the ethmoid.

More Anterior Portions of Midline/Parasagittal Anterior Skull Base

The foramen cecum is a small midline pit lying between the frontal and ethmoid bones, just anterior to the crista galli of the ethmoid (**Fig. 2.7**). It is close to 4 mm in diameter at birth, and the ossification is usually complete by 2 years but can sometimes be delayed until the age of 5 years.¹⁴ Ossification defects in the region of the foramen cecum, nose, and forehead can lead to the formation of three subtypes of frontoethmoidal (sincipital) cephaloceles: frontonasal (40–60%), nasoethmoidal (30%), and naso-orbital (10%) cephaloceles. Associated ocular or intracranial abnormalities are present in 80% of cases with frontoethmoidal cephaloceles.¹⁵

During early intrauterine life, a small anterior skull base fontanel at the anterior boundary of the anterior skull base, called

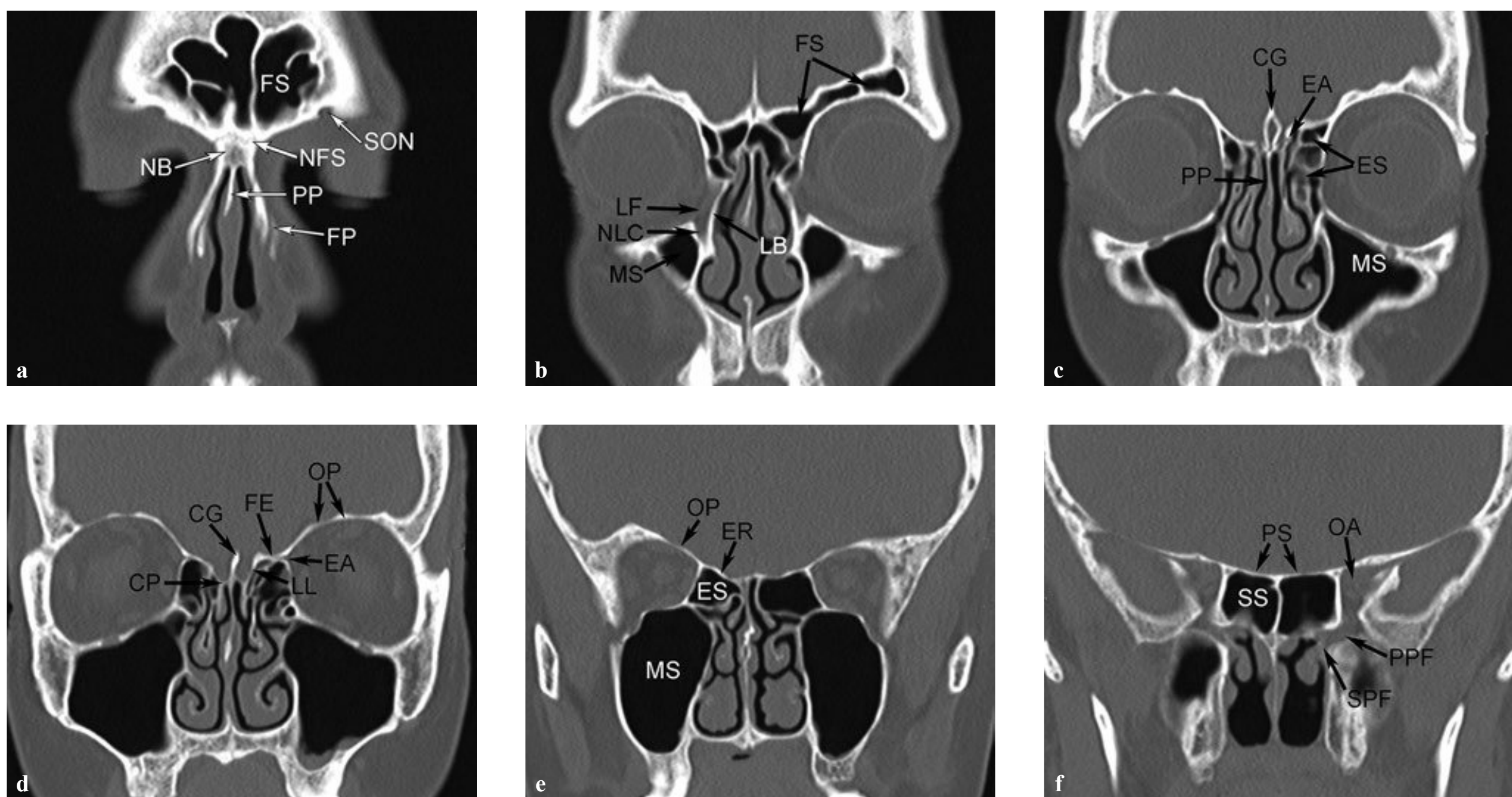


Fig. 2.3 Serial high-resolution computerized tomography (CT) coronal images through the anterior skull base, anterior to posterior. **(a)** Pneumatized frontal sinus (FS) air cells are seen bilaterally. The supraorbital notch (SON) marks the exit of the supraorbital nerve and associated vessels from the orbit to the forehead. The paired nasal bones (NBs) merge anteriorly at the nasal bridge and fuse superiorly at the nasofrontal suture (NFS). The perpendicular plate (PP) of the ethmoid bone forms the bony nasal septum superiorly. The inferior and lateral bony support of the nose is provided by the frontal process (FP) of the maxilla. **(b)** Frontal sinus (FS) air cells extend posteriorly above the orbital roof. There is a depression, the lacrimal fossa (LF), in the inferior and medial orbit that houses the lacrimal sac. The medial wall of the lacrimal fossa is formed by the lacrimal bone (LB). The lacrimal fossa is contiguous with the bony nasolacrimal canal (NLC). **(c)** More posteriorly, the crista galli (CG) is seen as a thin bony protrusion in the sagittal plane. The perpendicular plate (PP) of the ethmoid bone forms the bony nasal septum superiorly. The ethmoid sinus (ES) and maxillary sinus (MS) are seen at this level. A small foramen can be seen at this

level as the anterior ethmoid artery (EA) pierces the lateral lamella of the cribriform plate. **(d)** At this level, the anatomy of the cribriform plate and ethmoid roof are well demonstrated. The crista galli (CG) again seen as midline sagittal bone projecting above the cribriform plate (CP). The lateral margin of the cribriform plate is formed by a vertical portion of bone called the lateral lamella (LL) of the cribriform plate. The lateral roof of the ethmoid sinus is formed by a horizontal projection of bone that arises from the medial orbit, called the fovea ethmoidalis (FE). At this level, the proximal anterior ethmoid artery (EA) can be seen leaving the orbit as it extends anteromedially toward the cribriform plate. **(e)** More posteriorly, the cribriform plate and ethmoid roof (ER) flatten. The orbital plate of frontal bone separates the orbit from the frontal fossa. The posterior ethmoid (ES) and maxillary sinuses (MS) are shown. **(f)** More posteriorly, through the orbital apex (OA), the sphenoid sinus (SS) air cells are seen, along with the flat midline bony roof, the planum sphenoidale (PS). At this level, a portion of the pterygopalatine fossa (PPF), as well as the sphenopalatine foramen (SPF), can be seen.

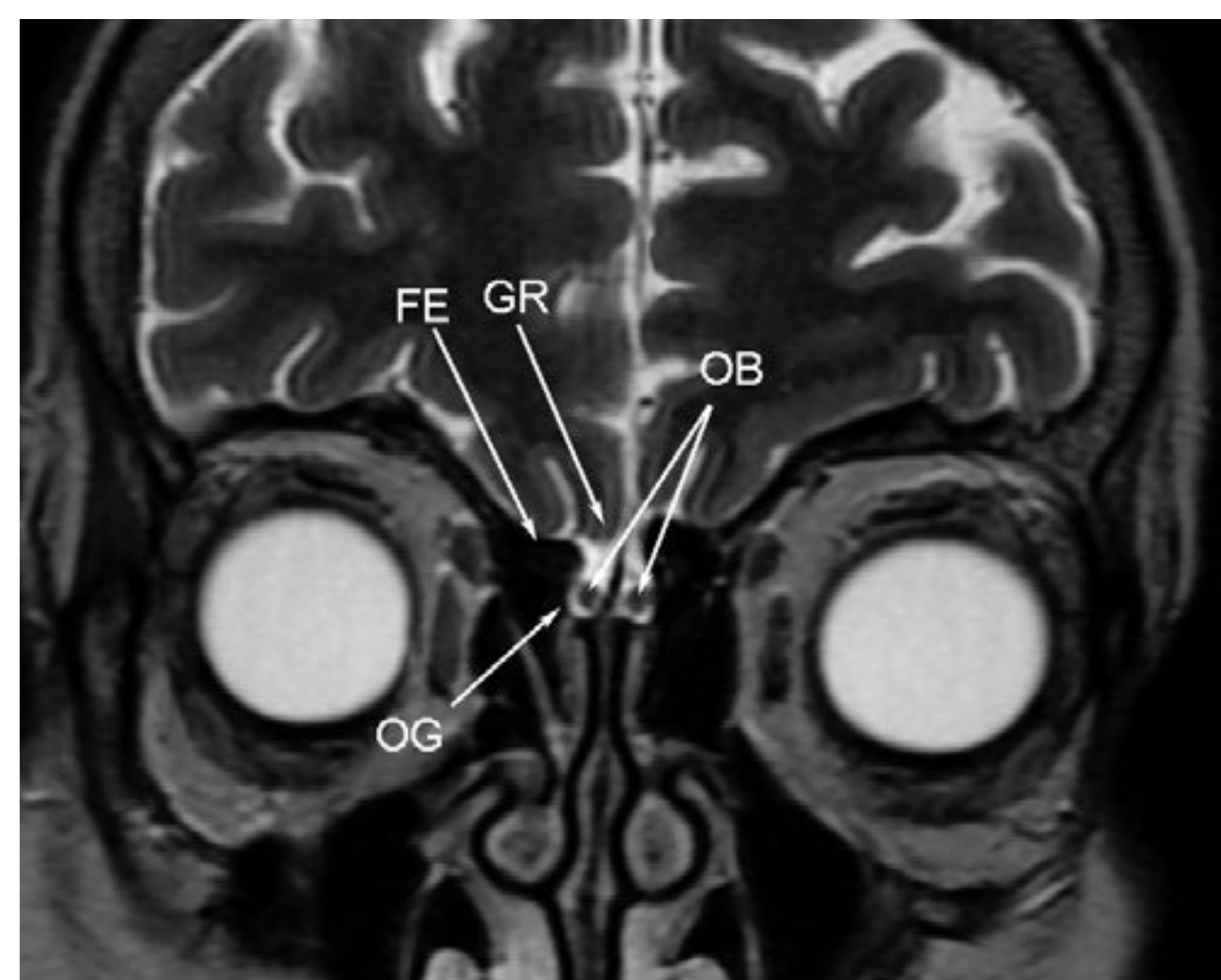


Fig. 2.4 Coronal T2-weighted magnetic resonance imaging through the orbits demonstrates the relationship of the frontal lobes, olfactory bulbs, and olfactory grooves. The olfactory bulbs (OBs) lie inferior to the gyrus rectii (GR) of the frontal lobes. The olfactory grooves (OGs) vary in depth in relationship to the ethmoid roof. The lateral aspect of the ethmoid roof is the fovea ethmoidalis (FE).

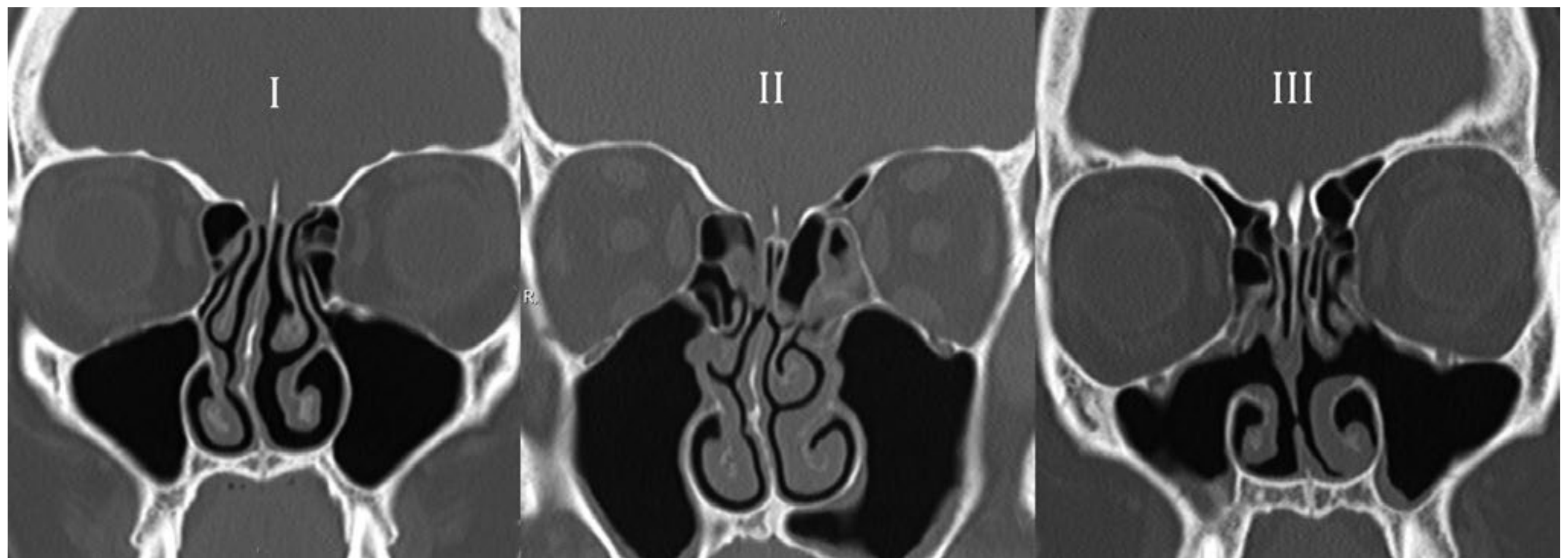


Fig. 2.5 Coronal computed tomography images in three different patients depicts the variable depth of the olfactory fossa, corresponding to the Keros classification, I–III. The image on the left shows a depth

of 3 mm (I). The middle image demonstrates a depth of 5 mm (II); the image on the right shows a depth of 8 mm (III).

the fonticulus frontalis, lies between the superior partially ossified frontal bone and inferior nasal bones. At this time, there is also a small space filled with dura just posterior to the developing nasal bones and anterior to the cartilage of the developing nasal capsule, called the prenasal space. When the chondrocranium begins to ossify, the fonticulus frontalis closes, and failure of its closure leads to development of a frontonasal cephalocele. In this condition, a small portion of meninges with (meningoencephalocele) or without (meningocele) brain herniates into the forehead at the region of the glabella or dorsum of the nose through a patent fonticulus frontalis, between the frontal bone superiorly and the nasal bones inferiorly.¹⁶

As a result of ossification of the chondrocranium of the anterior skull base from posterior to anterior, leaving a small portion of cartilage anteriorly for the nasal capsule and further ossification of nasal bones, the prenasal space lying between these becomes encased in bone and obliterates, leaving a small dural diverticulum called the foramen cecum just anterior to the site of the future crista galli. The foramen cecum can con-

nect anteroinferiorly to the skin of the nasal region transiently through a dura-lined stalk called the anterior neuropore, which later regresses. Defects in regression lead to a nasoethmoidal cephalocele through a midline foramen cecum defect into the prenasal space and nasal cavity. Mass effect by the cephalocele may bow the nasal bones anteriorly. The crista galli lies posterior to the anterior skull base foramen cecum defect and may be bifid or even absent, and an associated cribriform plate defect or absence may be seen.¹⁷ The least common subtype of an frontoethmoidal or sincipital cephalocele, called a naso-orbital cephalocele, develops as a result of defects in the lacrimal bones or frontal process of the maxilla with meninges and brain herniating inferomedially into the orbit.

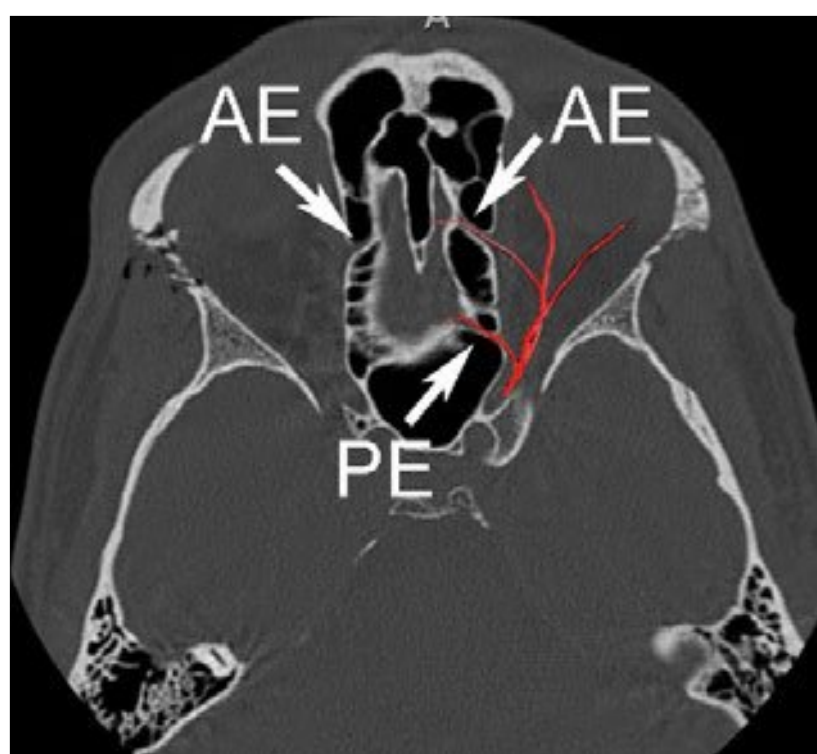


Fig. 2.6 Axial image through the level of the olfactory recess in patient with acute right orbital fracture. The anterior ethmoidal (AE) artery canals are demonstrated bilaterally. Superimposed illustration of the left ophthalmic artery branches also demonstrates the posterior ethmoid artery (PE) travelling more posteriorly.

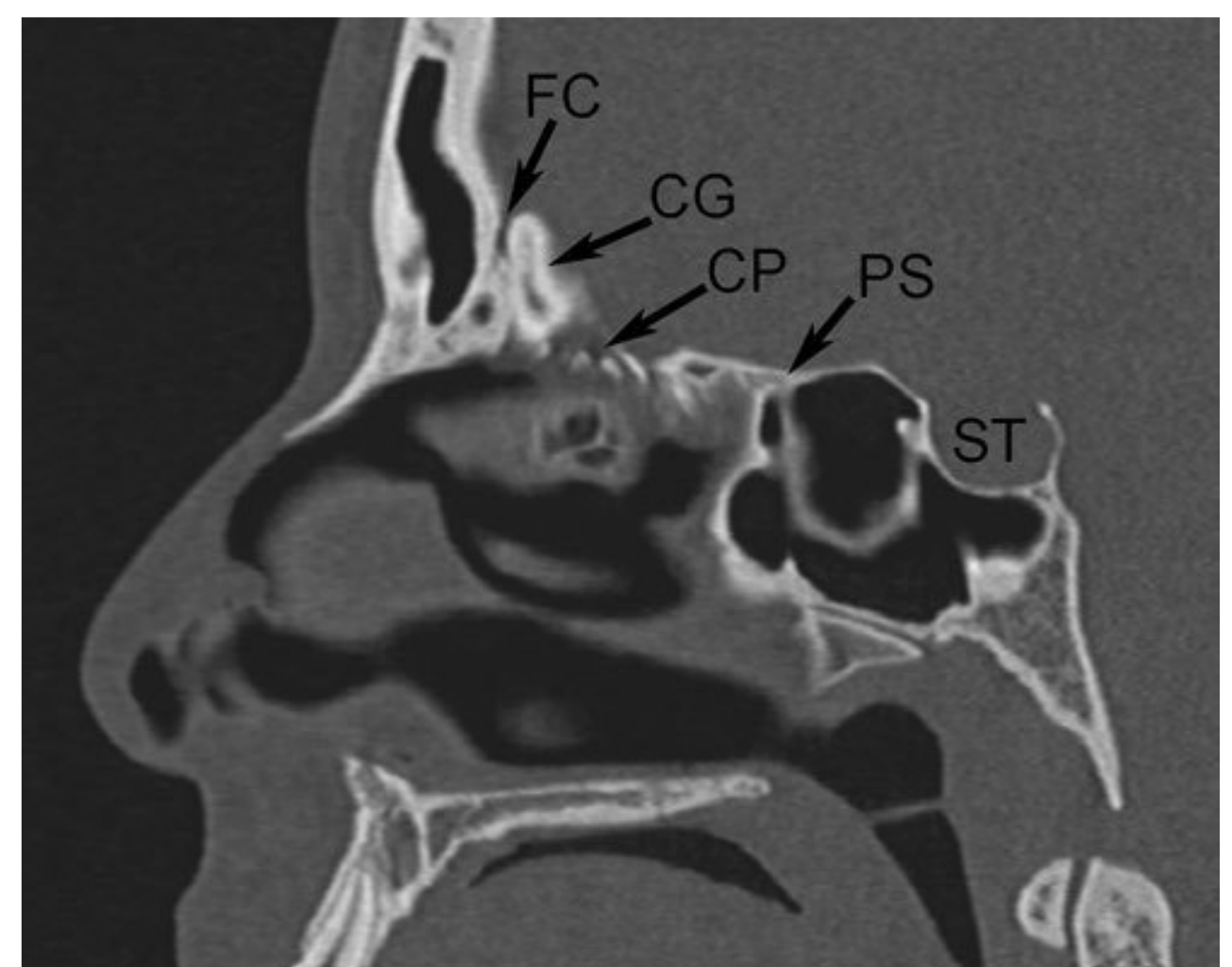


Fig. 2.7 Midline sagittal reformation of CT scan through the sinuses demonstrates midline structures from front to back. The residual foramen cecum (FC) is identified anterior to the crista galli (CG). The perforations along the cribriform plate (CP) can be seen. The planum sphenoidale (PS) is the flat, ventral roof of the sphenoid sinus, anterior to the sella turcica (ST).

Nasal dermal sinus with associated dermoid or epidermoid and nasal cerebral heterotopia (so-called nasal glioma), also present as congenital midline nasal masses, share common embryologic patterns and form the major differential diagnoses for frontoethmoidal cephaloceles. Nasal dermal sinus is lined by epithelial dermis, variably extends intracranially, and may be seen as a small nasal dimple. It does not contain brain or meninges but can be confused with a frontoethmoidal cephalocele when associated with a dermoid or epidermoid cyst somewhere along the tract. Nasal glioma (a misnomer because it contains nonneoplastic tissue) comprises of heterotopic dysplastic glial tissue without any demonstrable intracranial connection. Approximately two-thirds are extranasal and are located along the dorsum of the nose; the rest are under the nasal bones in an intranasal location.¹⁸

Anatomical Relationships of the Remainder of the Paranasal Sinuses with the Anterior Skull Base

The anatomy of the paranasal sinuses is given in detail in Chapter 17. Only the relevant anatomy of those portions of the paranasal sinuses associated with anterior skull base is discussed in this chapter.

The frontal sinuses are divided by a central septum into two parts, and multiple septa may be seen. The frontal recess, which is the drainage pathway of the frontal sinus, drains into the middle meatus of the nose, where the anterior ethmoid and maxillary sinuses also drain (**Fig. 2.8**). The uncinate process, which is attached inferiorly to the inferior turbinate of the nasal

cavity, forms the upper medial wall of maxillary sinus. It also forms the boundary of the ethmoid infundibulum, which is the common drainage pathway of maxillary and anterior ethmoid sinuses into the middle meatus. It may be attached superiorly, orienting laterally to the lamina papyracea (lateral ethmoid wall or medial orbital wall) or orienting medially to the nasal middle turbinate or anterior skull base. If the uncinate process attaches to the middle turbinate of nasal cavity or anterior skull base orienting medially, the frontal recess opens into the ethmoid infundibulum. The clinical importance of this anatomical relationship is that infection in the ethmoid infundibulum can affect the frontal sinus, resulting in combined involvement of the frontal anterior ethmoid and maxillary sinuses. On the other hand, if the uncinate process orients laterally and inserts into the lamina papyracea, the frontal recess has an isolated direct drainage into the anterior aspect of the middle meatus. In this case, the ethmoid infundibulum is closed superiorly by a blind-ending pouch known as the recessus terminalis¹⁹; hence, ethmoid infundibula inflammation results in anterior ethmoid and maxillary sinusitis without frontal sinus involvement; however, the presence of a recessus terminalis increases the incidence of frontal sinusitis, presumably because of the lack of an anatomical barrier between the frontal recess and middle meatus against the ascent of predisposing factors like allergens, irritants, and infections from the nasal cavity.²⁰

The posterior limit of the frontal recess is defined by the upward continuation of the bulla ethmoidalis (a prominent anterior ethmoid cell forming the superolateral margin of the ethmoid infundibulum) and the anterior ethmoidal artery, a branch of the ophthalmic artery.²¹ The anterior ethmoidal artery travels from the orbit through a canal piercing the lamina papyracea into the anterior ethmoid sinus immediately posterior to the frontal recess, crosses the sinus, and enters the anterior cranial fossa. As stated previously, injury to the anterior ethmoid foramen lying just anterolateral to the cribriform plate of the ethmoid should be avoided during surgery in this location. It gives off an anterior meningeal artery to the dura and also nasal branches, which re-enter the nasal cavity through the cribriform plate.

The frontal recess has a somewhat conical or inverted funnel shape with its superior apex at the frontal ostium.²² Anterior ethmoid cell pneumatization is variable, and both classic and accessory cells may compress the frontal sinus drainage pathway. The agger nasi cells and Kuhn's frontal recess cell types 1 to 4 occur along the anterior aspect of frontal recess, whereas suprabullar cells and frontal bullar cells are found posteriorly and supraorbital ethmoid cells posterolaterally.²³ Agger nasi (Latin for nasal mound) cells are the most anterior of the anterior ethmoid cells, lie anteroinferior to the frontal recess and inferior to the frontal sinus and are almost always present. These lie posterior to the frontal process of the maxilla, posteromedial to nasal bone, superomedial to the lacrimal bone, and superolateral to the uncinate process. They are seen inferior to the frontal recess and lateral to the middle turbinate on coronal CT scans, form important surgical landmarks, and are opened during endoscopic surgery to gain access to the frontal recess. Agger nasi cell inflammatory disease may obstruct the frontal recess, producing isolated opacification of the frontal sinus without involvement of the anterior ethmoid or maxillary sinuses.²⁴ There is a strong correlation between agger nasi cells and frontal sinus

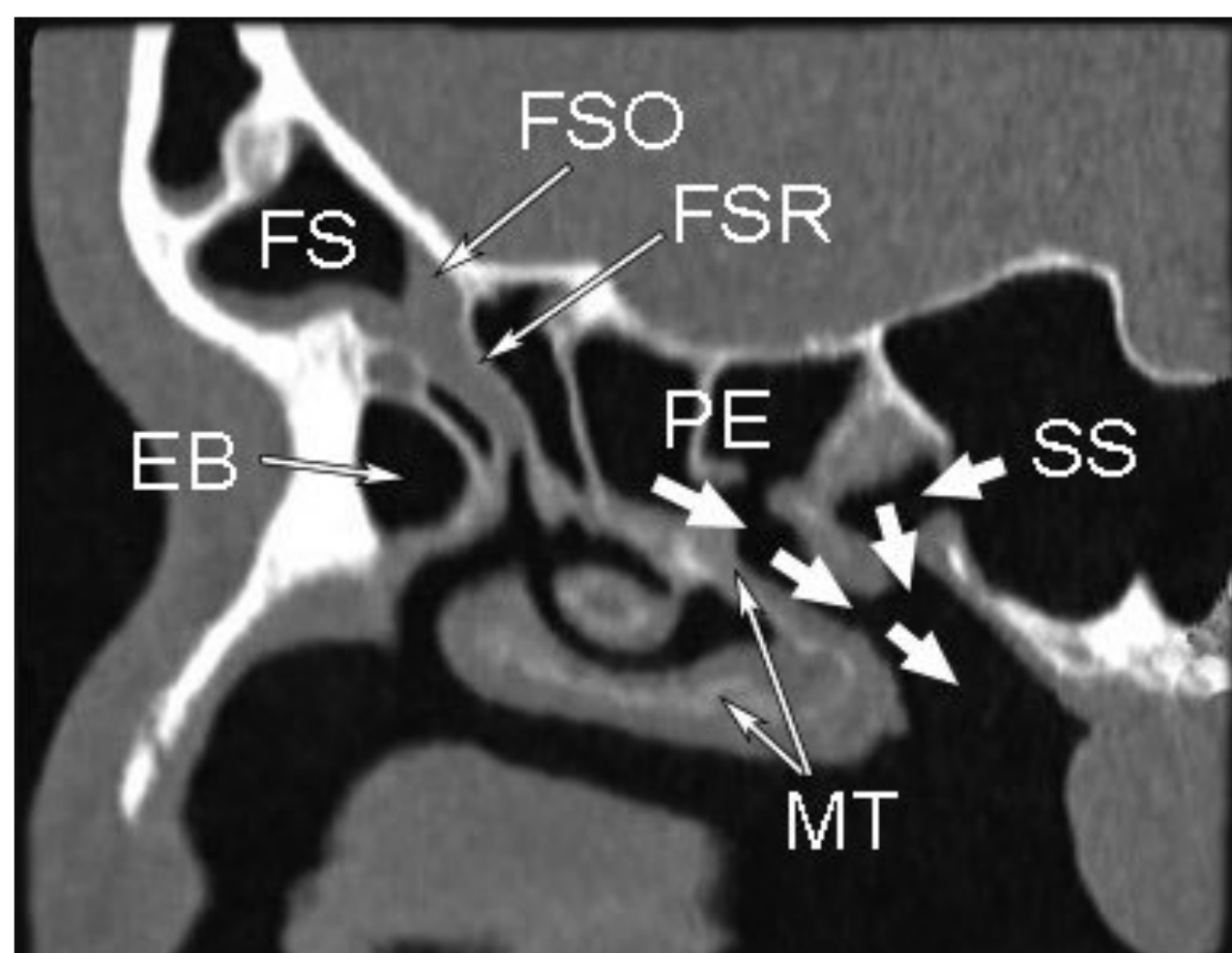


Fig. 2.8 Parasagittal reformation of CT scan through the sinuses demonstrates the frontal sinus (FS), the frontal sinus ostium (FSO), and the frontal sinus recess (FSR). The frontal sinus recess is conical shaped and extends inferiorly into the medial meatus. Also identified is the ethmoid bulla (EB), posterior ethmoid air cells (PE), and the sphenoid sinus (SS). The middle turbinate (MT) is labeled.

diseases on CT scans in patients undergoing revision functional endoscopic sinus surgery.²⁵

Frontal recess (Kuhn's) cells extend from the anterior ethmoid into the frontal recess, and these are all seen posterosuperior to the agger nasi cells. They are similar to agger nasi cells in that their posterior and superior walls appear as partitions within the frontal recess or within the frontal sinus in type 3 and 4 cells.²³ A type 1 cell is a single frontal recess cell superior to the agger nasi but below the floor of the frontal sinus. Type 2 cells are multiple cells in the frontal recess above the agger nasi that might extend into the frontal sinus. A type 3 cell is a single large frontal recess air cell that pneumatize superiorly into the frontal sinus. A type 4 cell is a single isolated cell within the frontal sinus. An intersinus cell is seen between the frontal sinuses, arises from the frontal sinus, and can sometimes narrow the frontal recess.²⁶ Mucosal inflammation is presumed to play a more crucial role than agger nasi cells and frontal recess cells 1–3 in the occurrence of frontal sinusitis.²⁷

As noted, accessory air cells along the posterior aspect of frontal recess include the frontal bullar cells, suprabullar cells, and supraorbital ethmoid cells. Frontal bullar cells are formed by anterior skull base pneumatization in the posterior frontal recess and extend through the frontal ostium into the true frontal sinus. Suprabullar cells are seen above the bulla ethmoidalis

and are also located in the posterior frontal recess similar to frontal bullar cells, but they do not extend into the frontal sinus. Supraorbital ethmoid cells are seen between the ethmoid roof and medial orbital wall and arise from anterior ethmoid sinus, and they might open into the lateral aspect of frontal recess. They pneumatize the orbital plate of frontal bone posterior to the frontal recess and superolateral to frontal sinus. These cells are found lateral to the frontal sinus in coronal CT scan images, whereas the frontal bullar cells are medial to the sinus.²⁸ The presence of accessory cells predispose one to a higher incidence of frontal sinusitis by narrowing the frontal sinus drainage pathway. Posteriorly, the suprabullar cells narrow the anteroposterior diameter of the frontal recess, frontal bullar cells narrow the frontal recess and also the more superior frontal ostium, and supraorbital ethmoid cells narrow the frontal ostium.²⁷

Another important paranasal sinus structure at the posterior aspect of the anterior skull base is the sphenoid Onodi cell, a posterior ethmoid air cell that extends superior and lateral to the anterior aspect of the sphenoid sinus and abuts the optic nerve. Dehiscence of the adjacent optic canal and carotid canal can be associated with an Onodi cell,²⁹ which can be seen as a bulge of the optic canal at transnasal endoscopy and should not be breached so as to avoid optic nerve injury.

References

- Harnsberger HR. Anterior skull base. In: Harnsberger HR, Osborn AG, Macdonald AJ, Ross JS AJ, eds. *Diagnostic and Surgical Imaging Anatomy: Brain, Head & Neck, Spine*. 1st ed. Philadelphia, PA: Amirsys; 2010:II12–II25
- Chapman PR, Bag AK, Tubbs RS, Gohlke P. Practical anatomy of the central skull base region. *Semin Ultrasound CT MR* 2013;34(5):381–392 [PubMed](#)
- Som PM, Park EE, Naidich TP, Lawson W. Crista galli pneumatization is an extension of the adjacent frontal sinuses. *AJNR Am J Neuroradiol* 2009;30(1):31–33 [PubMed](#)
- Kainz J, Heinz Stammberger. The roof of the anterior ethmoid: a place of least resistance in the skull base. *Am J Rhinol*. 1989;3:191–199
- Nuss DW, O'Malley BW. Surgery of the anterior and middle cranial base. In: Cummings CW, ed. *Cummings Otolaryngology Head and Neck Surgery*. 4th ed. St Louis, MO: Elsevier Mosby; 2005:3760–3775
- Meyers RM, Valvassori G. Interpretation of anatomic variations of computed tomography scans of the sinuses: a surgeon's perspective. *Laryngoscope* 1998;108(3):422–425 [PubMed](#)
- Stankiewicz JA, Chow JM. The low skull base: an invitation to disaster. *Am J Rhinol* 2004;18(1):35–40 [PubMed](#)
- Kim E, Russell PT. Prevention and management of skull base injury. *Otolaryngol Clin North Am* 2010;43(4):809–816 [PubMed](#)
- Messerklinger W. [Endoscopy technique of the middle nasal meatus] (author's transl). *Arch Otorhinolaryngol* 1978;221(4):297–305 [PubMed](#)
- Wigand ME. Transnasal, endoscopic sinus surgery for chronic sinusitis. II Endonasal ethmoidectomy. *HNO* 1981;29:287–293 [PubMed](#)
- Gray ST, Wu AW. Pathophysiology of iatrogenic and traumatic skull base injury. In: Bleier BS, ed. *Comprehensive Techniques in CSF Leak Repair and Skull Base Reconstruction*. *Adv Otorhinolaryngol*. 2013;74:12–23
- Keros P. [On the practical value of differences in the level of the lamina cribrosa of the ethmoid]. *Z Laryngol Rhinol Otol* 1962;41:809–813 [PubMed](#)
- Savvateeva DM, Guldner C, Murthum T, et al. Digital volume tomography (DVT) measurements of the olfactory cleft and olfactory fossa. *Acta Otolaryngol* 2010;130(3):398–404 [PubMed](#)
- Osborn AG. Anomalies of the skull and meninges. In: Osborn AG, ed. *Osborn's brain: imaging, pathology, and anatomy*. 1st ed. Salt Lake City, UT: Amirsys; 2013:1187–1208.
- Hoving EW, Vermeij-Keers C. Frontoethmoidal encephaloceles, a study of their pathogenesis. *Pediatr Neurosurg* 1997;27(5):246–256 [PubMed](#)
- Hedlund G. Congenital frontonasal masses: developmental anatomy, malformations, and MR imaging. *Pediatr Radiol* 2006;36(7):647–662, quiz 726–727 [PubMed](#)
- Barkovich AJ. Congenital malformations of the brain and skull. In: Barkovich AJ, ed. *Pediatric Neuroimaging*. 4th ed. Philadelphia: Lippincott Williams & Wilkins; 2005:308–313
- Barkovich AJ, Vandermark P, Edwards MS, Cogen PH. Congenital nasal masses: CT and MR imaging features in 16 cases. *AJNR Am J Neuroradiol* 1991;12(1):105–116 [PubMed](#)
- McLaughlin RB Jr, Rehl RM, Lanza DC. Clinically relevant frontal sinus anatomy and physiology. *Otolaryngol Clin North Am* 2001;34(1):1–22 [PubMed](#)
- Turgut S, Ercan I, Sayin I, Başak M. The relationship between frontal sinusitis and localization of the frontal sinus outflow tract: a computer-assisted anatomical and clinical study. *Arch Otolaryngol Head Neck Surg* 2005;131(6):518–522 [PubMed](#)
- Wormald PJ. Three-dimensional building block approach to understanding the anatomy of the frontal recess and frontal sinus. *Oper Tech Otolaryngol–Head Neck Surg* 2006;17:2–5
- Kuhn FA. Chronic frontal sinusitis: the endoscopic frontal recess approach. *Oper Tech Otolaryngol–Head Neck Surg* 1996;7:222–229

23. Lee WT, Kuhn FA, Citardi MJ. 3D computed tomographic analysis of frontal recess anatomy in patients without frontal sinusitis. *Otolaryngol Head Neck Surg* 2004;131(3):164–173 [PubMed](#)
24. Vattoth S, Sullivan JC. Face and Neck Anatomy. In: Canon CL, ed. *McGraw-Hill Specialty Board Review: Radiology*. 1st ed. New York: McGraw-Hill; 2010:99–114
25. Bradley DT, Kountakis SE. The role of agger nasi air cells in patients requiring revision endoscopic frontal sinus surgery. *Otolaryngol Head Neck Surg* 2004;131(4):525–527 [PubMed](#)
26. Coates MH, Whyte AM, Earwaker JW. Frontal recess air cells: spectrum of CT appearances. *Australas Radiol* 2003;47(1):4–10 [PubMed](#)
27. Lien CF, Weng HH, Chang YC, Lin YC, Wang WH. Computed tomographic analysis of frontal recess anatomy and its effect on the development of frontal sinusitis. *Laryngoscope* 2010;120(12):2521–2527 [PubMed](#)
28. Zhang L, Han D, Ge W, et al. Computed tomographic and endoscopic analysis of supraorbital ethmoid cells. *Otolaryngol Head Neck Surg* 2007;137(4):562–568 [PubMed](#)
29. Weinberger DG, Anand VK, Al-Rawi M, Cheng HJ, Messina AV. Surgical anatomy and variations of the Onodi cell. *Am J Rhinol* 1996;10(6):365–370

Introduction

The middle or central skull base has customarily been delineated from the anterior skull base by a horizontal line along the anterior sellar margin (tuberculum sellae), which extends laterally along the posterior margin of the lesser wing of the sphenoid bone on both sides and includes the medial anterior clinoid processes. The posterior boundary of the middle skull base is formed medially by the dorsum sella and laterally by the petrous ridges. The appearance of the skull base, as viewed from above and through an open calvaria, naturally separates the skull into its three classic anatomical divisions. The anatomical boundaries of the skull base coincide with the boundaries of the proposed intracranial spaces, producing the anterior, middle, and posterior cranial fossae. This archetypical approach does not take into account the practically important, three-dimensional (3D) connections of the middle skull base in the current era of advanced cross-sectional imaging or the availability of sophisticated surgical and radiation treatment methods.^{1,2}

The 3D anatomy of the middle skull base should encompass the contiguous anatomical regions of the orbital apex and optic canal, including the optic nerve leading posteriorly to the optic chiasm, the superior orbital fissure, the pterygopalatine fossa, and the sella. In addition, the suprasellar and parasellar structures, including the pituitary gland and stalk, cavernous sinus, internal carotid artery, cranial nerves, Meckel's cave, regional skull-base foramina, sphenoid sinus, clivus, petrous apex, petro-occipital fissure, foramen lacerum, and parts of the nasopharynx should also be incorporated as part of the middle skull base. This region can be conceptualized as having a roughly spherical shape with the optic chiasm at the superior pole, nasopharynx at the inferior pole, pterygopalatine fossa at the anterior pole, and the foramen ovale at the lateral and prepontine cistern at

the posterior poles, respectively. Attributing a 3D configuration to the middle skull base allows for compartmentalization of the anatomy, which in turn helps to predict pathology based on the knowledge of intrinsic structures dwelling in the particular location. In addition, it sheds light on the complex anatomical connections and aids in assessing the origin and spread of various trans-spatial disease processes. The lateral aspect of the middle skull base, constituted predominantly by the greater wing of the sphenoid bone, forms the floor of the middle cranial fossa, which houses the temporal lobes of the brain.^{1,3}

Center of the Sphere: Sphenoid Bone and Sphenoid Sinus

The sphenoid bone has a central body and is constituted on either side by the lateral greater and lesser wings and the inferior pterygoid process with the medial and lateral pterygoid plates. The body of the sphenoid contains the sella turcica superiorly and the sphenoid sinus inferiorly. Posteriorly, it forms the anterosuperior aspect of the clivus, joining the posteroinferior aspect from occipital bone at the spheno-occipital synchondrosis. The spheno-occipital synchondrosis separates the basisphenoid from the basiocciput (**Fig. 3.1**). Chordomas can arise from notochordal remnants near the synchondrosis, and the presence of vascularized bone marrow predisposes the clivus to pathologies like myeloma and metastasis. The lesser wing of the sphenoid forms the posterior margin of the anterior skull base—harboring the optic canal. The greater wing of sphenoid forms the floor of middle cranial fossa. The superior orbital fissure lies between

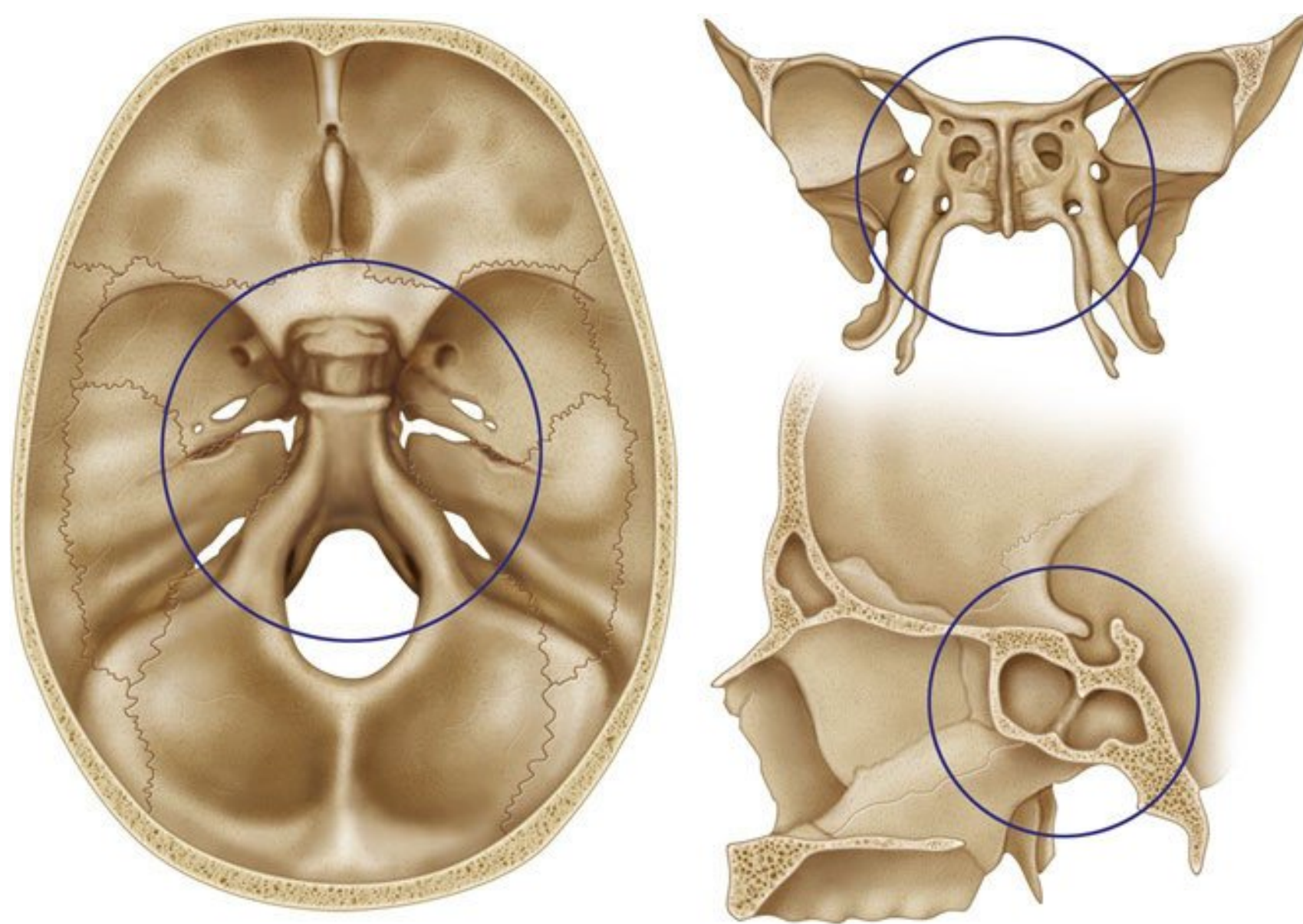


Fig. 3.1 Three-dimensional illustrations of the superior, anterior, and lateral views of the sphenoid bone and the osseous foundation of the central skull base. The outlined spherical region denotes the central skull base region and includes the adjacent endocranial structures including the pituitary gland and the exocranial structures of the neck including the nasopharynx.

the lesser wing of the sphenoid superomedially and the greater wing of the sphenoid inferolaterally, separated by the optic strut, a small bony bridge that projects from the anterior clinoid process of the lesser wing to the sphenoid body.^{4,5} The osseous architecture of the sphenoid bone, sphenoid sinus, and associated relationships with adjacent osseous skull base, canals, and foramina is best studied with high-resolution computed tomography (CT) scans using thin slices and bone algorithms (**Fig. 3.2, Fig. 3.3**).

The extent of sphenoid sinus pneumatization (or lack thereof) is classified as conchal, presellar, and sellar.⁶ In the conchal form, the sphenoid bone is essentially solid without development of an aerated sphenoid sinus. With presellar pneumatization, the sphenoid sinus is pneumatized but does not extend posteriorly to the coronal level of the anterior sellar. With sellar pneumatization, the sphenoid sinus extends posteriorly inferior to the sella and can extend to the posterior clival margin. The anterior wall and floor of sella are quite thin in the latter

subtype, measuring less than a millimeter in thickness. Sphenoid sinus pneumatization may extend into the optic strut and anterior clinoid process, resulting in thinning of the boundary with the optic canal and superior orbital fissure. Passage of the vidian canal through the body of sphenoid bone and the foramen rotundum, along the lateral aspect of sphenoid sinus roof, lies in close relation to sphenoid sinus.⁷ The sphenoid sinus lies close to the internal carotid arteries (ICAs) and cavernous sinuses. The ICA lies along a shallow groove on the intracranial side of the lateral wall of the sphenoid sinus. The variable intercarotid distance between the ICAs of both sides makes pituitary surgery more risky. Sphenoid sinus septation also varies considerably. Although it is usually single, septation can be multiple with septa deviating laterally, inserting near the carotid artery.⁸ Contiguous spread of pathology, bony destruction, and potential for iatrogenic injury to adjacent critical structures during surgery should be carefully estimated during presurgical imaging evaluation of the sphenoid sinus.

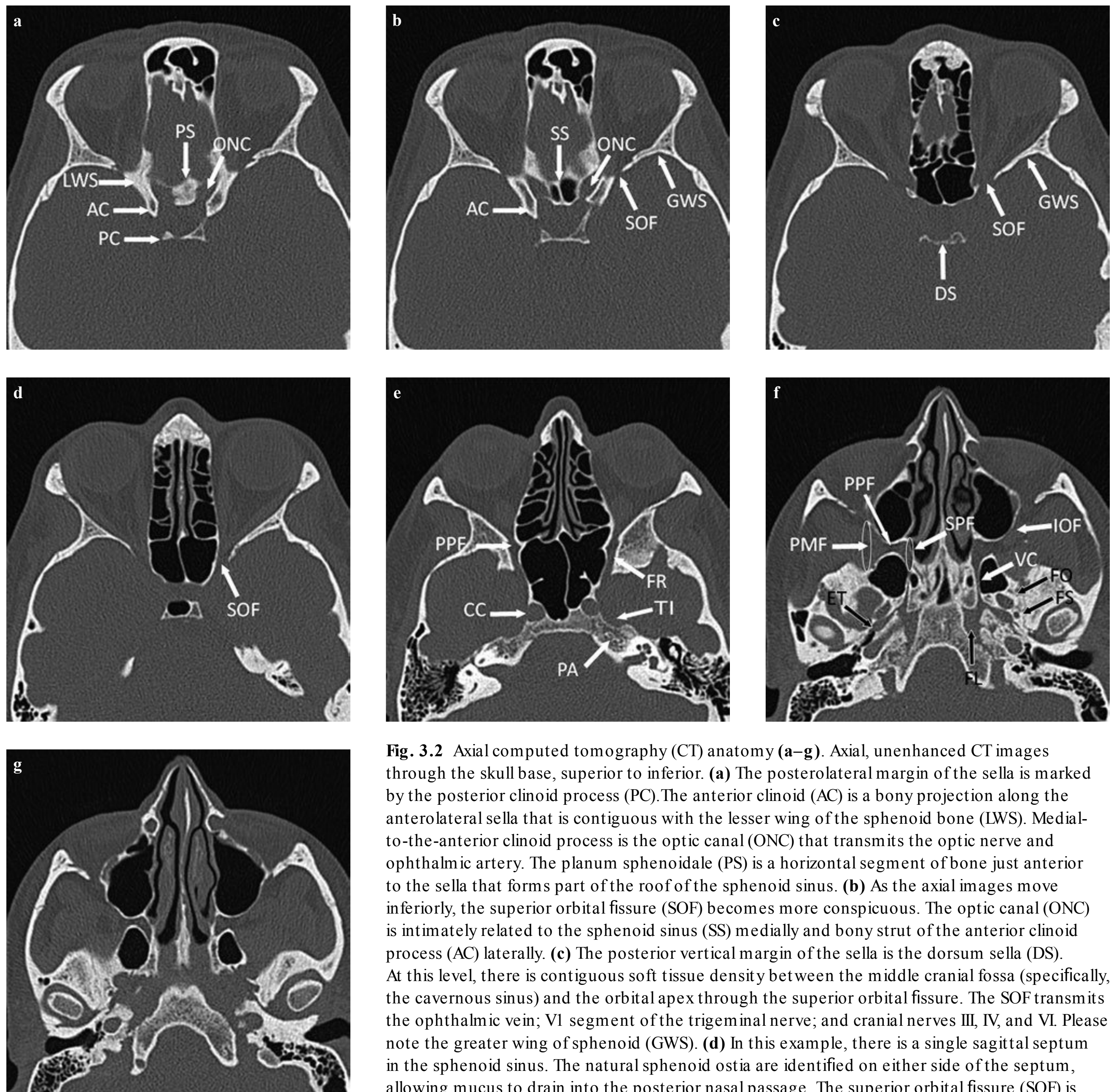


Fig. 3.2 Axial computed tomography (CT) anatomy (a–g). Axial, unenhanced CT images through the skull base, superior to inferior. **(a)** The posterolateral margin of the sella is marked by the posterior clinoid process (PC). The anterior clinoid (AC) is a bony projection along the anterolateral sella that is contiguous with the lesser wing of the sphenoid bone (LWS). Medial-to-the-anterior clinoid process is the optic canal (ONC) that transmits the optic nerve and ophthalmic artery. The planum sphenoidale (PS) is a horizontal segment of bone just anterior to the sella that forms part of the roof of the sphenoid sinus. **(b)** As the axial images move inferiorly, the superior orbital fissure (SOF) becomes more conspicuous. The optic canal (ONC) is intimately related to the sphenoid sinus (SS) medially and bony strut of the anterior clinoid process (AC) laterally. **(c)** The posterior vertical margin of the sella is the dorsum sella (DS). At this level, there is contiguous soft tissue density between the middle cranial fossa (specifically, the cavernous sinus) and the orbital apex through the superior orbital fissure. The SOF transmits the ophthalmic vein; V1 segment of the trigeminal nerve; and cranial nerves III, IV, and VI. Please note the greater wing of sphenoid (GWS). **(d)** In this example, there is a single sagittal septum in the sphenoid sinus. The natural sphenoid ostia are identified on either side of the septum, allowing mucus to drain into the posterior nasal passage. The superior orbital fissure (SOF) is noted (arrow). **(e)** At this level, the petrous apex (PA) can be seen as a pyramidal shaped, medial extension of the temporal bone. Along the superior and medial margin of the petrous apex is a shallow concavity, the trigeminal impression (TI). The medial opening of the carotid canal (CC) is seen, separated from the sphenoid sinus by thin cortical bone. The foramen rotundum (FR) opens into the upper recess of the pterygopalatine fossa (PPF). **(f)** The foramen lacerum (FL) is a triangular shaped, horizontal layer of cartilage between the clivus and petrous apex. The eustachian tube (ET) is seen just lateral to the carotid canal, extending lateral to medial and superior to inferior. The foramen ovale (FO) and foramen spinosum (FS) are seen in the lateral sphenoid bone. The vidian canal (VC) contains the vidian nerve and travels from a point near the foramen lacerum forward to the pterygopalatine fossa (PPF). The PPF connects with the masticator space laterally through the pterygomaxillary fissure (PMF, large oval) and medially through the sphenopalatine foramen (SPF, small oval) with the nasal cavity. The infraorbital nerve passes from the PPF into the inferior orbital fissure (IOF) on its way to the cheek. **(g)** At this level, soft tissues that form the roof of the nasopharynx begin to show up ventral to the clivus. Note that these soft tissues are directly contiguous with the region of the eustachian tube and foramen lacerum.

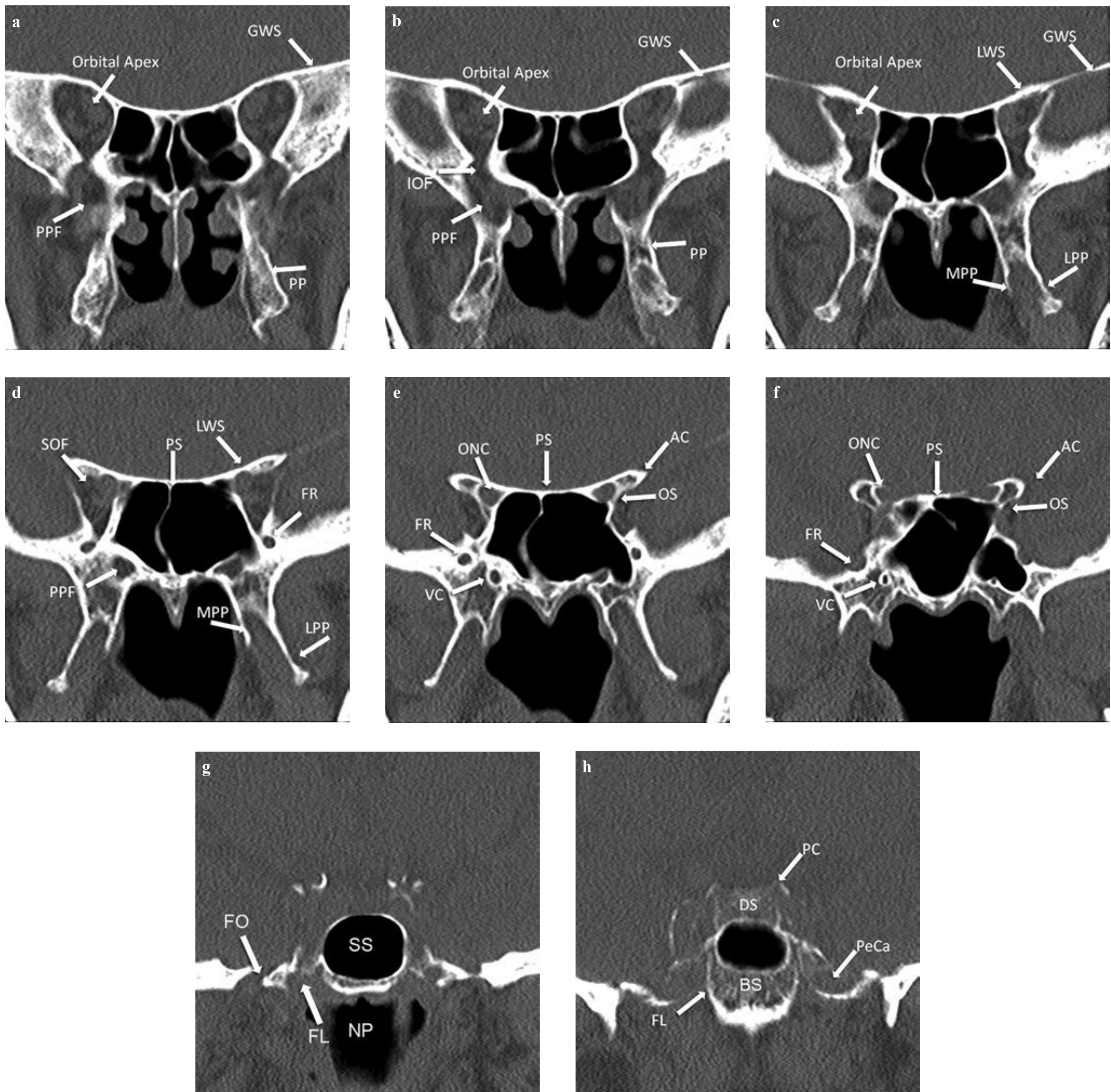


Fig.3.3 Coronal computed tomography (CT) anatomy, anterior to posterior (**a–h**). Coronal, unenhanced CT images through the central skull base. (**a**) Coronal image through orbital apices at the level of the pterygoid process (PP) demonstrates the relationship between the pterygopalatine fossa and the orbital apex. (**b**) The pterygopalatine fossa (PPF) contains fat, the distal branches of the internal maxillary artery, veins, the pterygopalatine ganglion, and its connections. The PPF is contiguous with the inferior orbital fissure (IOF) and, ultimately, the orbital apex. (**c**) Near the apex, the orbital roof is formed by the lesser wing of the sphenoid bone (LWS). The medial (MPP) and lateral (LPP) pterygoid plates project posteriorly from the pterygoid process (PP). (**d**) Near the apex, there is an obliquely oriented superolateral fissure, the superior orbital fissure (SOF), which transmits the ophthalmic vein; V1 segment of the trigeminal nerve; and cranial nerves III, IV, and VI. (**e**) The foramen rotundum (FR) opens into the upper recess of the pterygopalatine fossa (PPF). In the coronal plane,

the foramen rotundum is seen superolateral to the vidian canal (VC). (**f**) Coronal image through the sphenoid sinus demonstrates the relationship between the anterior clinoid process (AC) and the optic canal (ONC). The roof of the sphenoid sinus is flat and is referred to as the planum sphenoidale (PS). The optic strut (OS) is a thin bridge of bone defines the lateral margin of the optic canal. At this level, the foramen rotundum opens into the middle cranial fossa as V2 travels toward the lateral wall of the cavernous sinus. (**g**) Coronal image through sphenoid sinus demonstrates foramen ovale (FO) laterally, which transmits V3 into the masticator space and more poorly defined foramen lacerum (FL) medially. (**h**) Coronal image through the posterior aspect of the sella. The posterior clinoid processes (PC) can be seen as bilateral superolateral projections. The posterior wall of the sella is the dorsum sella (DS). The upper one-half of the clivus is formed from the sphenoid bone and is referred to as the basisphenoid (BS).

Intracranial Structures Superior to Center of the Sphere

Sella Turcica and Suprasellar Region

The sella turcica (Turkish saddle) is a saddle-shaped depression in the body of the sphenoid bone. The seat of the saddle supports the pituitary gland and is known as the hypophyseal fossa (**Fig. 3.4**). Its anterior margin is the tuberculum sella, and its posterior margin is the dorsum sella, with the superolateral posterior clinoid processes on either side. The dorsum sella is continuous posteriorly with the clivus. The chiasmatic sulcus lies just anterior to the tuberculum sella and medial to optic canals. The planum sphenoidale, a part of the anterior cranial fossa, lies in front of the tuberculum sellae and chiasmatic sulcus. The medial processes along lesser wings of sphenoid bilaterally form the sella's anterior clinoid processes. The floor of the pituitary fossa has a well corticated, less than 1-mm-thick bony wall known as the lamina dura. The diaphragma sellae is a slightly inferior, convex, thin dual fold covering the superior aspect of sella and is perforated centrally by the pituitary stalk. The pituitary stalk passes through the cerebrospinal fluid (CSF) filled suprasellar cistern on its way to the hypothalamus. The suprasellar cistern also houses the optic chiasm and circle of Willis. Large sellar or suprasellar lesions, including pituitary adenomas and craniopharyngiomas, can produce optic chiasm compression.

Cavernous Sinus

The cavernous sinuses, dural venous sinuses lying on either side of the sella connected by intercavernous sinuses, are fed by multiple tributaries, including the superior ophthalmic veins

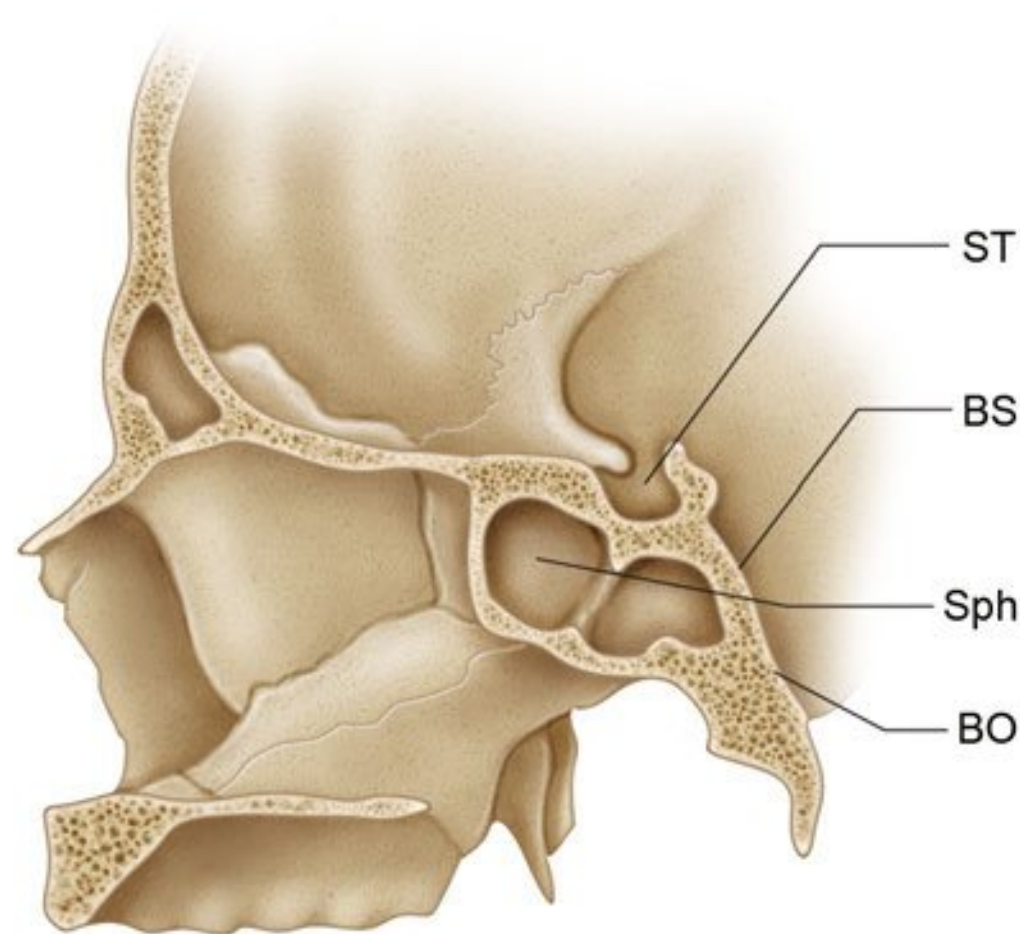


Fig. 3.4 Sagittal illustration through the central skull base demonstrates the bony anatomy of the sella turcica (ST). The anterior wall of the sella is very thin and separates the sella from the sphenoid sinus (Sph). The clivus is formed by the basisphenoid (BS) superiorly and the basiocciput (BO) inferiorly.

in the orbits, sphenoparietal sinuses seen along the anterior aspect of middle cranial fossa, basal vein of Rosenthal seen in the perimesencephalic cisterns draining toward the vein of Galen, pterygoid venous plexus seen in the masticator space, and the basilar venous plexus near the petrous apex. They drain through the superior petrosal sinus into the sigmoid sinus and through the inferior petrosal sinus into the internal jugular vein. In a carotid-cavernous fistula, venous channels may be engorged with high pressure arterialized flow and appear enlarged on magnetic resonance imaging (MRI) and CT scan images.⁹

The cavernous sinus has five walls.^{1,10} The medial wall of the cavernous sinus consists of an upper sellar component with a single-layered, thin, dural membrane separating it from the lateral margin of the pituitary gland, and a lower, thicker component adherent to the carotid sulcus. Tumor obliteration of the medial venous compartment of the cavernous sinus inferior to the cavernous ICA in a coronal MRI scan (called carotid sulcus venous compartment of cavernous sinus) has been shown to have a 95% positive predictive value (PPV) for cavernous sinus invasion by a pituitary adenoma.¹¹ Perimeter encasement of 67% or more of the cavernous segment of the ICA (100% PPV) and tumor spread beyond the border joining the lateral wall of the intracavernous and supracavernous ICAs (85% PPV), as seen on coronal MRI, both suggest cavernous sinus invasion. If the percentage of encasement of the perimeter of the intracavernous ICA is less than 25% or if adenoma invasion does not cross beyond the adjoining medial wall of the intracavernous and supracavernous ICAs, cavernous sinus invasion can then be ruled out with a negative predictive value of 100%.

Forming the medial margin of the temporal lobe, the bilaminar lateral wall of the cavernous sinus consists of a thin outer meningeal layer and a thicker inner dural layer that extends from the region of superior orbital fissure and the anterior clinoid process anteriorly to the petrous apex posteriorly. The oculomotor nerve (cranial nerve III, or CN III), the trochlear nerve (CN IV), and the ophthalmic segment of the trigeminal nerve (CN V1) are contained within the lateral wall layers, and the only truly intracavernous nerve, namely, the abducens nerve (CN VI), lies within the cavernous sinus itself, along with the cavernous segment of ICA (**Fig. 3.5**). Inferiorly, the medial and lateral walls fuse along the lateral margin of the body of sphenoid bone. It is interesting to note that this fusion occurs just superior to the maxillary nerve (second division of the trigeminal nerve, CN V2) and that the CN V2 and mandibular nerve (third division of the trigeminal nerve, CN V3) are not part of the cavernous sinus, even though they are invested by the contiguous dura.^{1,12}

The cavernous sinus becomes contiguous with the inferior petrosal sinus (which in turn drains through the petroclival fissure into internal jugular vein) posteriorly. The posterior wall of the cavernous sinus extends from the lateral margin of the dorsum sella to the superomedial aspect of Meckel's cave. Just posteroinferior to this is the petrous apex, over which the abducens nerve (CN VI) travels underneath the petrosphenoid ligament, goes through the Dorello's canal, enters the posterior wall of the cavernous sinus, and is seen within the substance of the cavernous sinus lateral to the cavernous ICA (**Fig. 3.6**). Petrous apicitis can lead to Gradenigo syndrome with CN VI palsy (resulting from involvement in Dorello's canal) and trigeminal distribution pain from spread of inflammation into the adjacent Meckel's cave, where the trigeminal ganglion resides.¹³

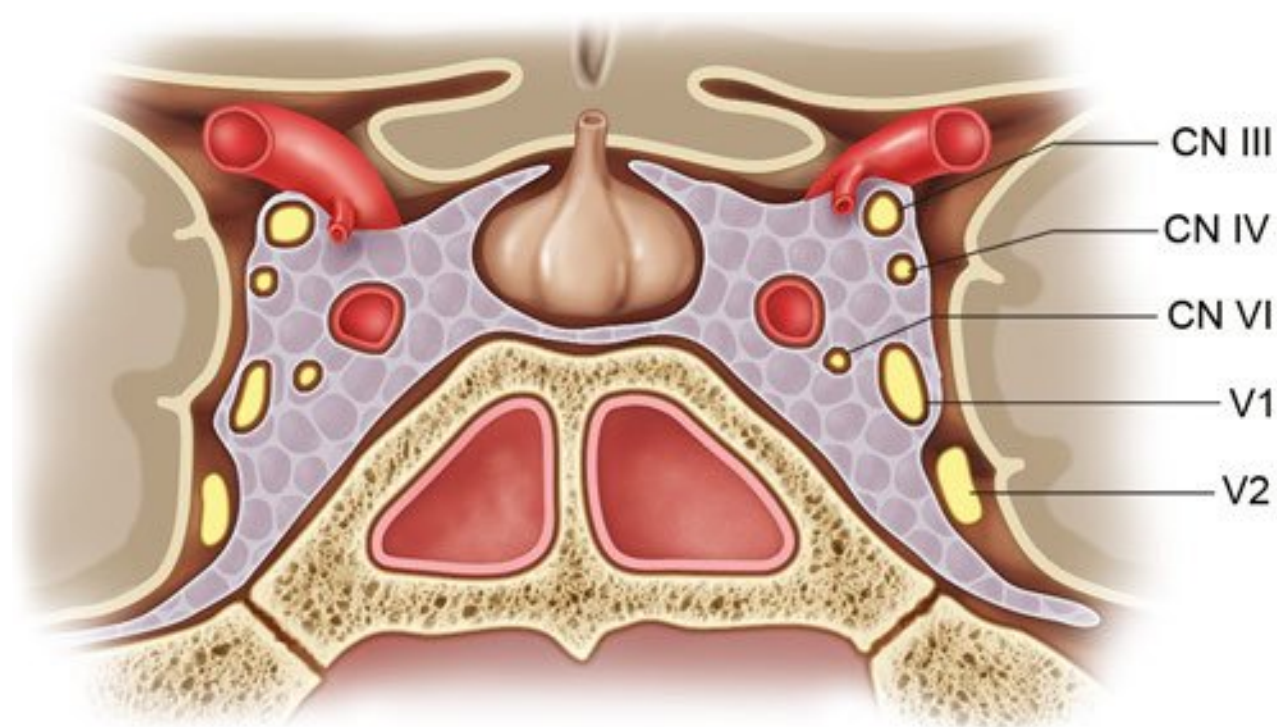


Fig. 3.5 Posterior view through the cavernous sinuses. The central location of the cavernous internal carotid artery is noted. Cranial nerve VI, the abducens, is the only nerve that is truly intracavernous. From superior to inferior, the oculomotor, trochlear, ophthalmic, and maxillary nerves are seen along the lateral margin of the cavernous sinus. The lateral wall is divided into two layers, an outer meningeal layer and an inner dural layer. The inner dural layer envelops the oculomotor, trochlear, and ophthalmic nerves.

The rectangular anterior wall of the cavernous sinus extends from the optic strut under the anterior clinoid process toward the superior orbital fissure, and its inferior margin forms the superior end of foramen rotundum carrying CN V2. The cavernous sinus roof extends from the optic strut and superior orbital fissure anteriorly to the petrous apex and the edge of the tentorium posteriorly. It is contiguous with the diaphragma sellae medially and is separated laterally from the lateral wall of cavernous sinus by the anterior petroclinoid fold. The anterior petroclinoid fold is a cordlike thickening of the dura extending from the anterior clinoid process anteriorly to tentorial edge posteriorly. The posterior petroclinoid fold is a separate fold extending from the posterior clinoid process to the tentorial edge, whereas the interclinoid fold is a thin band of dura that extends from the anterior clinoid process to the posterior clinoid process. The anatomical importance of these three folds is that they form a landmark triangle at the cavernous sinus roof—the oculomotor triangle (**Fig. 3.7**). CN III pierces the oculomotor triangle from a postero-superior aspect to pass through a short oculomotor cistern and enters within the bilaminar lateral wall of the cavernous sinus near the anterior clinoid process. CN IV enters the oculomotor triangle posterolaterally, just posterior to the oculomotor nerve.¹⁴

Internal Carotid Artery

The ICAs are important structures that are intimately related to the middle skull base, except for the proximal cervical and distal communicating segments. The widely used Bouthillier system divides the ICA into a seven-segment numerical scale along the superiorly oriented direction of blood flow according to a detailed understanding of the surrounding anatomy and the compartments through which it travels (**Fig. 3.8**),¹⁵ including the following segments from its origin in the neck to its termination at the circle of Willis: cervical (C1), petrous (C2), lacerum (C3), cavernous (C4), clinoid (C5), ophthalmic (C6), and communicating (C7) segments. Cervical C1 segment of the ICA has

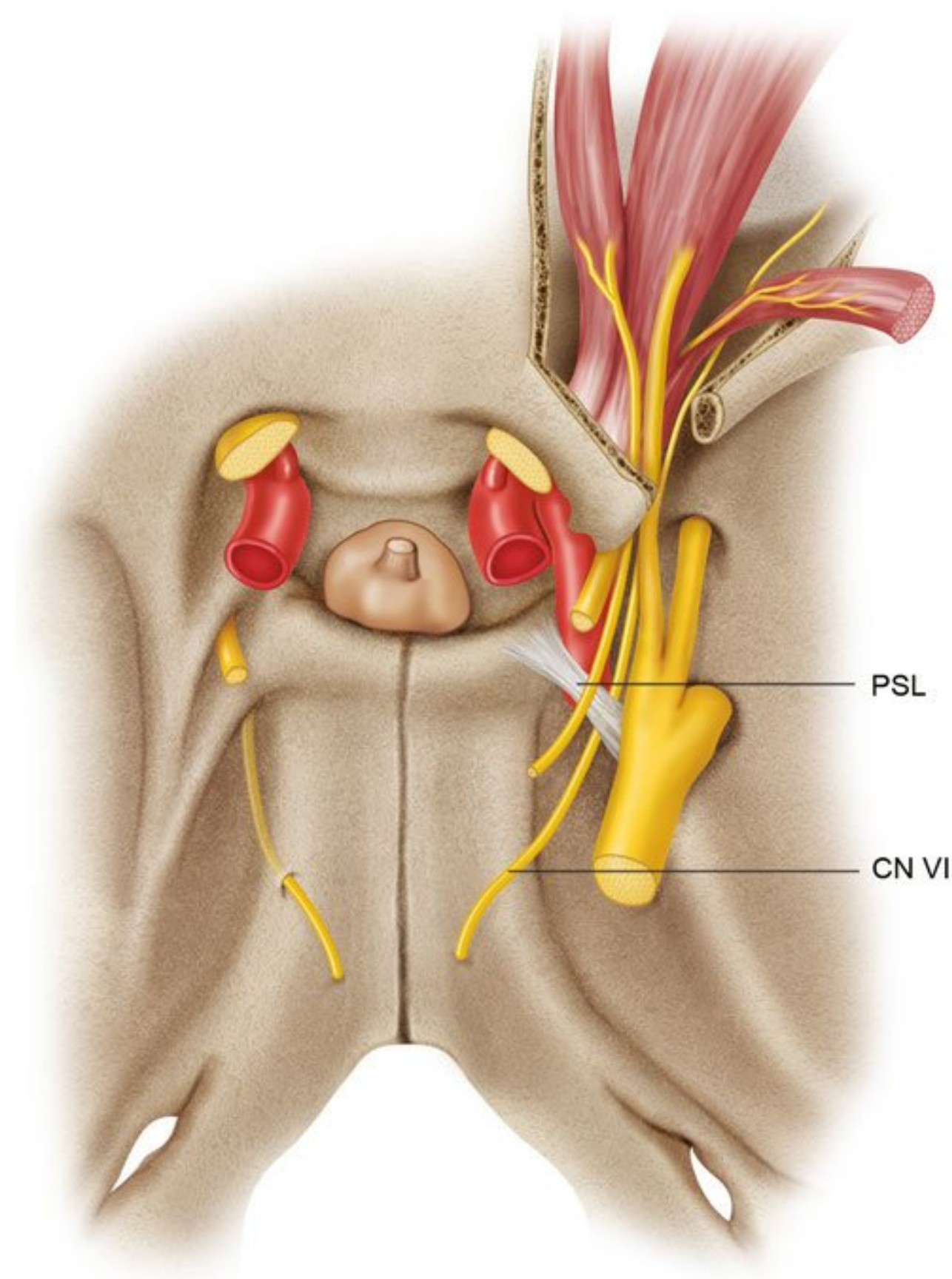


Fig. 3.6 The right cranial nerve (CN VI), the abducens nerve, enters the posterior wall of the cavernous sinus, beneath the petrosphenoid ligament, through Dorello's canal, and travels within the cavernous sinus, lateral to the cavernous internal carotid artery.

no branches, enters the carotid canal at the skull base, and travels medially in the carotid canal as the petrous C2 segment, surrounded by bone at its most solid posteromedial and relatively thinner anterolateral and inferior walls, with the roof being covered by dura. The petrous segment of ICA branches are the small caroticotympanic arteries, which enter the middle ear and the occasionally present vidian artery that usually arises from the maxillary artery, which in turn is a branch of the external carotid artery. The petrous carotid artery ends medially partially surrounded by fibrocartilaginous tissue contiguous with the cartilage of the foramen lacerum, over which the ICA passes as the lacerum C3 segment. The foramen lacerum is not within a single bone; rather, it is actually a cartilage-filled gap separating the petrous apex from the basisphenoid medially and the basiocciput posteriorly. Meningeal branches of the ascending pharyngeal artery pass through the cartilage-filled foramen.¹ Then the ICA turns superiorly on its way to the cavernous sinus, passing under a fibrous band called the *petrolingual ligament* (which extends from the petrous apex to the lingula of the carotid sulcus of the sphenoid body), after which the cavernous C4 segment begins. The petrosphenoid ligament or Gruber's ligament (which extends from the petrous apex to posterior clinoid process) is situated superior to the petrolingual ligament, and the abducens nerve (CN VI) lies just lateral and parallel

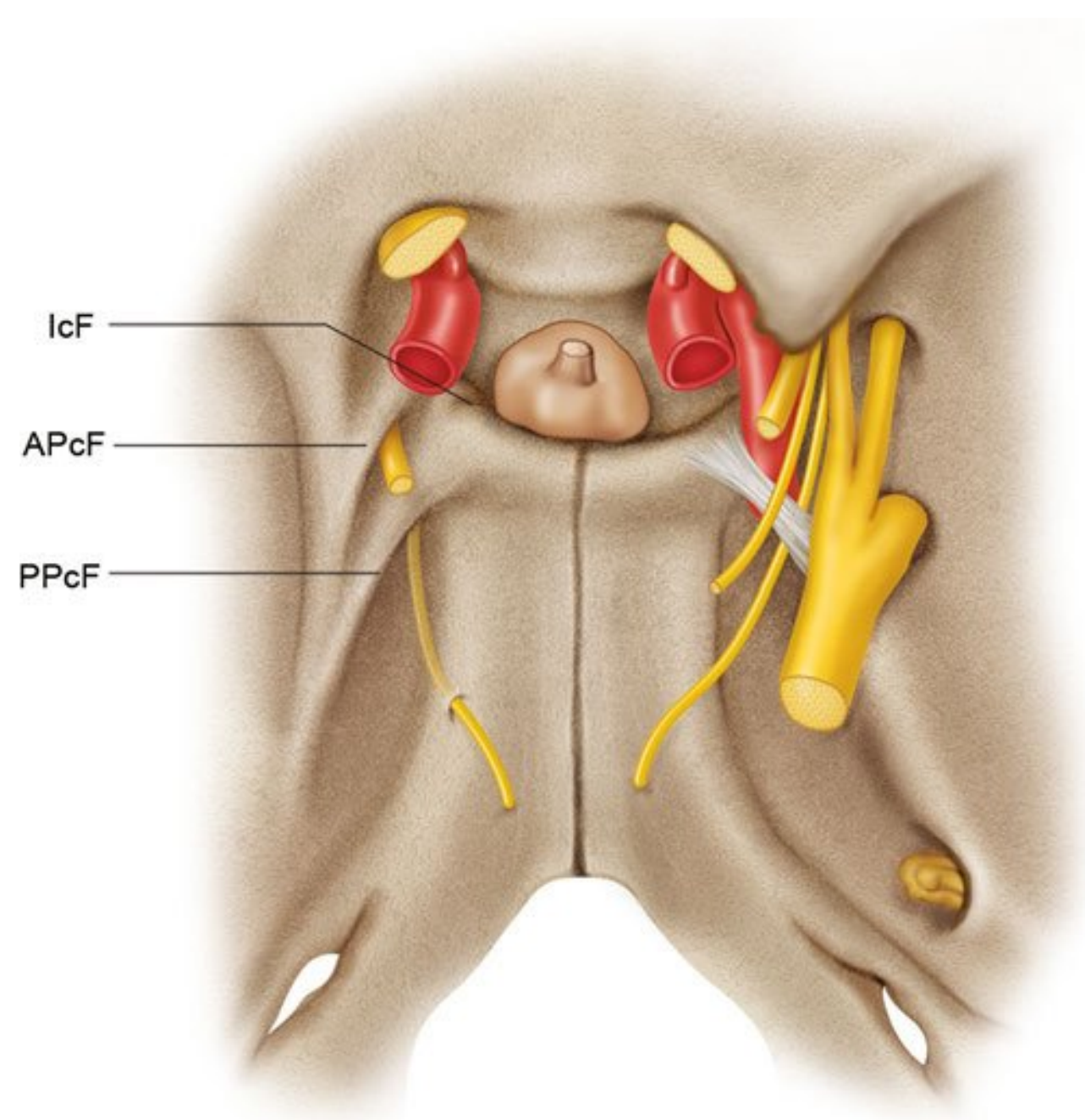


Fig. 3.7 Cranial nerve III, the oculomotor nerve, pierces the roof of the cavernous sinus on the left. Marginal thickening of the dura forms three distinct folds: the anterior petroclinoid fold (APcF), the posterior petroclinoid fold (PPcF), and the interclinoid (IcF) fold; these folds form the oculomotor triangle.

to the horizontal portion of the cavernous ICA underneath the petrosphenoid ligament.^{16–18}

The cavernous C4 segment travels superiorly and then turns anteriorly with a horizontal course along the cavernous sinus.

This horizontal portion of cavernous ICA lies in a shallow sulcus along the lateral aspect of body of sphenoid, called the carotid sulcus. Dehiscence of the bone in this location allows the ICA to project into the sphenoid sinus, potentially posing a risk during endoscopic trans-sphenoidal surgery. The characteristically described three named branches of the cavernous ICA are the meningohypophyseal trunk, inferolateral trunk, and capsular artery. The meningohypophyseal trunk (dorsal mainstem artery) arises from the cavernous ICA at the center of the outer convexity of its posterior genu, where the initial ascending segment turns anteriorly to become the horizontal segment, and subdivides into three vessels: the tentorial artery (artery of Bernasconi and Cassinari), the dorsal meningeal artery, and the inferior hypophyseal artery. The inferolateral trunk (lateral mainstem artery or artery of the inferior cavernous sinus) arises from the horizontal portion of the cavernous ICA segment itself and supplies small arterial branches to the intracavernous cranial nerves and tentorium. This artery is clinically important because it is anastomosed with the external carotid artery branches through the foramen rotundum, ovale, and spinosum. McConnell's capsular artery arises from the most superior segment of the intracavernous ICA and supplies the inferior and peripheral aspect of the anterior lobe of the pituitary gland and the diaphragma sellae.

The ICA then turns vertically near the anterior margin of the cavernous sinus and continues medially to the anterior clinoid process, where it passes through two dural rings, the proximal dural ring (which forms the true roof of the cavernous sinus anteriorly), and the distal dural ring (which represents the anatomical border between the extradural and intradural ICA). This short vertical segment of ICA medial to the anterior clinoid process between the proximal and distal dural rings is called the clinoid C5 segment, and it has no named branches. Differentiation of an ICA aneurysm, which has a neck in the proximal intra-

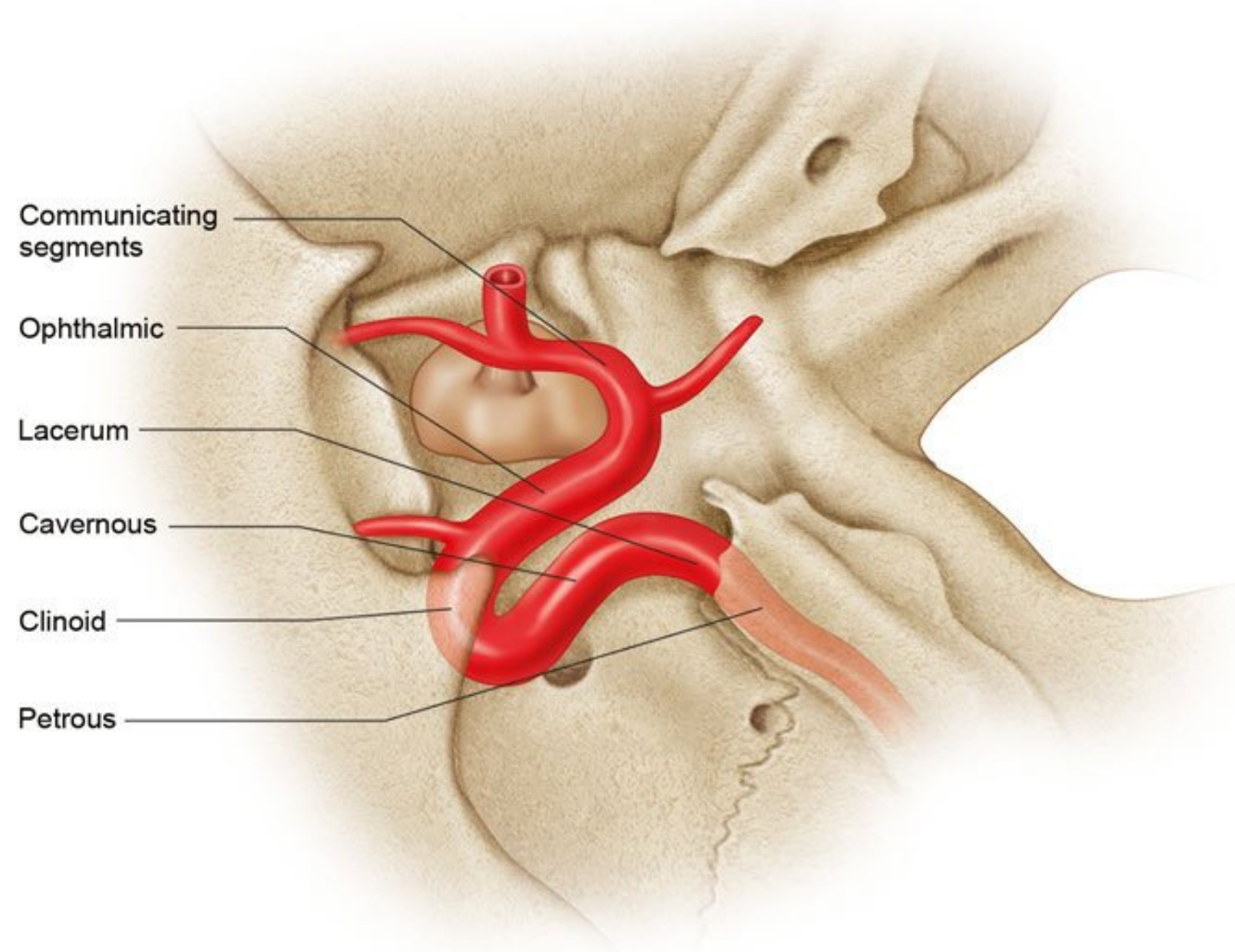


Fig. 3.8 The seven-segment classification system for the internal carotid artery. From proximal to distal, these include the (1) cervical (not shown), (2) petrous, (3) lacerum, (4) cavernous, (5) clinoid, (6) ophthalmic, and (7) communicating segments. All but the cervical segment are intimately related to the central skull base region.

dural segment that could produce a carotid–cavernous fistula if it bleeds, from one with a neck in the distal intradural segment, which can produce life-threatening subarachnoid hemorrhage, is extremely important. Although the dural rings are not seen at imaging, the location of the proximal dural ring can be assumed by the knowledge that (1) it forms the superomedial margin of the easily identifiable optic strut, a tiny bony process connected to the anterior clinoid process of the lesser wing of sphenoid; and (2) it separates the medial optic canal from the superior orbital fissure laterally.¹⁹ The distal dural ring, lying superior to the proximal dural ring, forms the real line of demarcation between the extradural and intradural ICA and can be assumed to be at the junction of the CSF and cavernous sinus on high-resolution coronal 3D CT cisternography or 3D T2 MRI.²⁰

After this, the ICA continues into the intradural subarachnoid space as the ophthalmic C6 segment, giving rise to the ophthalmic artery anteriorly and superior hypophyseal artery projecting posteroinferomedially into the sella. The terminal communicating C7 segment of the ICA begins just before the origin of its branch called the posterior communicating artery (PCOM) and ends by bifurcating into the anterior cerebral artery and middle cerebral artery. The anterior choroidal artery arises from the communicating segment immediately distal to the origin of the PCOM.

Structures Filling Posterior Aspect of the Sphere

Petrous Apex and Petroclival Junction

The petrous apex, the pyramidal obliquely oriented anteromedial extension of petrous temporal bone, must be considered a part of the 3D configuration of the middle skull base. Petrous apex pneumatization varies, being filled with bone marrow in 60%, pneumatized in 33% and sclerotic in 7% (**Fig. 3.9**). A pneumatized petrous apex may communicate directly with the mastoid or middle ear cavity and provide direct pathways for disease spread. Pneumatization is asymmetric in 5 to 10% and the T1 hyperintense marrow fat on the nonpneumatized side has the potential to mimic a lesion in MRI. Pneumatized petrous apices are more prone to apical petrositis and nonpneumatized marrow containing apices to disease processes like metastasis.^{21–23} The clinically important Dorello's canal, petro-occipital fissure, and Meckel's cave are in close relation to the petrous apex. Dorello's canal is a small channel between two layers of dura overlying the superomedial aspect of the petrous apex, where it is fused to the posterolateral sphenoid body below the posterior clinoid process. This channel transmits the abducens nerve (CN VI) and is surrounded by the inferior petrosal sinus, which in turn is continuous with the cavernous sinus anteriorly and drains into inferior petrosal sinus. Petro-occipital (petroclival fissure) fissure is the oblique cartilaginous junction of inferomedial petrous temporal bone and inferolateral clivus. This cartilage-filled fissure appears lucent on CT scans, but it can be variably ossified and dense and is the classic site of origin for skull base chondrosarcoma.²⁴

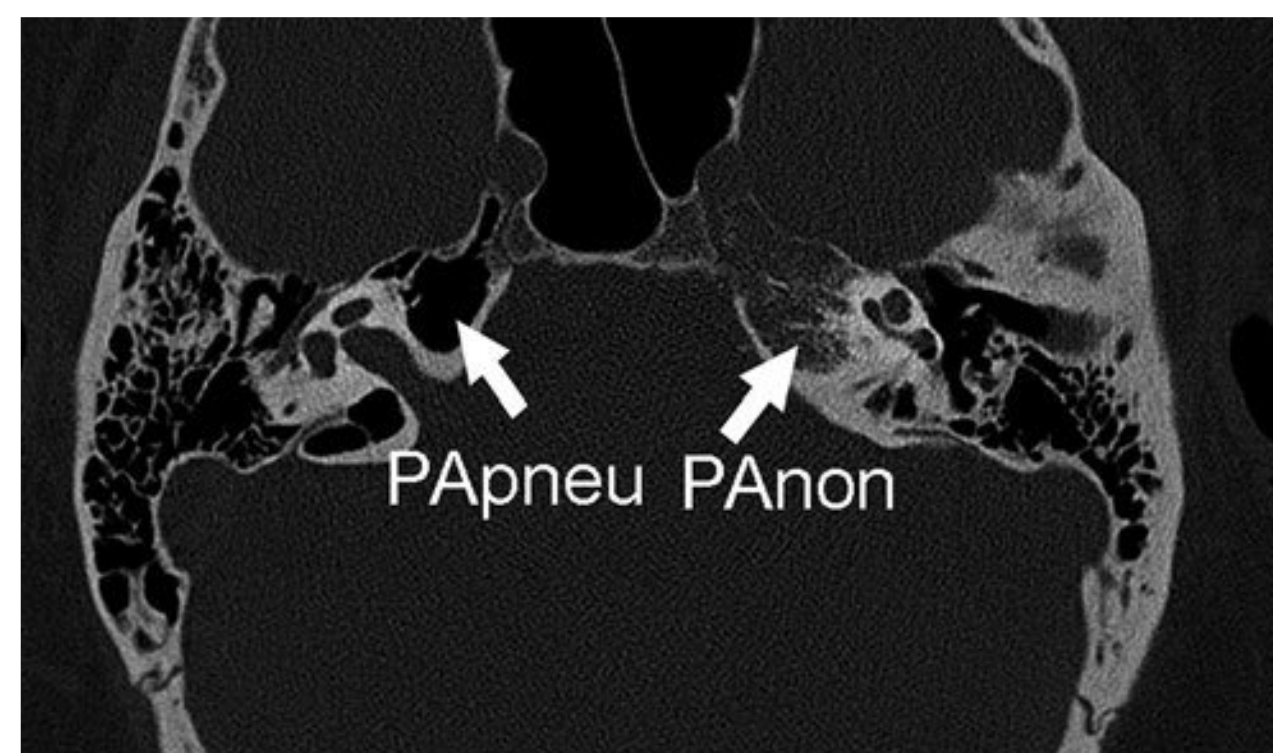


Fig. 3.9 Axial computed tomography image through the petrous apex demonstrates the variability in pneumatization of the petrous apex. The petrous apex on the right is well pneumatized and demonstrates air density (PApneu); the contralateral petrous apex is nonpneumatized and demonstrates bone trabecular bone density (PAnon).

Meckel's Cave

Meckel's cave is a localized dural outpouching over the petrosphenoid junction at the posteromedial aspect of middle cranial fossa. It houses the trigeminal (Gasserian) ganglion within its anteroinferior aspect and the caval segment of trigeminal nerve more posteriorly. Immediately posterior to Meckel's cave, the trigeminal nerve lies in close relation to a small depression in the superior aspect of the petrous apex, just lateral to petrosphenoid junction, called the trigeminal impression. The trigeminal nerve then travels into the posterior fossa as the cisternal segment and enters the pons at the root entry zone. Anteromedially, Meckel's cave is closely opposed to the posteroinferolateral aspect of the cavernous sinus and is just lateral to the ICA near the lacerum or proximal cavernous segment, where the artery begins to run anterosuperiorly into the cavernous sinus. The three major divisions of trigeminal nerve arise within the Meckel's cave. The ophthalmic division (V1) runs anteromedially to enter the lateral wall of cavernous sinus, whereas the maxillary division (V2) runs anteriorly underneath the cavernous sinus to enter into foramen rotundum, and the mandibular division (V3) extends inferolaterally along the foramen ovale into the masticator space.²⁵

Extracranial Structures Lying Anterior/Inferior to Center of the Sphere

Orbital Apex and Pterygopalatine Fossa

The orbital apex is contiguous with the middle skull base through the optic canal in the lesser wing of the sphenoid, superior orbital fissure between the lesser and greater wings and the pterygopalatine fossa through the inferior orbital fissure. Orbital tumors like optic nerve sheath meningioma, inflamma-

tory lesions like orbital apex pseudotumor, and infections like invasive fungal disease can extend into the middle skull base and vice versa. Orbital apex syndrome can produce vision loss, ophthalmoplegia, and multiple cranial neuropathies as a result of the connections with cavernous sinus and pterygopalatine fossa. Superior ophthalmic vein thrombosis, which usually arises from infections in the dangerous triangle of the face, can lead to cavernous sinus thrombosis. Despite classic assumptions that the absence of valves in the facial and superior ophthalmic veins is thought to facilitate infectious spread from the midface region to the cavernous spread, a recent cadaveric stereomicroscopic study has demonstrated valves in these veins. The consistent communications between the facial vein and cavernous sinus and the direction of blood flow are important in the spread of infection rather than absence of valves.²⁶

The optic canal is the pathway of optic nerve and ophthalmic artery and lies entirely within the lesser wing of sphenoid. The optic strut (inferior root of lesser wing), along with the anterior clinoid process of the lesser wing of sphenoid, which it is connected to, separates the optic canal from the superior orbital fissure laterally. The fatty bone marrow in the optic strut may have high T1 MRI signal and may be seen projecting inferomedially from the anterior clinoid process, separating the optic nerve from the oculomotor and other cranial nerves. The anterolateral aspect of body of the sphenoid bone forms the medial boundary of optic canal, and a thin bony bridge called the superior root of the lesser wing forms its roof.²⁷ Within the dural sheath in optic canal, the ophthalmic artery lies inferolateral to optic nerve. It later leaves the dura and crosses above the optic nerve from lateral to medial sides, giving rise to the central retinal artery as it winds around the nerve. The ciliary ganglion lies in the posterior orbit between the optic nerve and lateral rectus muscle at the lateral aspect of ophthalmic artery.

The superior orbital fissure (SOF) is an oblique gap between the lesser wing of sphenoid superomedially and the greater wing of sphenoid inferolaterally (**Fig. 3.10**). It connects the orbit and middle cranial fossa via the cavernous sinus. It is divided by the annulus of Zinn, a tough fibrous aponeurotic ring at the orbital apex, into a medial intraconal compartment (containing CN III, CN VI, and the nasociliary nerve) and a lateral extraconal compartment (containing CN IV, frontal, and lacrimal nerves, and the superior ophthalmic vein). The extraocular muscles arise from the annulus of Zinn, except the inferior oblique muscle, which originates at anteroinferior orbital rim. In addition to the medial SOF compartment, the annulus also surrounds the optic canal, and hence the optic nerve and ophthalmic artery become intraconal structures.

The intraconal medial SOF is wider, lies directly anterior to the cavernous sinus, and contains the oculomotor nerve (CN III), which immediately divides into the superior division (to supply superior rectus and levator palpebrae superioris muscles) and the inferior division (to supply the medial rectus, inferior rectus, and inferior oblique muscles). The medial compartment also contains the abducens nerve (CN VI to supply lateral rectus muscle) lying immediately lateral to the CN III superior division and the nasociliary nerve further superiorly. Note that the nasociliary nerve is one of the three branches of the sensory ophthalmic division of trigeminal nerve (CN V₁) branching within the distal cavernous sinus before entering the orbit.

The other two branches of the ophthalmic CN V₁, namely, the frontal and lacrimal nerves, lie within the smaller extraconal lateral compartment of SOF inferiorly and superolaterally respectively. The trochlear nerve (CN IV to supply the superior oblique muscle) enters the orbit at the extraconal lateral SOF compartment outside the annulus of Zinn and lies here above the frontal nerve and inferomedial to the lacrimal nerve. The

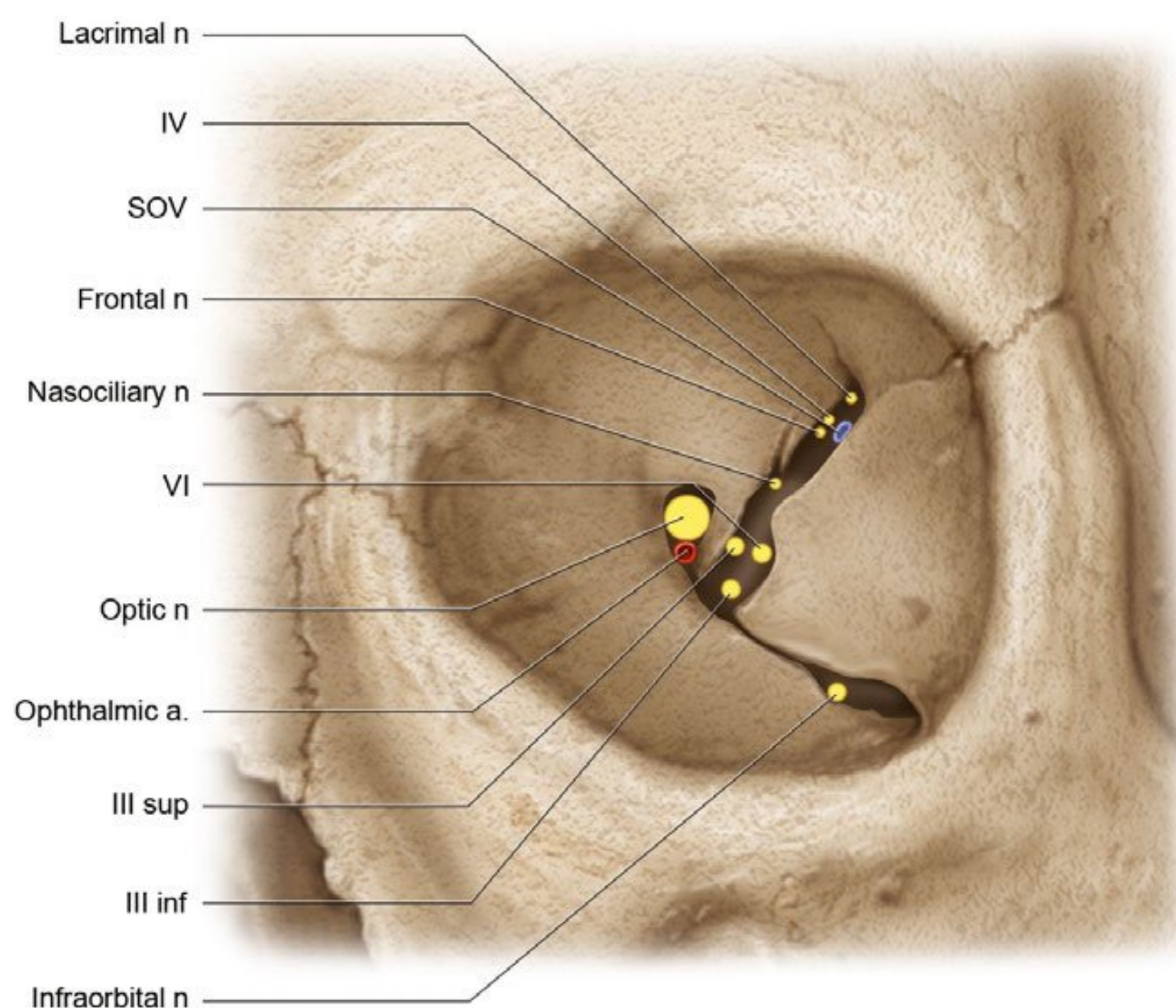


Fig. 3.10 Orbital apex. The superior, medial, inferior, and lateral rectus muscles converge posteriorly and attach to a dense fibrous ring, the annulus of Zinn. The ring circumscribes the optic canal and the inferomedial aspect of the superior orbital fissure. The optic canal contains the optic nerve and ophthalmic artery. The oculomotor nerve (CN III) enters the medial superior orbital fissure and divides into superior and inferior divisions. The nasociliary and abducens (CN VI) nerves also enter through the medial compartment. Laterally, the superior orbital fissure contains the trochlear nerve (CN IV), the lacrimal nerve, the frontal nerve, and the superior ophthalmic vein (SOV).

superior ophthalmic vein lies further lateral to the nerves in the lateral SOF compartment.

The inferior orbital fissure is an oblique gap situated between the floor and lateral wall of orbit (greater wing of sphenoid). It communicates with the pterygopalatine fossa and masticator space and contains the infraorbital nerve and zygomatic nerve (branches of the maxillary division of the trigeminal nerve CN V2), inferior ophthalmic vein division, or emissary veins between the inferior ophthalmic vein and the pterygoid plexus.^{28,29}

The pterygopalatine fossa (PPF) is a fat-filled space between the maxillary sinus anteriorly and pterygoid process of sphenoid bone posteriorly. Medially, it is partially bound by a portion of the perpendicular plate of the palatine bone (**Fig. 3.11**). The PPF contains the small pterygopalatine ganglion at its medial aspect, the maxillary nerve (V2) entering via the foramen rotundum, and the distal internal maxillary artery entering via the pterygomaxillary fissure. It is difficult to differentiate the ganglion from nerves and vessels in the PPF, even with high-resolution CT/MRI. Although it is quite small, the PPF has important connections with the middle skull base, orbit, palate, and nasal cavity and can act as a junctional area for the spread of infiltrating or perineural tumor and infection.

Masticator Space

The pterygomaxillary fissure is the lateral opening of PPF into the nasopharyngeal masticator space (infratemporal fossa). The sphenopalatine foramen is its mucosa-covered medial opening into the superior meatus of the nose through a gap in its medial boundary formed by the palatine bone. Nasopharyngeal angiofibromas arise in this region. The PPF communicates superi-

orly with the SOF. The inferior orbital fissure is its anterior opening into the orbit, which transmits the infraorbital nerve (CN V2 continuation branch) and artery. The foramen rotundum is the pathway along which the intracranial maxillary nerve (CN V2) passes into the PPF after traveling in the dura underneath the lateral wall of the cavernous sinus. The canal can be easily identified in axial CT and MRI connecting the PPF to middle cranial fossa alongside the lateral wall of the cavernous sinus and in coronal imaging superior to an occasionally pneumatized lateral recess of the sphenoid sinus. The vidian canal is a channel that runs through the body of the sphenoid bone connecting the PPF to the foramen lacerum, which in turn is the anteroinferomedial cartilaginous floor of the horizontal petrous ICA canal situated between the sphenoid and temporal bones. In coronal sections, the vidian canal is seen inferomedial to the foramen rotundum with an occasionally pneumatized lateral recess of the sphenoid sinus between them. The pterygopalatine canal is the common inferior canal leading from the PPF and carrying the palatine nerves, and ultimately it divides into an anterior greater palatine foramen and posterior lesser palatine foramen at the hard palate.^{30,31}

The masticator space, containing the mastication muscles, is intimately related to the middle skull base through (1) the foramina in the greater wing of sphenoid (e.g., foramen ovale transmitting mandibular division of trigeminal nerve, CN V3); (2) the lesser petrosal nerve, accessory meningeal branch of maxillary artery and emissary vein; and (3) the tiny foramen spinosum, just posterolateral to it (transmitting the middle meningeal artery and vein and meningeal branch of CN V3). These foramina are easily identified on CT images just anterolateral to the horizontal petrous carotid canal. As described already herein, the masticator space is connected with the PPF through the pterygomaxillary fissure. These connections allow perineural

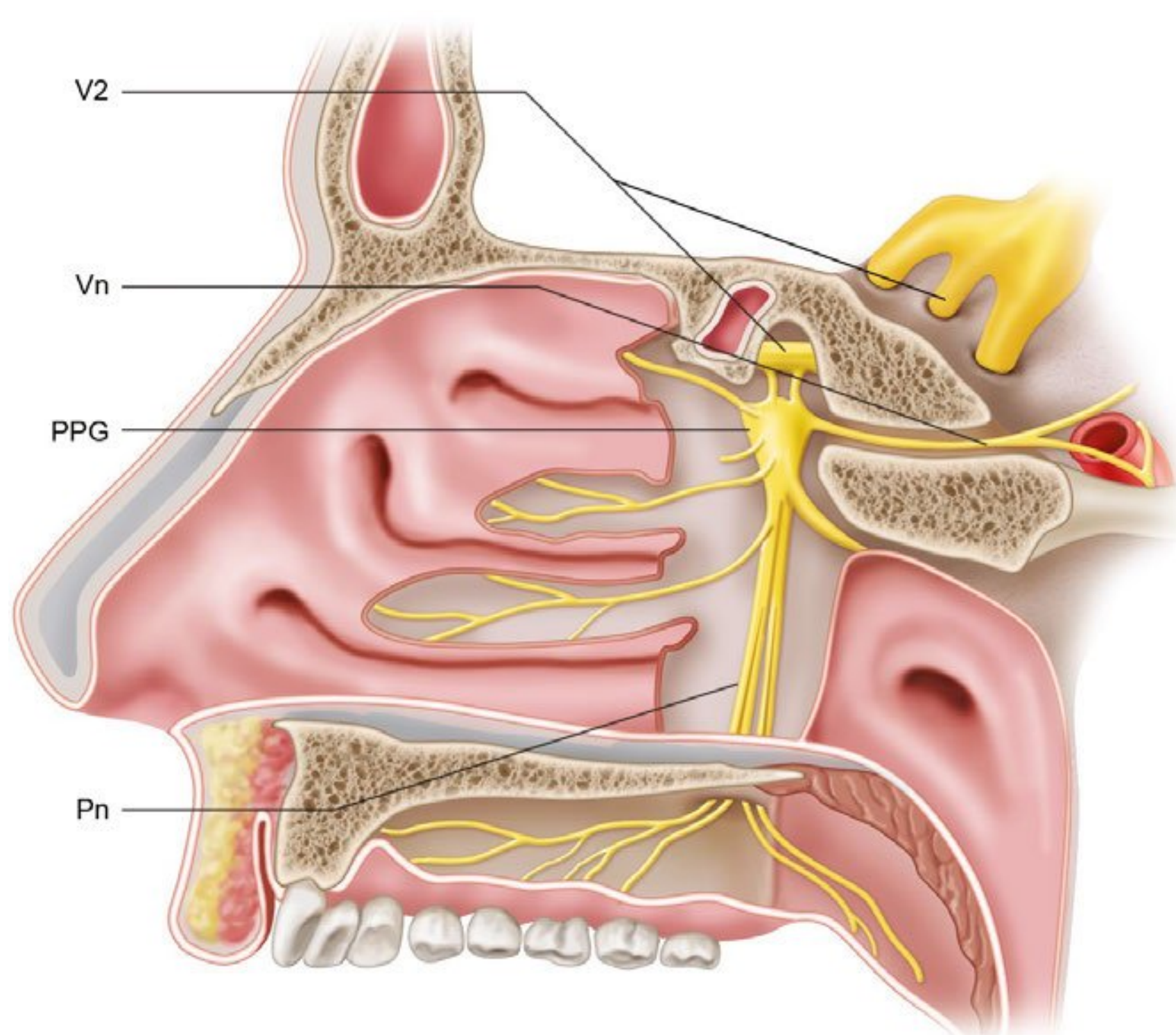


Fig. 3.11 Pterygopalatine fossa (PPF). The posterior aspect of the lateral nasal wall has been dissected, exposing the sphenopalatine foramen and pterygopalatine fossa. The pterygopalatine ganglion (PPG) has multiple neural connections. The maxillary nerve (V2) traverses the upper aspect of the PPF. The vidian nerve (VN) is seen passing from the ganglion into the vidian canal. The greater and lesser palatine nerves (Pn) descend into the palatine canal and into the submucosa of the palate.

tumor spread within the middle skull base. Aggressive masticator space lesions can also erode bone and extend intracranially. The superficial layer of the deep cervical fascia splits to enclose this space, which extends inferiorly to the attachment of medial pterygoid and masseter muscles onto the mandible and superiorly abuts the skull base, with the foramen ovale and foramen spinosum included in this space. Superolaterally, the masticator space extends along the outer surface of the skull as far as the temporalis muscle.³²

Nasopharynx

The nasopharynx lies immediately inferior to the basisphenoid and clival region of the middle skull base and is an important area to evaluate for contiguous intracranial spread of tumor or aggressive infection (**Fig. 3.12**). It extends from the posterior nasal choana anterosuperiorly to the retropharyngeal and prevertebral space posteriorly and the parapharyngeal spaces lie laterally. Anteroinferiorly, the soft palate separates it from the oropharynx with the posterior side of the soft palate considered part of nasopharynx and its anteroinferior side part of oropharynx. The separation posterior to the soft palate is arbitrary, using an imaginary horizontal line along the hard palate or superior edge of the anterior arch of C1 or through the atlantoaxial articulation.^{33,34}

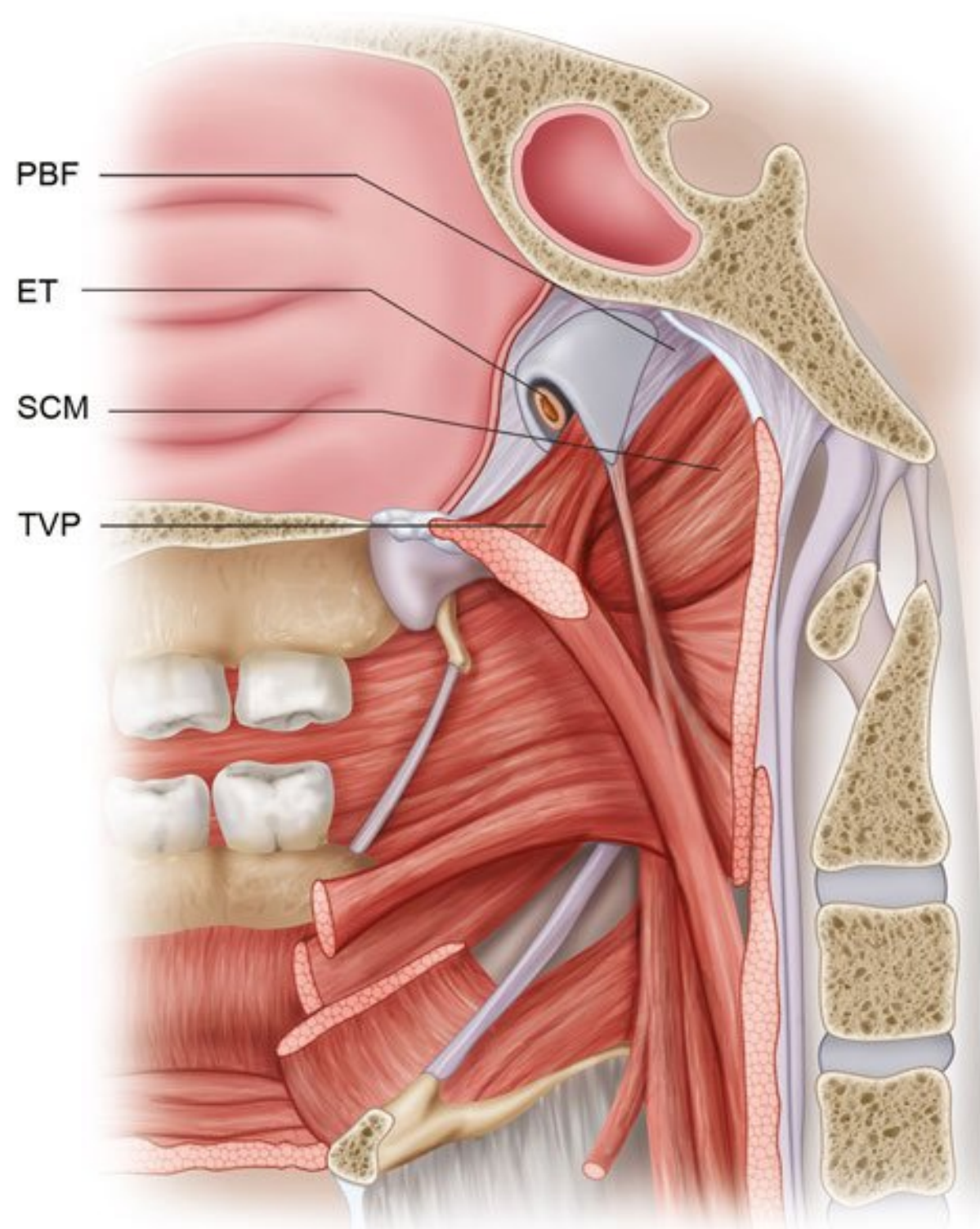


Fig. 3.12 Illustration of the submucosal nasopharynx. The superior constrictor muscle (SCM) attaches to the skull base via the pharyngobasilar fascia (PBF). The eustachian tube (ET) passes through a defect in the PBF referred to as the sinus of Morgagni. The tensor veli palatini (TVP) muscle is seen arising from the cartilaginous eustachian tube and extending inferiorly to the lateral margin of the soft palate.

The middle visceral or pharyngeal mucosal layer of the deep cervical fascia encloses the pharynx; hence, the oropharynx and nasopharynx are collectively called the visceral space or pharyngeal mucosal space (PMS). The nasopharyngeal superficial mucosa consists of epithelium of the PMS and can give rise to nasopharyngeal squamous cell carcinoma.⁵ The submucosal space contains lymphoid tissue, accessory salivary glands, and cellular notochord remnants, which can give rise to benign and malignant lesions like lymphoma, salivary gland tumors, and chordoma. The nasopharyngeal tonsils are called adenoids; they lie at the midline roof of the nasopharynx and are usually prominent in children.

The pharyngeal tubercle of the occipital bone provides posterior attachment to the midline pharyngeal raphe and the paired superior constrictor muscles of the pharynx; however, the superior constrictor muscle of either side fans forward to attach to the lower portion of the medial pterygoid plate. This exposes a gap between the muscles and the skull base, which is filled by the pharyngobasilar fascia, a tough aponeurosis that surrounds the pharynx and attaches to the skull base. The pharyngobasilar fascia attaches to the medial pterygoid plate anteroinferiorly and extends superiorly to the skull base. It fills the gap between the muscles and skull base as it proceeds posteriorly, attaching to the body of sphenoid bone, petrous apex, foramen lacerum, and more posteriorly as it processes to the occipital pharyngeal tubercle and prevertebral muscles. Therefore, the foramen lacerum lies within the attachment of this fascia to the skull base, whereas the foramen ovale is seen lateral to this fascia. The eustachian tube and levator veli palatini muscle enter the nasopharynx through a posterolateral defect of the pharyngobasilar fascia called the sinus of Morgagni. Protection from tumor spread from the nasopharynx to the middle skull base and vice versa by the tough pharyngobasilar fascia is deficient at the sinus of Morgagni and at the foramen lacerum, even though fibrocartilage closes this foramen.³⁵

The tensor veli palatini and levator veli palatini muscles reside in the nasopharynx. The torus tubarius is the prominent medial end of the cartilaginous eustachian tube, which together with the levator veli palatini muscle and the overlying mucosa forms a ridgelike protrusion into the nasopharynx.³³ The eustachian tube orifice is a mucosa-lined recess in front of the torus tubarius. The lateral pharyngeal recess or fossa of Rosenmüller is another mucosa-lined recess located posterosuperior to the torus tubarius. The fossa of Rosenmüller is an important site of origin of nasopharyngeal carcinoma and appears to be posterior to the eustachian tube orifice on axial images and superior on coronal images owing to the configuration of the torus tubarius.

The eustachian tube connects the middle ear to the nasopharynx (**Fig. 3.13**). The posterolateral bony portion begins along the anterior wall of the tympanic cavity and travels anteroinferomedially toward the nasopharynx and is seen just inferolateral to the prominent landmark of proximal petrous carotid canal in axial CT scan images. The bony portion of the tube continues as the cartilaginous portion at the sphenopetrous groove, which is the gap between the posterior margin of the greater wing of sphenoid and the anterior margin of petrous temporal bone. The cartilaginous portion can be seen as a soft tissue density immediately posterior to the foramen ovale and foramen spinosum on axial CT scans and continues into the nasopharynx as described already. Mass lesions in the nasophar-

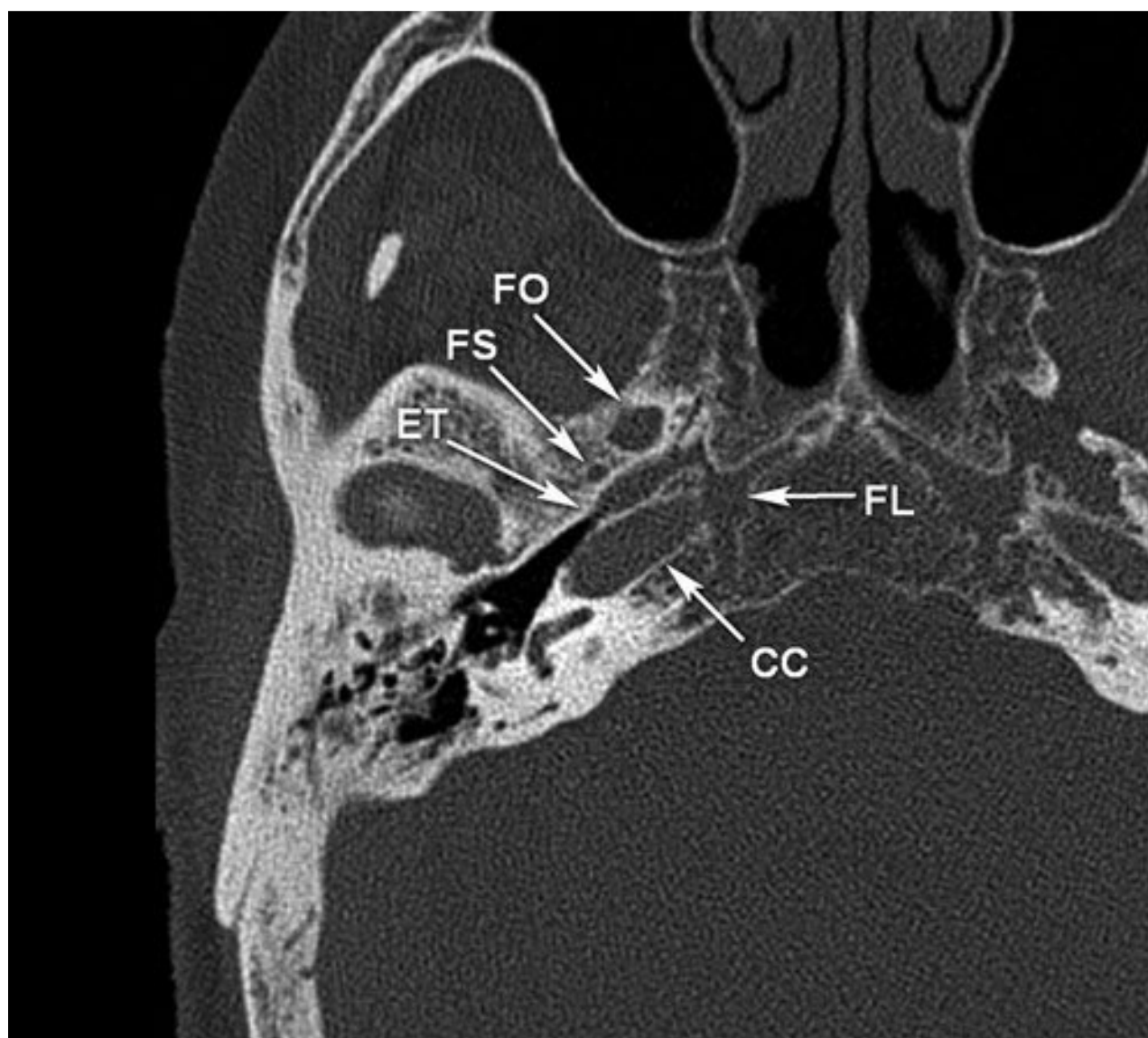


Fig. 3.13 Axial computed tomographic image through the skull base demonstrates the relationships between various foramina, fissures, and canals along the lateral margin of the central skull base region. The internal carotid artery passes obliquely through the carotid canal (CC) and exits the canal just above cartilage-filled gap, the foramen lacerum (FL). The eustachian tube (ET) consists of bony and cartilaginous segments and passes both medially and inferiorly from the middle ear to the nasopharynx. Note the intimate relationship between the eustachian tube, the carotid canal and the foramen spinosum (FS).

ynx, especially those in the fossa of Rosenmüller, can compress the eustachian tube opening and lead to the development of middle ear and mastoid effusions. It is extremely important to evaluate for any nasopharyngeal mass lesion when unilateral middle ear or mastoid effusion is identified on a brain or paranasal sinus CT scan.

The retropharyngeal space (RPS) lies behind the pharynx, immediately posterior to the middle (visceral) layer of deep cervical fascia and anterior to deep (prevertebral) layer of deep

cervical fascia. The nasopharyngeal RPS extends superiorly to the basiocciput and the thin horizontal alar fascia extending from the skull base to cervicothoracic region divides the space into an anterior true RPS and posterior danger space. Anywhere between the C6 and T4 level, the alar fascia fuses with the anterior middle (visceral) layer of the deep cervical fascia and terminates at the inferior extent of the true RPS; however, the posterior danger space continues inferiorly as a potential source of skull-base infection spread into the posterior mediastinum. The RPS harbors normal fat and retropharyngeal lymph nodes, especially laterally. The retropharyngeal lymph nodes (RPLNs) are divided into a lateral group that overlie the prevertebral fascia at the level of the upper cervical vertebral transverse processes and are more commonly involved by pathology especially from squamous cell carcinomas of the nasopharynx, oropharynx, hypopharynx, and nasal cavity and an inconsistent small medial group. It is important to note that only those nodes lying medial to the ICA and within 2 cm of the skull base are classified as RPLN on imaging-based classification. If a lymph node situated within 2 cm of the skull base lies anterior, lateral, or posterior to the carotid sheath, it is classified as a level II node. Nodes inferior to a level 2 cm below the skull base are not named RPLN.³⁶

The prevertebral space (PVS), which lies immediately posterior to the RPS, is surrounded by the deep (prevertebral) layer of deep cervical fascia. In the suprahyoid neck, the PVS contains prevertebral muscles longus colli and capitis, vertebral body, cervical intervertebral disk, spinal canal, vertebral arteries, and the phrenic nerve. Specifically, at the nasopharyngeal level, the larger longus capitis and the smaller anterior rectus capitis muscles behind it reside in this location. Differentiation of PVS lesions from the anterior RPS and lateral carotid space lesions is sometimes challenging, especially if the lesions are large. Useful hints for imaging include the fact that a PVS abscess elevates the prevertebral muscles, whereas a RPS abscess does not. Likewise, bony erosion of adjacent anterior portion of vertebral body favors a PVS tumor like rhabdomyosarcoma, whereas erosion along the lateral aspect of a vertebra favors a carotid space tumor like neuroblastoma.^{1,29}

References

1. Chapman PR, Bag AK, Tubbs RS, Gohlke P. Practical anatomy of the central skull base region. *Semin Ultrasound CT MR* 2013;34(5): 381–392 [PubMed](#)
2. Borges A. Imaging of the central skull base. *Neuroimaging Clin N Am* 2009;19(3):441–468 [PubMed](#)
3. Morani AC, Ramani NS, Wesolowski JR. Skull base, orbits, temporal bone, and cranial nerves: anatomy on MR imaging. *Magn Reson Imaging Clin N Am* 2011;19(3):439–456 [PubMed](#)
4. Laine FJ, Nadel L, Braun IFCT. CT and MR imaging of the central skull base. Part 1: Techniques, embryologic development, and anatomy. *Radiographics* 1990;10(4):591–602 [PubMed](#)
5. Laine FJ, Nadel L, Braun IFCT. CT and MR imaging of the central skull base. Part 2. Pathologic spectrum. *Radiographics* 1990;10(5): 797–821 [PubMed](#)
6. Rhoton AL Jr. The sellar region. *Neurosurgery* 2002;51(4, Suppl): S335–S374 [PubMed](#)
7. Unal B, Bademci G, Bilgili YK, Batay F, Avci E. Risky anatomic variations of sphenoid sinus for surgery. *Surg Radiol Anat* 2006;28(2): 195–201 [PubMed](#)
8. Hamid O, El Fiky L, Hassan O, Kotb A, El Fiky S. Anatomic variations of the sphenoid sinus and their impact on trans-sphenoid pituitary surgery. *Skull Base* 2008;18(1):9–15 [PubMed](#)
9. Vattoth S, Cherian J, Pandey T. Magnetic resonance angiographic demonstration of carotid-cavernous fistula using elliptical centric time resolved imaging of contrast kinetics (EC-TRICKS). *Magn Reson Imaging* 2007;25(8):1227–1231 [PubMed](#)
10. Miyazaki Y, Yamamoto I, Shinozuka S, Sato O. Microsurgical anatomy of the cavernous sinus. *Neurol Med Chir (Tokyo)* 1994;34(3): 150–163 [PubMed](#)
11. Cottier JP, Destrieux C, Brunereau L, et al. Cavernous sinus invasion by pituitary adenoma: MR imaging. *Radiology* 2000;215(2):463–469 [PubMed](#)
12. Tubbs RS, Hill M, May WR, et al. Does the maxillary division of the trigeminal nerve traverse the cavernous sinus? An anatomical study and review of the literature. *Surg Radiol Anat* 2008;30(1):37–40 [PubMed](#)
13. Hardjasudarma M, Edwards RL, Ganley JP, Aarstad RF. Magnetic resonance imaging features of Gradenigo's syndrome. *Am J Otolaryngol* 1995;16(4):247–250 [PubMed](#)

14. Isolan GR, Kraysenbühl N, de Oliveira E, Al-Mefty O. Microsurgical anatomy of the cavernous sinus: measurements of the triangles in and around it. *Skull Base* 2007;17(6):357–367 [PubMed](#)
15. Bouthillier A, van Loveren HR, Keller JT. Segments of the internal carotid artery: a new classification. *Neurosurgery* 1996;38(3):425–433 [PubMed](#)
16. Liu XD, Xu QW, Che XM, Mao RL. Anatomy of the petrosphenoidal and petrolingual ligaments at the petrous apex. *Clin Anat* 2009;22(3):302–306 [PubMed](#)
17. Chapman PR, Gaddamanugu S, Bag AK, Roth NT, Vattoth S. Vascular lesions of the central skull base region. *Semin Ultrasound CT MR* 2013;34(5):459–475 [PubMed](#)
18. Tubbs RS, Hansasuta A, Loukas M, et al. Branches of the petrous and cavernous segments of the internal carotid artery. *Clin Anat* 2007;20(6):596–601 [PubMed](#)
19. Hashimoto K, Nozaki K, Hashimoto N. Optic strut as a radiographic landmark in evaluating neck location of a paraclinoid aneurysm. *Neurosurgery* 2006;59(4):880–895, discussion 896–897 [PubMed](#)
20. Watanabe Y, Nakazawa T, Yamada N, et al. Identification of the distal dural ring with use of fusion images with 3D-MR cisternography and MR angiography: application to paraclinoid aneurysms. *AJNR Am J Neuroradiol* 2009;30(4):845–850 [PubMed](#)
21. Connor SE, Leung R, Natas S. Imaging of the petrous apex: a pictorial review. *Br J Radiol* 2008;81(965):427–435 [PubMed](#)
22. Isaacson B, Kutz JW, Roland PS. Lesions of the petrous apex: diagnosis and management. *Otolaryngol Clin North Am* 2007;40(3):479–519, viii [PubMed](#)
23. Razek AA, Huang BY. Lesions of the petrous apex: classification and findings at CT and MR imaging. *Radiographics* 2012;32(1):151–173 [PubMed](#)
24. Balboni AL, Estenson TL, Reidenberg JS, Bergemann AD, Laitman JT. Assessing age-related ossification of the petro-occipital fissure: laying the foundation for understanding the clinicopathologies of the cranial base. *Anat Rec A Discov Mol Cell Evol Biol* 2005;282(1):38–48 [PubMed](#)
25. Woolfall P, Coulthard A. Pictorial review: Trigeminal nerve: anatomy and pathology. *Br J Radiol* 2001;74(881):458–467 [PubMed](#)
26. Zhang J, Stringer MD. Ophthalmic and facial veins are not valveless. *Clin Experiment Ophthalmol* 2010;38(5):502–510 [PubMed](#)
27. Daniels DL, Mark LP, Mafee MF, et al. Osseous anatomy of the orbital apex. *AJNR Am J Neuroradiol* 1995;16(9):1929–1935 [PubMed](#)
28. Aviv RI, Casselman J. Orbital imaging: Part 1. Normal anatomy. *Clin Radiol* 2005;60(3):279–287 [PubMed](#)
29. Vattoth S, Sullivan JC. Face and neck anatomy. In: Canon CL, ed. *McGraw-Hill Specialty Board Review: Radiology*. 1st ed. New York: McGraw-Hill; 2010:99–114
30. Daniels DL, Mark LP, Ulmer JL, et al. Osseous anatomy of the pterygopalatine fossa. *AJNR Am J Neuroradiol* 1998;19(8):1423–1432 [PubMed](#)
31. Curtin HD, Williams R. Computed tomographic anatomy of the pterygopalatine fossa. *Radiographics* 1985;5(3):429–440
32. Harnsberger HR. Anterior skull base. In: Harnsberger HR, Osborn AG, Macdonald AJ, Ross JS AJ, eds. *Diagnostic and Surgical Imaging Anatomy: Brain, Head & Neck, Spine*. 1st ed. Philadelphia, PA, Amirsys; 2010:II26–II35
33. Siddiqui A, Connor SEJ. Imaging of the pharynx and larynx. *Imaging* 2007;19:83–103
34. Dubrulle F, Souillard R, Hermans R. Extension patterns of nasopharyngeal carcinoma. *Eur Radiol* 2007;17(10):2622–2630 [PubMed](#)
35. Som PM, Curtin HD. Fascia and Spaces of the Neck. In: Som PM, Curtin HD, eds. *Head and Neck Imaging*. Vol 2. 3rd ed. St. Louis: Mosby; 2003:1805–1827
36. Som PM, Curtin HD, Mancuso AA. Imaging-based nodal classification for evaluation of neck metastatic adenopathy. *AJR Am J Roentgenol* 2000;174(3):837–844 [PubMed](#)

4

Soft Tissue of the Scalp and Temporal Regions

Noriyuki Koga

Introduction

The scalp is the soft tissue covering the calvaria. It anatomically positioned in the cranial side of the line connecting the supraorbital border of the forehead, the frontal process of the zygomatic bone, the superior margin of the zygomatic arch, the external acoustic foramen, the mastoid process of the temporal bone, and the superior nuchal line of the occipital bone.¹ The major difference between the scalp and other skin in terms of appearance is that it has hair in almost all areas, excluding the forehead. In a cross-section, the scalp reveals a layered structure, usually divided into five layers, excluding the temporal region, as follows, from the outermost layer down: skin, subcutaneous fat (dense connective tissue), galea aponeurotica (aponeurotic layer), loose connective tissue; and pericranium (**Fig. 4.1**). Among these layers, the skin, subcutaneous tissue, and galea aponeurotica layer are closely connected, making it difficult to bluntly separate each layer. Therefore, these layers from the skin to galea aponeurotica are lumped together and also called the superficial fascial layer, whereas loose connective tissue is also called the deep fascial layer.²

Scalp (Skin) and Subcutaneous Fat Layer

The structure of the scalp is fundamentally similar to the skin in other regions; however, the dermis is thick compared with that in other parts of the body and is rich in blood vessels. Furthermore, it has an abundance of hair.

Subcutaneous tissue comprises an abundance of hair follicles and sweat glands. Moreover, there are many fibrous septa, similar to that of the palms of the hands and soles of the feet, closely connecting the skin and the galea aponeurotica layer. Therefore, subcutaneous fat is separated into small fat lobes by these fibrous septa. In this layer are many perforating arteries and veins heading to the skin from the main vascular network of the scalp inside the galea aponeurotica, along with the small sensory nerves transmitting cutaneous sensation.

Galea Aponeurotica

The galea aponeurotica is the intermediate aponeurosis of the occipitofrontalis muscle and is connected to the frontalis muscle at the front as well as to the occipitalis muscle at the rear (**Fig. 4.2**). The frontalis muscle originates from the galea aponeurotica and attaches to the dermis of the eyebrow after inter-

secting with the orbicularis oculi muscle and procerus muscle near the supraorbital border. Generally, frontalis muscles run obliquely downward superolaterally to inferomedially; therefore, there is a V-shaped area in the center of the forehead between the bilateral frontalis muscles and the galea aponeurotica that extends to the front in this V-shaped part of the forehead. The occipitalis muscle originates from the highest nuchal line of the occipital bone, runs upward, and attaches to the galea aponeurotica. These frontalis and occipitalis muscles are both innervated by the facial nerve; the temporal branch innervates the frontalis muscle, and the occipitalis muscle is innervated by the posterior auricular nerve. It is the role of the frontalis muscle to lift the eyebrows, thereby forming horizontal wrinkles on the forehead. The occipitalis muscle has a role of pulling the galea aponeurotica and placing tension on the scalp; however, it is degenerative and weak, only having the effect of supporting the frontalis muscle. In the temporal region, the galea aponeurotica transitions to the superficial temporal fascia, which is a part of the superficial musculoaponeurotic system (SMAS).^{3,4} The superficial temporal fascia contains the temporoparietal muscle and superior auricular muscle in the same plane. Major blood vessels of the scalp run in the galea aponeurotica layer and give off multiple branches toward the skin and subcutaneous fat layer. Therefore, massive bleeding is commonly observed when separating the galea aponeurotica and subcutaneous fat layer.

Loose Connective Tissue

This layer is also known as the subgaleal fascia and subaponeurotic plane (**Fig. 4.3**). It is found between the galea aponeurotica or pericranium, providing mobility to the scalp. It is approximately 1 to 3 mm thick and is grossly observed as a semitransparent, foamy layer. Chayen et al reported that this loose connective tissue layer is a three-layer structure comprising two loose areolar tissue layers and a dense fascial layer between two loose areolar tissue layers, an outer layer (loose areolar tissue), a dense fascial layer, and a deep layer (loose areolar tissue).⁵ Although blood vessels are not grossly observed in this layer, it is macroscopically observed as layers having blood vessels. The blood circulation of this layer is supplied via two strains wherein the first is the perpendicular blood flow from the vascular plexus inside the galea aponeurotica layer using perforating vessels; the second is the blood flow by the blood vessel system directly flowing in from the main blood vessel of the scalp to the loose connective tissue layer, such as a superficial temporal artery, supraorbital artery, and supratrochlear artery. Using these blood circulations, it is used as a flap when very thin soft tissue flaps are required during auricular reconstruction and such procedures.⁶

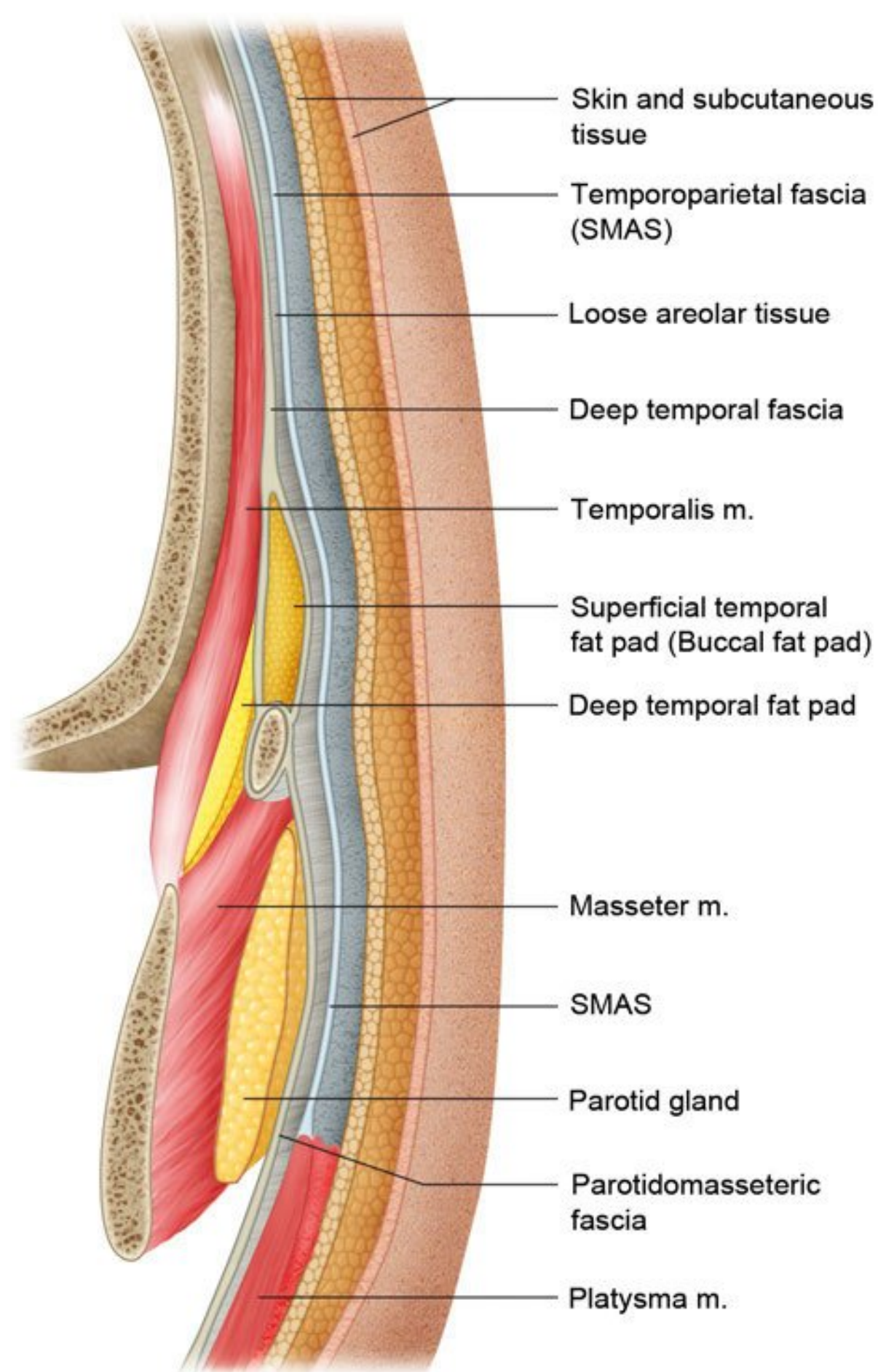


Fig. 4.1 The layers of the scalp. The scalp is divided into five layers from the surface down: skin (S), subcutaneous fat (dense connective tissue) (C), galea aponeurotica (A), loose connective tissue (L), and pericranium (P).

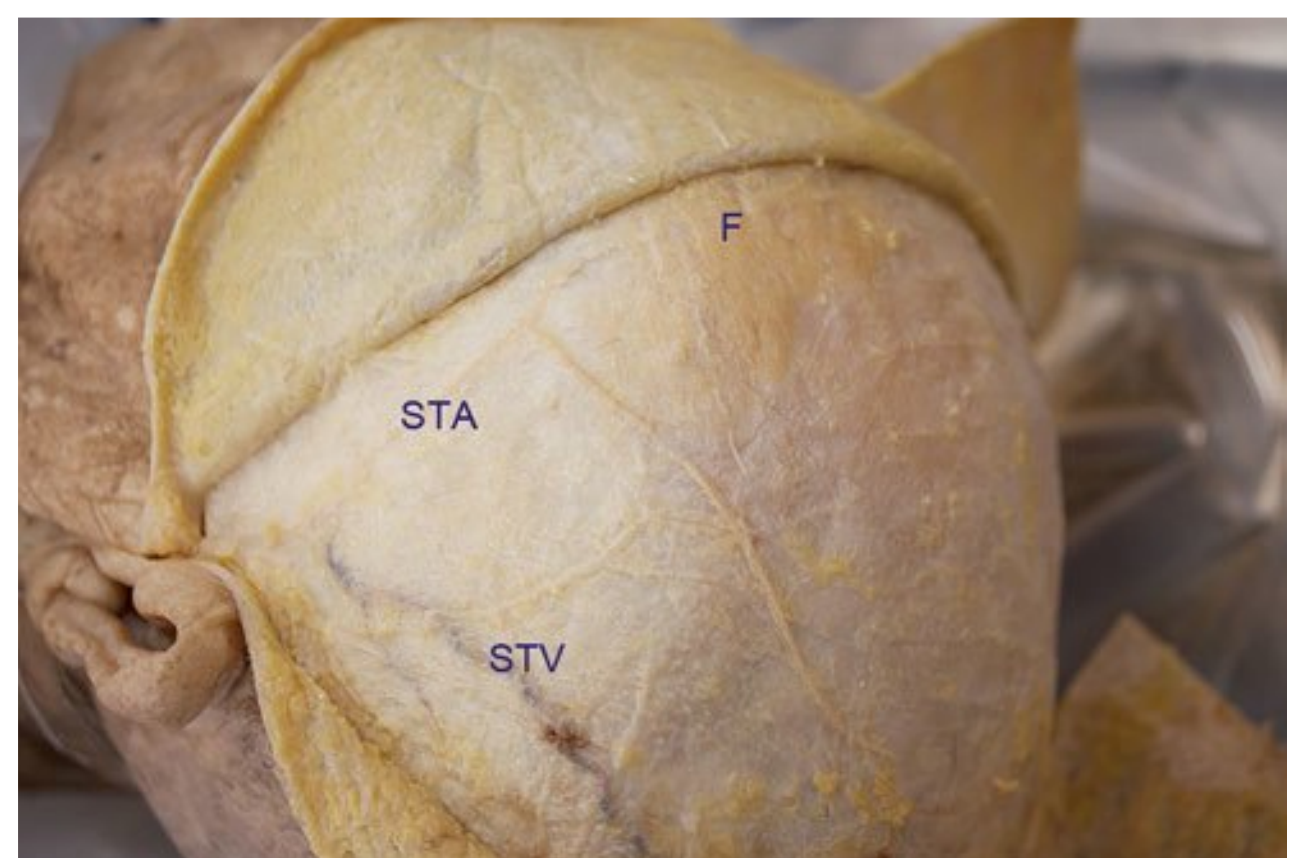


Fig. 4.2 Galea aponeurotica (cadaver dissection picture of the left superior view.) Left frontalis muscle, galea aponeurotica, and superficial temporal fascia are exposed. F, frontalis muscle; STA, superficial temporal artery; STV, superficial temporal vein.

Pericranium

This soft tissue layer is positioned in the deepest subcutaneous tissue. The pericranium of the head is continuous with the temporal fascia in the temporal region and is not observed underneath the temporalis muscle of the temporal fossa.

Blood Circulation Morphology of the Scalp

Regarding the arterial blood supply to the scalp, the supra-orbital artery and supratrochlear artery, branching from the

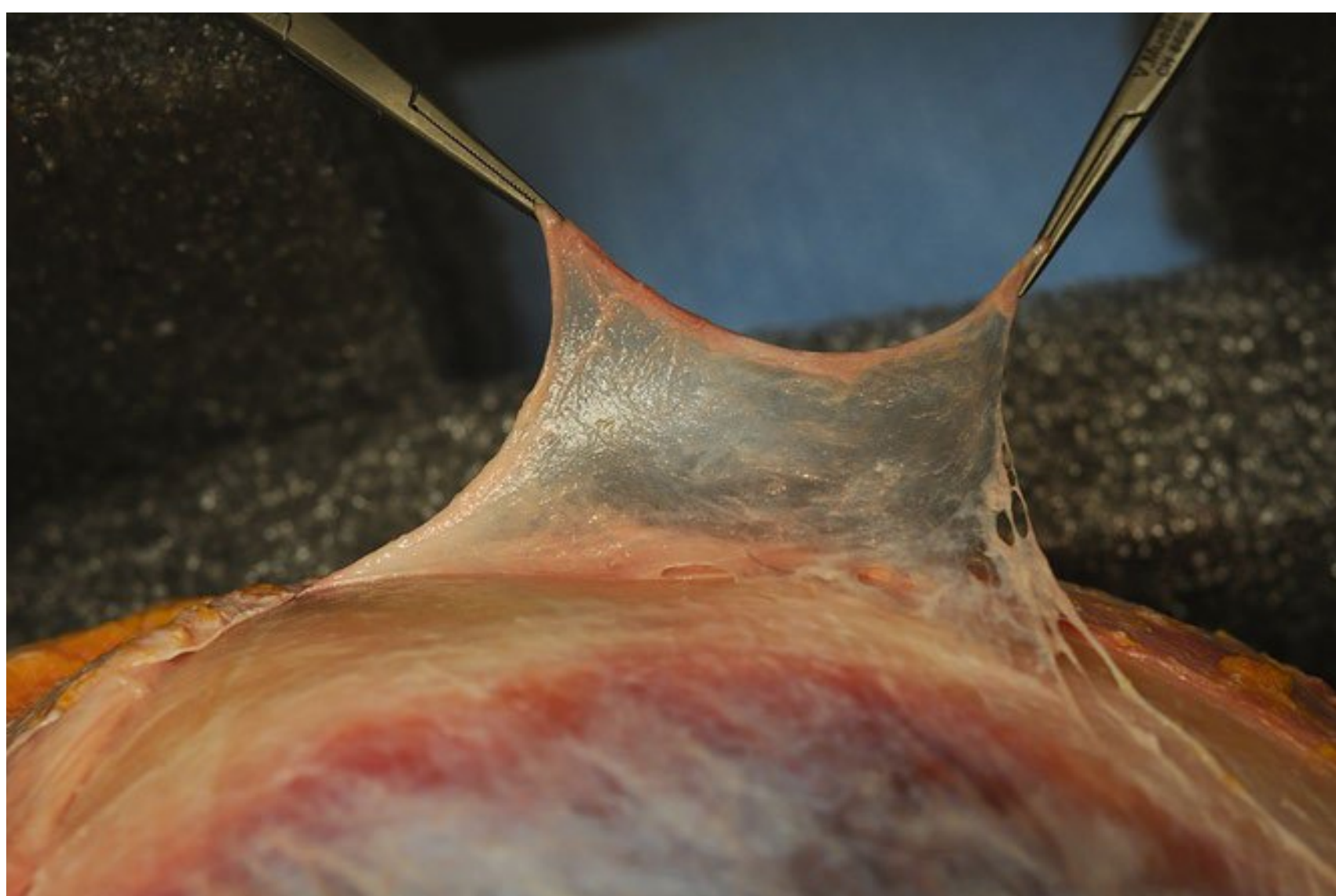


Fig. 4.3 Loose connective tissue layer (cadaver dissection picture).

Table 4.1 Blood circulation morphology of the scalp

Artery	Origin	Distribution
Supraorbital artery	Ophthalmic artery (a branch of the internal carotid artery)	Anterior part of the scalp
Supratrochlear artery	Ophthalmic artery (a branch of the internal carotid artery)	Anterior part of the scalp
Superficial temporal artery	External carotid artery	Lateral part of the scalp
Posterior auricular artery	External carotid artery	Posterior part of the scalp
Occipital artery	External carotid artery	Posterior part of the scalp

ophthalmic artery, supply blood flow to the anterior scalp; the superficial temporal artery, posterior auricular artery, and occipital artery, branching from the external carotid artery, supply blood flow to the lateral and posterior sides of the scalp, respectively (**Table 4.1**). These arteries are connected to each other in the parietal region, forming a dense vascular network. These blood vessels form the vascular plexus in the galea aponeurotica layer, thereby branching blood vessels vertically toward the superficial layer (that is, the subcutaneous fat layer) or deep layer (loose connective tissue layer and the pericranium). These main arteries of the scalp form the vascular plexus also in the loose connective tissue, and this vascular network connects with the perforator vessels from the network in the galea aponeurotica.

The veins mainly run parallel with the arteries, flowing into the internal jugular vein via veins with the same names as the arteries, that is, the supratrochlear vein, supraorbital vein, superficial temporal vein, posterior auricular vein, and occipital vein. The supratrochlear and supraorbital veins flow into the internal jugular vein via the facial vein; however, some flow inside the orbit toward the intracranial cavernous sinus. Moreover, the superficial temporal vein is connected to the superior sagittal sinus in the cranial cavity via the emissary vein passing through the parietal foramen. This vein causes sustained bleeding from the parietal bone during subperiosteal dissection in the parietal region.

Surgical Annotation

Scalp Flap

This skin flap is the first considered in cases requiring various reconstructions of the soft tissue defect in the head. Although known as a skin flap, it is actually raised underneath the galea aponeurotica. Although it is often fundamentally used as a random pattern flap, it may also be used as an axial pattern flap, including the main arteries distributing the scalp, such as the superficial temporal artery.

Frontal Musculopericranial Flap

The frontal musculopericranial flap is useful in the reconstruction of the anterior cranial base required after injury or tumor

excision because it provides good blood circulation in addition to being strong but thin and flexible (**Fig. 4.4**). A periosteal flap in the frontal region is sometimes used for repairing anterior skull-base defects. When creating a large periosteal flap such as covering the entire anterior skull base, the blood circulation in the peripheral region of the flap often becomes unstable; then, in cases of large defects, the frontalis muscle flap should be raised with the periosteum.

Characteristics of the Layered Structures of Soft Tissue in the Temporal Region

The layered structures of the soft tissues in the temporal region is greatly different from the layered structures of other parts of the scalp. The following are the two main differences: (1) the temporalis muscle is in the deepest layer, and (2) the pericranium is not present underneath the temporalis muscle, and the pericranium of other parts of the head is continuous with the deep temporal fascia. From these differences, the layered structure of the temporal region is basically as follows, from the surface down: skin, subcutaneous tissue, superficial temporal fascia, subgaleal fascia (also called innominate fascia or loose areolar tissue layer), deep temporal fascia (divided into two layers inferiorly: the superficial layer and the deep layer), temporalis muscle, and subperiosteum (tissues below the pericranium).

The superficial temporal fascia is continuous with the galea aponeurotica layer in other parts of the head upward, in addition to being continuous with the SMAS in the face and continuous with the platysma in the neck.^{3,4} The superficial temporal fascia layer anatomically has the superior auricular muscle, temporoparietal muscle, and so forth, which are mimetic muscles in relation to the auricle; however, these muscles are difficult to appreciate during surgery and to recognize as the fascia of the superficial layer.

The subgaleal fascial layer consists of a loose connective tissue covering the entire calvarial region, as well as the temporal region, and it has a role of supporting the mobility of the scalp. Blood circulation of this layer is rich in the temporal region as a result of the abundant axial blood supply from the superficial